THE UNIVERSITY OF CHICAGO

THE INTEGRATED STRESS RESPONSE IN HYPOXIA INDUCED DIFFUSE WHITE MATTER INJURY

A DISSERTATION SUBMITTED TO
THE FACULTY OF THE DIVISION OF THE BIOLOGICAL SCIENCES
AND THE PRITZKER SCHOOL OF MEDICINE
IN CANDIDACY FOR THE DEGREE OF
DOCTOR OF PHILOSOPHY

COMMITTEE ON NEUROBIOLOGY

BY

BENJAMIN LAWRENCE LYNNER CLAYTON

CHICAGO, ILLINOIS

AUGUST 2016

Copyright

Table of Contents

List of Figures

List of Tables

List of Abbreviations

ATF4 – activating transcription factor 4

ATF6 – activating transcription factor 6

Axin2 – axin inhibition protein 2

BiP – binding immunoglobulin protein

CHOP – CAAT-enhancer binding protein homologous protein

CMT – Charcot-Marie Tooth disease

CNP - 2',3'-cyclic-nucleotide 3'-phosphodiesterase

CNS – central nervous system

CreP – constitutive repressor of eIF2α phosphorylation

DMSO – dimethyl sulfoxide

DWMI – diffuse white matter injury

EAE – experimental autoimmune encephalomyelitis

EGF – endothelial growth factor

eIF2α - eukaryotic initiation factor 2 alpha

ER – endoplasmic reticulum

GADD34 – growth and arrest DNA-damage 34

GalC – galactosylceramidase

GCN2 – general control nodepressible 2

Hr – hour

HRI – heme-regulated inhibitor

IFN-ɣ - interferon-gamma

IRE1 – inositol requiring enzyme

ISR – integrated stress response

KO – knockout

Lef1 – lymphoid enhancer-binding factor 1

LPS – lipopolysaccharide

MAG – myelin associated glycoprotein

MBP – myelin basic protein

MCH – mild chronic hypoxia

MCT – monocarboxylate transporters

MEF – mouse embryonic fibroblasts

MS – multiple sclerosis

NORM – normoxia

O_2 – oxygen

OGD – oxygen-glucose deprivation

OPC – oligodendrocyte progenitor cell

P0/MPZ – myelin protein zero

PDGFAA – platelet derived growth factor alpha

peIF2α - phosphorylated eIF2α

PERK – PKR-like endoplasmic reticulum kinase

PKR – protein kinase double-stranded RNA-dependent

PLP – proteolipid protein

PMD – Pelizaeus-Merzbacher disease

PMP22 – peripheral myelin protein 22

PNS – peripheral nervous system

PP1 – protein phosphatase 1

RA – room air

RPL13A – ribosomal protein L13a

SAH – severe acute hypoxia

SCIP/Oct6 – octamer-binding protein 6

SOX2 – SRY-Box 2

UPR – unfolded protein response

VEGF – vascular endothelial growth factor

VWMD – vanishing white matter disease

WT – wildtype

XBP1 – x-box binding protein 1

Acknowledgements

First and foremost, I would like thank my advisor and mentor Dr. Brian Popko, because of you I am a better scientist. I greatly appreciate your unwavering support, guidance, and patience through a process that took longer than we had initially hoped. You never lost faith in me and my potential as a scientist and I will be forever grateful. I'd like to also thank you for taking a chance and dedicating significant time and resources on a project that represented a new direction for the lab, being able to work on a something I'm passionate about made all the difference.

I would like to also thank my committee members Dr. Dan McGehee, Dr. David Gozal, and Dr. Richard Kraig. At every committee meeting you helped me remember why I chose to pursue a Ph.D. in the first place. No matter how frustrated I was when I entered our meetings, I always left with a renewed excitement for the potential of my next set of experiments.

Thank you to the members of the Popko lab past and present for their technical help and scientific insight. I'd like to especially thank Robin Avila-Carey and Sharon Way.

Thank you to my family. Thank you to my parents, for your constant support and encouragement and for never giving me a hard time about making it to my 30's without having a "real job". Without my parents I would not have my love of learning and respect for knowledge that guided me to science in the first place. Thank you Eric for introducing me to outdoors, and for marrying me to Ali. Thank you to my siblings: Brianna, Alec, Taylor, Zac, and our new addition little Maximo! You all inspire me.

I have made some amazing friends during my time in Chicago, I'd like to specifically thank Josh Aaker, we got through this together. Thank to everyone else within the Neurofam and to all of the wonderful people I met outside of school. Thank you for putting up with me as

commissioner of our fantasy football league, and remember we can always say we were co-ed flag football champs at the University of Chicago!

Finally, for my wife Ali, there is not enough gratitude in the world. This accomplishment is half yours. Thank you for staying with me on late nights at the lab, for bringing me dinner, for picking me up at the end of long days, for spending your weekends with me in the lab labelling tubes and taking notes, thank you for being there during the highs and the lows, for always taking care of me, and for the countless other things you quietly do that I'm too dense to notice. I can't wait for more adventures with you, I love you and GO UTES!!!!

Abstract

In this thesis two distinct but related studies are presented. The first study is on the role of the integrated stress response (ISR) in a hypoxia induced white matter disorder of prematurity, and the second is on the effect of neonatal hypoxia on myelination of the peripheral nervous system (PNS). The goal of both studies is to furthering our understanding of hypoxia induced injuries suffered by premature infants with the hope of informing the future development of novel therapeutics.

With advancement in medical interventions a greater percentage of premature infants, especially those weighing less than 1500g, are surviving. Unfortunately, neurological disabilities due to white matter injury continue to be a leading cause of morbidity among survivors of premature birth. While in past decades the predominant lesion in the premature brain was necrotic white matter injury caused by hypoxia and ischemia, today the most frequently observed lesion is diffuse white matter injury (DWMI) caused by hypoxia alone. Hypoxia leads to selective damage of oligodendrocyte progenitor cells (OPCs), therefore, a better understanding of the response of OPCs to hypoxia is crucial for developing strategies that would increase their survival and function. The ISR is a conserved stress-induced signaling pathway that is activated by, and provides protection to, a variety of cytotoxic insults. ISR signaling leads to the phosphorylation of the α subunit of eukaryotic translation initiation factor 2 (eIF2α), resulting in inhibition of global protein synthesis and the selective expression of cytoprotective genes. Importantly, hypoxia is an activator of the ISR through the eIF2α kinase PKR-like endoplasmic reticulum kinase (PERK), indicating a potential role for the ISR in hypoxia-induced DWMI. We hypothesized that the PERK arm of the ISR plays an active role in hypoxia induced DWMI and that inhibition of this pathway will exacerbate DWMI while enhancement of the PERK pathway

will protect oligodendrocytes and myelin from hypoxia induced DWMI. We demonstrate that *in vitro* hypoxia activates the ISR in primary OPCs and that genetically inhibiting the PERK arm of the ISR in differentiating OPCs increases their susceptibility to *in vitro* hypoxia. We also show that an *in vivo* mild chronic hypoxia (MCH) model of DWMI activates part of the ISR. Nonetheless, genetic inhibition of the PERK pathway does not have a significant effect on MCH-induced DWMI, and moreover, genetic enhancement of the ISR exacerbates the negative effects of MCH. In addition, we establish a new severe acute hypoxia (SAH) model of DWMI that also activates part of the ISR, although neither genetic inhibition nor genetic enhancement of the ISR appear to have a significant effect on SAH-induced DWMI. These studies suggest that while the ISR protects OPCs from severe hypoxia *in vitro*, it does not play a major role in either mild chronic or SAH-induced DWMI and is therefore not likely to be a valid target for therapies aimed at improving neurological outcome in preterm neonates with hypoxia-induced DWMI.

The adverse effects of neonatal hypoxia, associated with premature birth, on central nervous system (CNS) myelination are well known. However, the effects of neonatal hypoxia on PNS myelination have not been addressed. Damage to Schwann cells in the PNS can lead to myelin disorders that cause significant motor deficits. Furthermore, evidence suggests that motor impairments are a risk factor for behavioral and cognitive deficits experienced by approximately 50% of survivors of premature birth. A better understanding of the effects of neonatal hypoxia on PNS myelination could provide novel opportunities for therapeutic intervention. We hypothesized that neonatal hypoxia would lead to hypomyelination of the PNS with sustained motor deficits. We demonstrate that neonatal hypoxia results in thinner PNS myelin and delayed development of axon bundles in mice leading to electrophysiological and motor deficits that persist into adulthood. These findings provide support for a role of hypoxic damage to the PNS

in persistent motor deficits commonly experienced by premature infants and suggest that therapies designed to protect PNS myelin may improve clinical outcomes in premature infants.

Chapter 1. Introduction

1.1 Myelination in the vertebrate nervous system

Oligodendrocytes of the central nervous system (CNS) and Schwann cells from the peripheral nervous system (PNS) are glia cells responsible for producing the myelin sheath that wraps axons (Fig 1.1). Myelin is a multi-lamellar structure that wraps axons in multiple layers of compact lipid membrane and specialized proteins with a cytoplasmic channel next to the periaxonal space. Oligodendrocytes simultaneously myelinate multiple axonal segments while Schwann cells myelinate a single segment of axon. The original function attributed to the myelin sheath was simply that of an electrical insulator to promote fast conduction of action potentials through salutatory conduction (Buttermore, Thaxton, and Bhat 2013).

Our understanding of myelinating glia and the diversity in their function and the function of myelin has grown significantly over the past three decades and we now know that myelinating glia are more than just passive observers within the nervous system. The presence of myelinating glia is necessary for clustering of sodium channels within the axonal membrane at nodes of Ranvier (Ching et al. 1999; Rasband et al. 1999) and potassium channels at the juxtaparanode region (Fig 1.2) (Baba et al. 1999). Moreover, myelin and myelinating glia are critical for the development and maintenance of axonal integrity through metabolic support (Nave 2010; Nave and Ehrenreich 2014; Nave and Werner 2014; Simons and Nave 2016). Disruption of certain oligodendrocyte proteins can lead to axonal pathology even in the absence of gross demyelination. For example, ablation of the oligodendrocyte specific protein 2',3'-cyclic-nucleotide 3'-phosphodiesterase (CNP) in mice causes axonal damage such as axonal swelling,

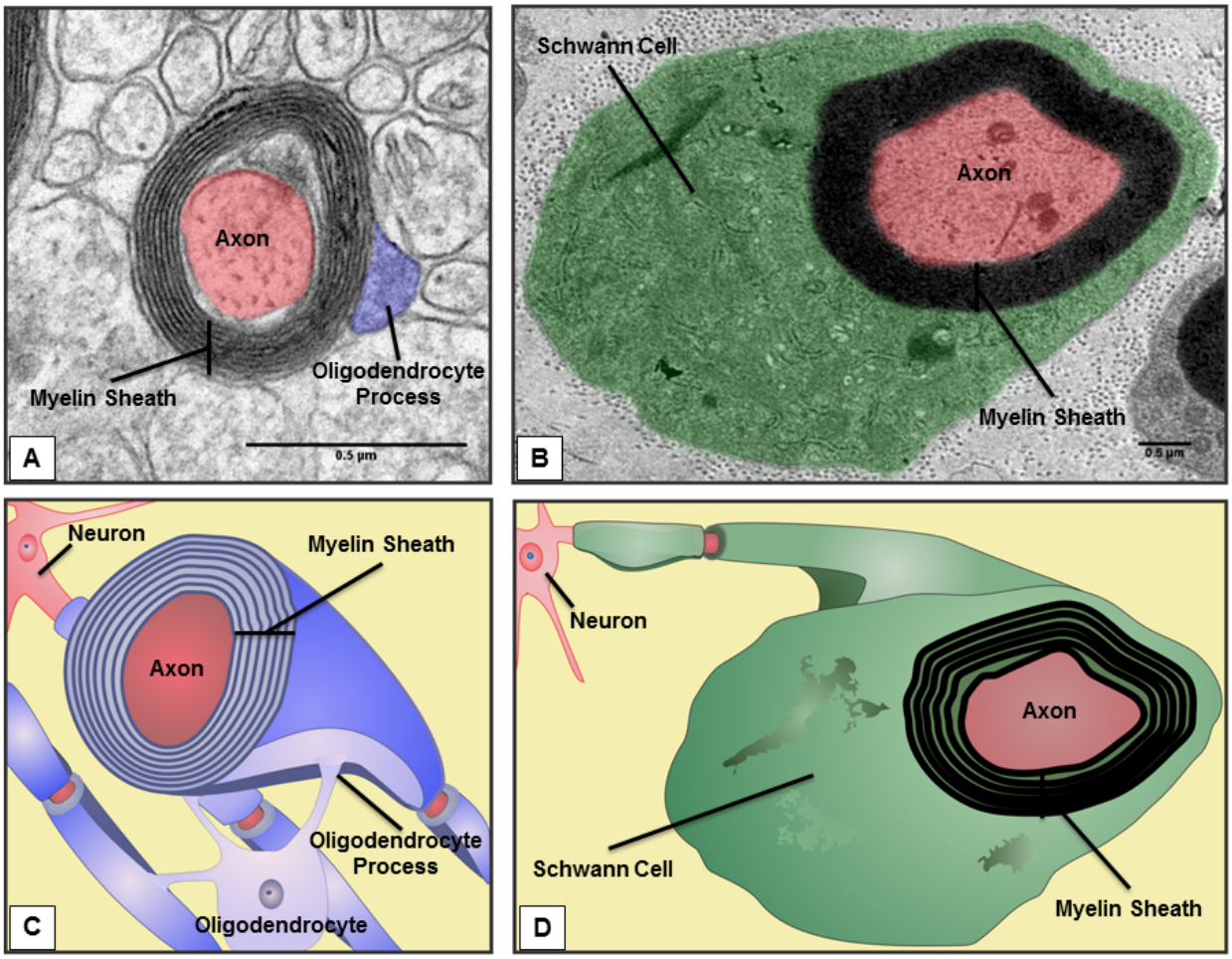

Figure 1.1 Oligodendrocyte and Schwann cell electron micrographs. ((A) False color electron microscopy image and (C) schematic of a myelinated axon in the CNS with an oligodendrocyte process (blue) forming the myelin sheath. (C) Oligodendrocytes will myelinate multiple axon segments in the CNS. B) False color electron microscopy image and (D) schematic of a myelinated axon in the PNS. The Schwann cell body (green) engulfs the axon and will only produce the myelin sheath for a single axon segment.

despite the presence of compact myelin (Griffiths et al. 1998; Lappe-Siefke et al. 2003). In addition, myelinating glia play an important role in providing metabolic energy to the axon through the myelin sheath. Although local energy production along the axon is likely necessary

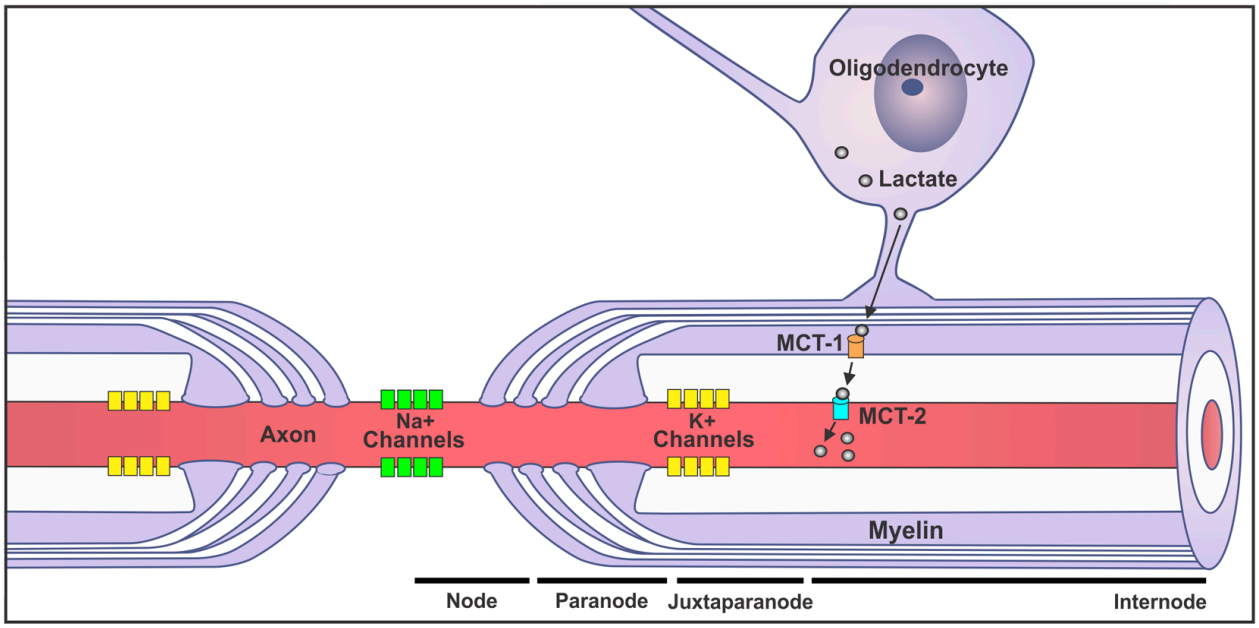

Figure 1.2. Myelinated axon domains and metabolic support of axons by oligodendrocytes. Contact with oligodendrocytes is necessary for clustering of Na^+ channels at nodes and K^+ channels at juxtaparanodes that are required for fast saltatory conduction of action potentials. Oligodendrocytes also metabolically support axons by shuttling lactate through oligodendrocyte expressed MCT-1 into the periaxonal space where it is taken up into the axon through the neuron expressed MCT-2.

to maintain proper function, compact myelin covers much of the axonal surface area, thus limiting access of the axon to extracellular glucose for energy production. Recent findings indicate that myelinating glia act as energy providers via monocarboxylate transporters (MCTs). MCTs transport lactate and pyruvate across the cell membrane with MCT1 localized to oligodendrocytes while MCT2 is found in neurons (Rinholm et al. 2011; Lee et al. 2012). Importantly, oligodendrocyte-specific down regulation of *Mct1* causes axonal pathology (Lee et al. 2012) without death of oligodendrocytes that is likely due to the ability of oligodendrocytes to survive on aerobic glycolysis (Fünfschilling et al. 2012). These results suggest a system in which lactate, a product of glycolysis, is transported from myelin to axons via MCT1 and MCT2, such that myelinating glia provide metabolic support for axons isolated from extracellular glucose

(Fig 1.2). The dependence on myelinating glia for formation of axonal domains and metabolic support clearly demonstrate that myelin is more than a passive electrical insulator. Indeed, myelination has been shown to be a major step in the evolution of the vertebrate nervous system with critical roles in motor, sensory, and cognitive function (Bercury and Macklin 2015).

1.2 Common disorders of myelin and myelinating glia

The importance of myelin and myelinating glia is unmistakable given the devastating effects of disorders of myelin including multiple sclerosis (MS), Pelizaeus-Merzbacher disease (PMD), Vanishing White Matter Disease (VWMD), and Charcot-Marie-Tooth disease (CMT). MS is a CNS demyelinating disorder involving T cell-mediated autoimmunity that results in inflammation, loss of oligodendrocytes, demyelination, and axonal damage leading to worsening neurological outcomes that significantly decrease quality of life (Franklin et al. 2012). PMD is a genetic demyelinating disorder of the CNS with childhood onset caused by mutations in the *PLP1* gene, which encodes proteolipid protein (PLP), a major protein component of myelin; prognosis varies by mutation from gait abnormalities to progressive neurological decline until death (Garbern 2007). VWMD is an autosomal-recessive disorder characterized by CNS hypomyelination and abnormal "foamy" oligodendrocytes that occurs following minor head trauma or febrile infection causing episodes of rapid and progressive neurological deterioration (van der Knaap, Pronk, and Scheper 2006). CMT is a genetic disorder that affects PNS myelin and one form, CMT1, is caused by dominant mutations in genes that encode peripheral myelin proteins. CMT affects both motor and sensory nerves but is not fatal (Theocharopoulou and Vlamos 2015). These diseases demonstrate the variety in causes and prognosis of myelinating

disorders. However, there is a common element within these diseases which is the involvement of the PERK arm of the integrated stress response (ISR).

1.3 The integrated stress response (ISR)

The ISR is a conserved eukaryotic stress response pathway activated by a variety of seemingly disparate cellular insults that converge upon phosphorylation of the alpha subunit of eukaryotic initiation factor 2 (eIF2α) (Fig. 1.3). The ISR is initiated by activation of one of the following four stress sensing kinases; PKR-like endoplasmic reticulum kinase (PERK; also known as eukaryotic initiation factor 2-alpha kinase 3 [EIF2AK3]), general control nondepressible 2 (GCN2; also known as EIF2AK4), protein kinase double-stranded RNA-dependent (PKR; also known as EIF2AK2), and heme-regulated inhibitor (HRI; also known as EIF2AK1). Each eIF2α kinase responds to a variety of stress stimuli. PERK is primarily activated by accumulation of misfolded or unfolded proteins within the endoplasmic reticulum (ER), causing ER stress and is a component of the unfolded protein response (UPR) that maintains ER homeostasis (Walter and Ron 2011; Cao and Kaufman 2012). In addition, PERK is activated by oxidative stress, ischemia, and importantly hypoxia (Kumar et al. 2001; Harding et al. 2003; Koumenis et al. 2002). GCN2 is activated by amino acid deprivation, glucose deprivation, and UV irradiation (Deval et al. 2009; Ye et al. 2010; Grallert and Boye 2007). PKR is primarily activated by viral infection, however it has also been implicated in ER stress (Dar, Dever, and Sicheri 2005; Onuki et al. 2004). Finally, HRI responds to iron deprivation and proteasome inhibition (J. J. Chen 2007; Yerlikaya, Kimball, and Stanley 2008).

Regardless of the initiating stress, activation of one of the four eIF2α kinases leads to phosphorylation of eIF2α, which decreases global protein translation through inhibition of the

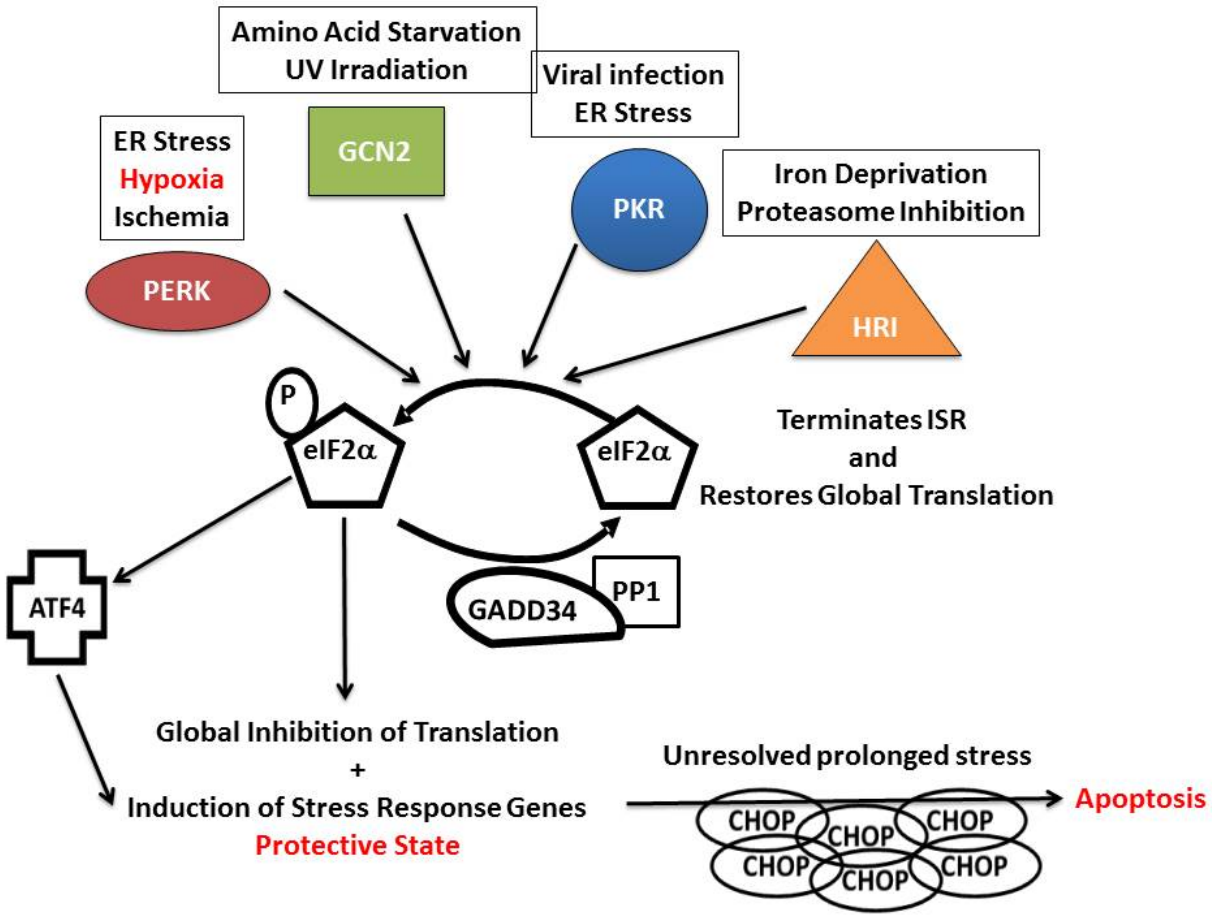

Figure 1.3. The integrated stress response. The integrated stress response is activated by one of four stress sensing kinases that phosphorylate eIF2α in response to various cellular insults. Phosphorylation of eIF2α inhibits global translation while inducing stress response genes via ATF4. ATF4 also increases expression of CHOP, which then induces GADD34. GADD34 then complexes with PP1 to dephosphorylate eIF2α and terminate the ISR. The ISR is initially protective however, in the face of unresolved stress CHOP can accumulate and lead to apoptosis.

guanine nucleotide exchange factor eukaryotic initiation factor 2B (eIF2B). Increased levels of phosphorylated eIF2α (peIF2α) somewhat paradoxically leads to increased translation of a subset of transcripts with regulatory upstream open reading frames (uORF) (Walter and Ron 2011; Pavitt and Ron 2012). One of these transcripts is activating transcription factor 4 (ATF4), ATF4 contains two regulatory uORFs, under non-stressed conditions the translation initiation

complex forms at a high enough rate to translate both uORFs with the second uORF inhibiting translation of ATF4, however, under stressed conditions inhibition of eIF2B by peIF2α slows formation of the translation initiation complex allowing the ribosome to scan pass the second inhibitory uORF and translate ATF4 (Pavitt and Ron 2012). Other components of ISR signaling also contain regulatory uORFs that allow for increased translation efficiency when levels of peIF2α are high, however the mechanisms of regulation differs depending upon the transcript revealing a diversity in uORF regulated translation initiation. ATF4 then furthers ISR signaling by inducing stress response genes aimed at resolving the initiating stress (Donnelly et al. 2013). Activation of the ISR is initially protective due to this combination of translation inhibition and induction of stress response genes. ATF4 then induced expression of the transcription factor CAAT-enhancer binding protein homologous protein (CHOP; also known as DNA-damage-inducible transcript 3 [DDIT3]) (Harding et al. 2003). CHOP transcriptionally increases expression of growth and arrest DNA-damage 34 (GADD34; also known as protein phosphatase 1 regulatory subunit 15A [PPP1R15A]). GADD34 is a regulator of protein phosphatase 1 (PP1) and complexes with PP1 to dephosphorylate eIF2α terminating the ISR and restoring global translation (Novoa et al. 2001; Marciniak et al. 2004). As mentioned above, activation of the ISR is initially cytoprotective, however, in the face of unresolved stress accumulation of CHOP can become pro-apoptotic by directly repressing expression of pro-survival protein B cell lymphoma 2 (Bcl-2) and indirectly by prematurely increasing GADD34 expression and terminating the protective ISR under stress condition (Li et al. 2014; Marciniak et al. 2004; Zinszner et al. 1998). Although, it should be mentioned that the role of CHOP within myelinating glia is controversial as a recent report shows overexpression of CHOP in oligodendrocyte lineage cells does not cause apoptosis (Southwood et al. 2016).

1.4 The integrated stress response and the unfolded protein response, bridged by the PERK pathway

The PERK pathway is also a part of the UPR that monitors ER homeostasis for disruption in protein folding, lipid synthesis, or calcium depletion (Walter and Ron 2011). The UPR is a highly conserved eukaryotic signaling network orchestrated by three transmembrane UPR signal transducers including PERK, inositol requiring enzyme 1 (IRE1), and activating transcription factor 6 (ATF6) (Cao and Kaufman 2012). These three arms of the UPR coordinate a response that decreases protein folding load, increases folding capacity of the ER, and induces cytoprotective genes (Walter and Ron 2011). UPR activation is cytoprotective while the cell corrects for the initiating insult that caused ER; however, if ER stress is left unresolved the UPR can become pro-apoptotic (Li et al. 2014). While activation of PERK leads to decreased translation reducing the demand on the ER, IRE1 and ATF6 act to decrease protein folding load and increase ER protein folding capacity via increased ER associated degradation of mRNA, induced expression of ER resident chaperones and increased ER biogenesis through activation of lipid biosynthesis genes (Cao and Kaufman 2012). IRE1 signaling begins with splicing of X-box binding protein 1 (XBP-1) mRNA, this produces an active transcription factor that increases expression of protein-folding chaperones and lipid biosynthesis and ER biogenesis genes (Calfon et al. 2002; Peschek et al. 2015). In response to ER stress ATF6 is trafficked to the Golgi complex where it is cleaved by Site-1 and Site-2 proteases prior to entering the nucleus as a transcription factor (Ye et al. 2000). Cleaved-ATF6 is largely responsible for increased expression of ER-resident proteins involved in protein folding (Walter and Ron 2011). The PERK pathway is a component of both the ISR and the UPR due to the central role of translation inhibition in response to various stress conditions. This role in translation inhibition seems to be

especially important in myelinating glia since during myelination these cells produce vast amounts of lipid and myelin enriched proteins that assert a high burden on the secretory system; in fact, morphometric analysis indicates that myelinating glia have a surface area a thousand times greater than a typical mammalian cell (Clayton and Popko 2016; Pfeiffer, Warrington, and Bansal 1993). Because of this when referring to the PERK pathway the terms integrated stress response and unfolded protein response are sometimes used interchangeably.

1.5 The important of PERK and the ISR/UPR in disorders of myelin and myelinating glia

PERK expression in the brain is highest within cells of the oligodendrocyte lineage (Y. Zhang et al. 2014) and as mentioned above while producing myelin, myelinating glia place a heavy load on their secretory pathways and require PERK to respond to insults. As such, it has been shown that the PERK arm of the ISR/UPR as well as IRE1 and ATF6 arms of the UPR alone play a role in many disorders of myelin and myelinating glia, including the common disorders discussed earlier. Again PERK plays a role in both the ISR and UPR, for clarity in this work activation of PERK will be attributed to the ISR alone, unless evidence of ER stress is present in which case PERK will be attributed to activation of the ISR/UPR.

1.5.1 The ISR/UPR in multiple sclerosis

MS is a demyelinating disorder that affects approximately 2.3 million individuals world-wide, occurring in both children and adults (Karussis 2014). MS is an autoimmune disease that involves inflammation, loss of oligodendrocytes, demyelination, and axonal damage (Franklin et al. 2012). Different forms of MS range in severity from relapsing-remitting MS, in which patients experience transient immune-mediated attacks on myelin followed by remission and

remyelination, to primary progressive MS, where neurological symptoms steadily worsen and no remission occurs (Barnett and Prineas 2004). Although the etiology of MS remains controversial, studies have found the presence of apoptotic oligodendrocytes prior to immune infiltration (Barnett and Prineas 2004). In addition, a recent report showed that early experimentally-driven death of oligodendrocytes resulted in a late-onset, immune-driven demyelinating disorder in mice (Traka et al. 2015). Together these findings suggest that MS may be initiated by oligodendrocyte death and myelin damage in the CNS. A number of studies have also established ER stress and the ISR/UPR as participants in MS and its primary animal model experimental autoimmune encephalomyelitis (EAE) (Stone and Lin 2015; Way and Popko 2016). Evidence of ISR/UPR activation, including increased *CHOP* and *ATF4* mRNA, is found in demyelinating lesions of MS patients (Cunnea et al. 2011) and CHOP immunoreactivity is seen in multiple cell types, including oligodendrocytes, in active MS lesions (Mháille et al. 2008; McMahon et al. 2012). In agreement with the human MS findings, studies have detected evidence of ISR/UPR activation such as increased levels of phosphorylated eIF2α and CHOP protein in multiple cell types, including oligodendrocytes, within white matter lesions of EAE mice and rats (Ní Fhlathartaigh et al. 2013; Chakrabarty, Danley, and LeVine 2004; Chakrabarty et al. 2005; W. Lin et al. 2007). Nevertheless, *Chop* gene ablation has been reported to have no effect on the EAE disease course (Deslauriers et al. 2011).

Considerable work has focused on genetic manipulation of cells and mice to examine the role of the ISR/UPR in EAE and inflammatory-mediated demyelination (Way and Popko 2016). To model inflammation, interferon-gamma (IFN-ɣ), a cytokine that is expressed by T cells and plays a crucial role in MS and EAE, is often used (Lees and Cross 2007; Popko et al. 1997). IFN-ɣ causes ER stress and apoptosis in cultured rat oligodendrocytes, and when ectopically

expressed by astrocytes in the mouse CNS during development, the cytokine induces ER stress in oligodendrocytes and hypomyelination (W. Lin et al. 2005). Using IFN-ɣ it was also shown that ISR/UPR signaling through PERK protects oligodendrocytes. When mice heterozygous for a *Perk*-null mutation were exposed to IFN-ɣ during developmental myelination they had more severe hypomyelination and increased mortality compared to *Perk* wild-type mice exposed to IFN-ɣ (W. Lin et al. 2005). Likewise, PERK was found to play a protective role in EAE. When IFN-ɣ was administered at different times during the EAE disease course, contrasting effects on EAE disease severity were found (W. Lin et al. 2007; W. Lin et al. 2006). Genetically-driven CNS-specific expression of IFN-ɣ prior to EAE onset protects oligodendrocytes and myelin and ameliorates EAE disease severity (W. Lin et al. 2007). Nevertheless, CNS expression of IFN-ɣ later in the EAE disease course inhibits remyelination and recovery (W. Lin et al. 2006). Importantly, PERK plays a protective role in both situations. IFN-ɣ expression prior to EAE disease onset, protects oligodendrocytes and myelin and ameliorates EAE disease course. Nevertheless, these protective effects are lost in heterozygous *Perk*-null mice (W. Lin et al. 2007), demonstrating that the protective effects of prophylactic IFN-ɣ expression are at least in part dependent upon PERK. Using a similar approach, when the IFN-ɣ was expressed later in *Perk* haploinsufficient mice, the detrimental effects of the cytokine on remyelination and recovery were exacerbated, demonstrating again that activating PERK protects oligodendrocytes and myelin (W. Lin et al. 2006). These studies laid the foundation for the ISR/UPR as a potential therapeutic target in MS. Further studies have built upon these studies to examine the cell-specific role of PERK-mediated ISR/UPR activation in oligodendrocytes in both active EAE disease and recovery. Conditional deletion of *Perk* from oligodendrocytes worsens EAE disease severity and increases oligodendrocyte loss (Hussien, Cavener, and Popko 2014). In addition,

using a combined small molecule and genetic approach, it was shown that oligodendrocyte-specific activation of PERK protects mice against EAE and protects remyelinating oligodendrocytes during recovery from EAE (W. Lin et al. 2013). These studies demonstrate that the protective effects of PERK activation are, at least in part, due to a cell autonomous effect within oligodendrocytes.

With the establishment of the protective role of the PERK in the MS model EAE, there has been considerable interest in finding compounds that could pharmacologically enhance the ISR/UPR for therapeutic benefit. Such an approach would be particularly beneficial because current MS therapies are primarily immunomodulatory, and there are no approved therapies that directly protect oligodendrocytes and/or myelin. In addition, genetic manipulations of a second major UPR target, GADD34, were performed to better understand its role in the protective pathway. GADD34 complexes with protein phosphate 1 (PP1) to dephosphorylate eIF2α, terminating the UPR. As predicted, a loss of function mutation in *Gadd34* resulted in enhancement of the eIF2α phosphorylation in oligodendrocytes (W. Lin et al. 2008). Therefore, it was postulated that functional deletion of *Gadd34* should inhibit the dephosphorylation of eIF2α and prolong the protective effects of the peIF2α. In agreement with this hypothesis, GADD34 inactivation increases the percentage of phosphorylated eIF2α positive oligodendrocytes and protects oligodendrocytes and myelin from IFN-ɣ-induced immune mediated hypomyelination (W. Lin et al. 2008). In addition, treatment of rat hippocampal slice cultures exposed to IFN-ɣ with the small molecule salubrinal, which blocks formation of eIF2α phosphatase complexes, increases phosphorylated eIF2α protein levels and protects oligodendrocytes and myelin (W. Lin et al. 2008). Unfortunately, salubrinal is not desirable for use in humans due to its low solubility in aqueous solutions, which requires use of potentially

toxic dimethyl sulfoxide (DMSO) as a solvent. In addition, prolonged inhibition of both eIF2α phosphatase complexes can be lethal, making salubrinal a potentially dangerous drug with a narrow window of utility (Boyce et al. 2005; Pavitt and Ron 2012). Importantly, another small molecule, guanabenz, was found that inhibits GADD34-PP1 complex formation, prolongs eIF2α phosphorylation, and protects cells against ER stress (Tsaytler et al. 2011). Guanabenz prolongs phosphorylation of eIF2α and protects mice against IFN-ɣ-induced oligodendrocyte loss in the CNS. Guanabenz also ameliorates the disease course in EAE mice, which correlates with the protection of oligodendrocytes and decreased CNS T-cell presence (Way et al. 2015). Disease amelioration is also seen in a relapsing-remitting EAE model of MS when guanabenz is given after the initial onset of disease (Way et al. 2015). In addition, a highly specific inhibitor of GADD34 has been developed called Sephin1 (Das et al. 2015). It will be of interest to determine whether Sephin1 can improve upon the protective effects of guanabenz in EAE. With the success of GADD34 inhibition in mouse models of MS, guanabenz has entered into clinical trials.

1.5.2 The ISR/UPR in Pelizaeus-Merzbacher disease

Pelizaeus-Merzbacher disease (PMD) is an X chromosome-linked disease that causes dysmyelination of the CNS due to one of more than 60 known mutations in *Plp1,* which encodes for proteolipid protein (PLP) and its alternative spliced isoform DM20 (Garbern 2007). PLP is a major myelin protein in the CNS, making up approximately 50% of total CNS myelin protein (Greer and Lees 2002). Severity of PMD varies broadly depending upon the mutation, and studies in PMD animal models have suggested that severity depends upon the ability of PLP/DM20 to translocate out of the ER, with more severe disease caused by mutations where PLP/DM20 are abnormally sequestered within the ER (Gow and Lazzarini 1996; Garbern 2007).

Two genetic mouse models of PMD that carry authentic human PLP mutations illustrate the role of mutant PLP/DM20 ER retention on disease severity. The *myelin-synthesis deficient mouse* has a phenotype caused by an A242V amino acid substitution that is similar to the severe PMD phenotype in humans (Gow and Lazzarini 1996). This A242V mutation in *Plp1* causes an increase in PLP localized to the ER and DM20 localized to the Golgi, with neither mutant protein reaching the cell surface (Gow and Lazzarini 1996; D'Antonio, Feltri, and Wrabetz 2009). In contrast, in the *rumpshaker* mouse that carries an I186T mutation that causes mild disease in both mouse and humans, DM20 does not accumulate in the ER while PLP is still retained in the ER (Gow and Lazzarini 1996; D'Antonio, Feltri, and Wrabetz 2009). Further evidence that PLP/DM20 ER retention is central to disease severity is provided by *Plp1*-null mice in which PLP/DM20 protein is absent, instead of misfolded, and the phenotype is mild (Klugmann et al. 1997; Rosenbluth et al. 2006). It is important to note that while classical PMD is caused by mutations in *PLP1* there are also PMD-like diseases caused by mutations in other genes coding for myelin proteins. One example comes from a recent report in which the authors describe a mutation in the gene encoding the myelin associated glycoprotein (MAG) protein, which was found in three siblings exhibiting PMD-like disease phenotype (Lossos et al. 2015). In these patients, mutant MAG protein did not properly fold and was retained in the ER and caused an increase in the UPR marker binding immunoglobulin protein (BiP), which is a protein chaperone that binds to and inhibits activation of PERK, IRE1, and ATF6 until sequestered by misfolded proteins leading to activation of the UPR, suggesting a role for ER stress in PMD-like disorders (Lossos et al. 2015).

Evidence from human patients, mouse models, and *in vitro* studies of PMD support the initial observation and hypothesis that ER stress plays a central role in PMD. In mice with

mutant PLP, increases in CHOP protein localization to mature oligodendrocytes, which recapitulates the increase in oligodendrocyte-localized CHOP expression in PMD patients (Southwood et al. 2002). Indeed, microarray analysis in optic nerves from mice with mutant PLP show a significant increase in expression of the ISR/UPR genes encoding CHOP, ATF4, and BiP protein (Southwood et al. 2013). In addition, a recent study using induced pluripotent stem cells (iPSCs) harvested from PMD patients and differentiated into mature oligodendrocytes shows PLP accumulation in the ER (Numasawa-Kuroiwa et al. 2014). Interestingly, there is no increase in UPR markers in the PMD derived oligodendrocytes compared to those derived from a healthy patient. Nevertheless, PMD derived oligodendrocytes from a patient with a severe phenotype have increased sensitivity to mild ER stress, such that might occur during active myelination (Numasawa-Kuroiwa et al. 2014). In support of the role of ER stress in PMD severity, PMD derived oligodendrocytes from a second patient with a more mild disease were more resistant to ER stress compared to the oligodendrocytes from the severe PMD patient (Numasawa-Kuroiwa et al. 2014). Oligodendrocytes derived from both PMD patients also showed increased apoptosis, produced abnormal myelin structure, and had disrupted ER morphology compared to cells from a healthy patient (Numasawa-Kuroiwa et al. 2014).

Attempts to genetically manipulate the ISR/UPR in PMD mouse models have been met with surprising results. As mentioned, in most cell types and contexts, CHOP is pro-apoptotic (Zinszner et al. 1998; Marciniak et al. 2004). Nevertheless, *Chop* ablation from *rumpshaker* mice exacerbates disease severity dramatically (Southwood et al. 2002). *Rumpshaker* mice without CHOP have increased oligodendrocyte apoptosis and die around 5 weeks of age, whereas *rumpshaker* mice with normal expression of CHOP have lifespans similar to wildtype mice (Southwood et al. 2002). These results demonstrate that modulating the ISR/UPR can affect

PMD disease severity, but that surprisingly, CHOP in oligodendrocytes is protective within this disease context. This paradoxical role of CHOP in oligodendrocytes is still not fully understood. A suggested hypothesis is that CHOP targets a different set of genes in oligodendrocytes compared to other cell types, which is supported by the lack of induced downstream CHOP genes in PMD (Southwood et al. 2002). More studies are needed to better understand the disparate roles of CHOP in oligodendrocytes and disease models.

1.5.3 The ISR/UPR in Vanishing White Matter disease

Vanishing white matter disease (VWMD) is an autosomal-recessive disorder characterized by hypomyelination and abnormal "foamy" oligodendrocytes (van der Knaap, Pronk, and Scheper 2006). The clinical course of VWMD is chronic and progressive with minor head trauma and febrile infection, causing episodes of rapid neurological deterioration (van der Voorn et al. 2005). VWMD is caused by a mutation in any of the genes encoding the five subunits of eIF2B, a guanine nucleotide exchange factor that promotes the formation of an active eIF2-GTP complex necessary for protein translation (van der Knaap, Pronk, and Scheper 2006). ER stress leading to phosphorylation of eIF2α reduces the activity of eIF2B by forming an inactive phosphorylated eIF2α-eIF2B complex that inhibits translation initiation (van der Voorn et al. 2005). It has been proposed that mutant eIF2B perturbs the oligodendrocyte response to ER stress (van der Knaap, Pronk, and Scheper 2006). Support for this hypothesis has been shown *in vitro*, expression of eIF2B mutations in an oligodendrocyte cell line causes a higher basal level of UPR markers and cells expressing mutant eIF2B have a heightened UPR response and increased cell death compared to controls (Kantor et al. 2008; N. Chen et al. 2015).

Markers of ER stress and activation of PERK and the other two arms of the UPR have been seen in oligodendrocytes of VWMD patients (van der Voorn et al. 2005; van Kollenburg et al. 2006). Increased levels of *BiP*, *ATF4*, *CHOP*, and *GADD34* mRNA is seen in postmortem tissue from VWMD patients as well as increased *XBP-1* mRNA splicing and increased immunostaining for XBP-1, BiP, and ATF6 in oligodendrocytes (van Kollenburg et al. 2006). In another study, increased immunostaining for phosphorylated PERK, phosphorylated eIF2α, and ATF4 was also seen in oligodendrocytes from VWMD patient tissue (van der Voorn et al. 2005).

Mouse models that reproduce the characteristics of VWMD have been difficult to produce (Lin et al., 2014b). Point mutations in eIF2B reproduce some white matter deficits but to a much milder degree than seen in VWMD. While the role that ER stress plays in the phenotype of these mouse models has not been examined (Geva et al. 2010), a recent study using transgenic mice provides evidence for a role of ER stress in VWMD (Lin et al., 2014b). *PLP/Fv2E-PERK* transgenic mice allow for oligodendrocyte-specific expression of a chimeric protein that contains the luminal eIF2α kinase domain of PERK fused to a small molecule-driven artificial dimerizing domain. When the small molecule dimerizing agent AP20187 is injected into the mouse PERK dimerizes and activates (Y. Lin, Huang, et al. 2014)LIN 2014. Using this transgenic mouse, the authors demonstrate that strong activation of PERK specifically in oligodendrocytes leads to impaired eIF2B activity in young developing mice, resulting in a VWMD-like phenotype including myelin loss and "foamy" oligodendrocytes (Lin et al., 2014b). Strong activation of PERK was accomplished by using mice homozygous for *PLP/Fv2E-PERK* with high doses of the small molecule dimerizer compared to moderate PERK activation that has no effect on developmental myelination in hemizygous *PLP/Fv2E-PERK* mice with low doses of dimerizer (Lin et al., 2014a). This study provides evidence of cell autonomous decreased eIF2B

activity in oligodendrocytes as causative in VWMD. In addition, it presents the basis for a hypothesis regarding one of the mysteries of VWMD, namely how do mutations in a gene necessary for protein translation cause selective damage to white matter and oligodendrocytes? The authors propose that inhibition of eIF2B is biphasic in nature. Modest inhibition of eIF2B is protective (W. Lin et al. 2013; Y. Lin, Huang, et al. 2014) while strong inhibition of eIF2B, such as would happen with the combination of eIF2B mutation and phosphorylation of eIF2α by ER stress, is damaging to oligodendrocytes during active myelination and may explain the severe demyelination seen in VWMD following acute stress (Lin et al., 2014b). This hypothesis deserves further investigation.

1.5.4 The ISR/UPR in Charcot-Marie Tooth disease

Charcot-Marie-Tooth disease is a group of dominant genetic disorders affecting PNS myelin and categorized based on whether the disease originates from mutations in genes expressed by myelinating Schwann cells (Charcot-Marie-Tooth 1 or CMT1) or neurons (Charcot-Marie-Tooth 2 or CMT2) (Theocharopoulou and Vlamos 2015). Charcot-Marie-Tooth affects 1 in 2,500 individuals, making it one of the most common inherited neurological disorders. Most CMT1 cases are caused by mutations in genes that encode peripheral myelin proteins (Theocharopoulou and Vlamos 2015). CMT1 is further categorized based on the affected protein. The most prevalent form of CMT1A is caused by defects in the gene that encodes peripheral myelin protein 22 (PMP22), with the most common form resulting from duplication of the chromosomal region containing *PMP22* (Hoyle et al. 2015). Studies in *Trembler* mice, which carry the same missense mutations found in some forms of human CMT1A patients, have shown that mutant PMP22 is misfolded and abnormally localizes to the

ER where it forms aggregates and associates with the ER chaperone calnexin (Dickson et al. 2002). Nevertheless, *Trembler* mice do not show evidence of UPR activation (Dickson et al. 2002). A second category of CMT1 is CMT1B, which is caused by one of over 120 mutations found in the gene that encodes myelin protein zero (MPZ), the most abundant protein in PNS myelin (Theocharopoulou and Vlamos 2015). Similar to CMT1A, many of these mutations cause MPZ to be retained in the ER instead of being transported to the myelin sheath. In contrast to CMT1A, CMT1B mouse models display evidence of ISR/UPR activation in Schwann cells (Theocharopoulou and Vlamos 2015).

The P0S63del mutant mouse is a mouse model of CMT1B that carries the same S63 deletion in *Mpz* that causes CMT1B in humans (Wrabetz et al. 2006). Studies of this mouse show that mutant MPZ is retained in the ER and activates PERK and the other branches of the UPR in Schwann cells. Increased levels of phosphorylated eIF2α, ATF4, and CHOP indicate activation of the PERK pathway, spliced XBP-1 is evidence of IRE1 activation, and cleavage of ATF6 is also detected in P0S63del mice (Pennuto et al. 2008; Wrabetz et al. 2006). Moreover, activation of the UPR in the nerves of these mice is dose-dependent, strongly suggesting that increased activation of the UPR is directly related to increased levels of mutant MPZ protein in the ER (Wrabetz et al. 2006). As previously mentioned, CHOP is generally considered to be pro-apoptotic and *Chop* deletion protects cells from ER stress-induced apoptosis (Walter and Ron 2011). In agreement with this classical role, *Chop* ablation from P0S63del mice reduces the number of demyelinated fibers and lessens the electrophysiological and behavioral defects typically found in P0S63del mice (Pennuto et al. 2008). Surprisingly, CHOP deletion neither decreases the number of apoptotic Schwann cells nor increases the myelin thickness of P0S63del nerves. Similarly, another mouse model of CMT1B that contains the human R98C mutation in

the *Mpz* locus, also exhibits ER retention of mutant MPZ and activation of the ISR/UPR (Saporta et al. 2012). In addition, treatment of R98C mice with curcumin, which has been shown to relieve ER stress, is protective. However, *Chop* ablation in this model did not provide therapeutic benefit (Saporta et al. 2012; Patzkó et al. 2012).The results of *Chop* ablation in the CMT1B mouse models again point to an apparent distinct role that CHOP plays in myelinating glia, which requires further investigation (Pennuto et al. 2008). A more recent study continued to expand on the therapeutic potential of ISR/UPR manipulation in cases of CMT1B. Utilizing microarray analysis of P0S63del nerves, D'Antonio et al. reported that UPR transcripts are upregulated in P0S63del nerves prior to the onset of myelination and prior to induction of any apoptotic or inflammatory transcripts (D'Antonio et al. 2013). These results, coupled with the protective effects of *Chop* deletion, suggest that the ISR/UPR is maladaptive in the P0S63del model of CMT1B. Interestingly, GADD34 mRNA and protein was increased in P0S63del nerves and returned to normal levels in P0S63del nerves absent CHOP (D'Antonio et al. 2013). This led the authors to hypothesize that premature termination of the ISR/UPR by GADD34 is maladaptive in P0S63del nerves. To examine the role of GADD34 in CMT1B nerves, P0S63del mice were crossed with GADD34-null mice. Removal of GADD34 function from P0S63del nerves restores motor performance, lessens the electrophysiological deficits in P0S63del mice, decreases the number of demyelinated axons, and increases myelin thickness (D'Antonio et al., 2013). Importantly, treatment of P0S63del mice with the GADD34 inhibitor salubrinal has the same effect as genetic removal of GADD34 function (D'Antonio et al. 2013). The protective effects of GADD34 inhibition are accompanied by increased levels of phosphorylated eIF2α and ATF4, showing an increase in PERK signaling (D'Antonio et al. 2013). Treatment with the specific GADD34 inhibitor Sephin1 restores motor function and rescued myelin deficits in

P0S63del nerves compared to vehicle treated controls (Das et al. 2015). These results in a CMT1B mouse model highlight the therapeutic potential of targeting the ISR/UPR in the treatment of CMT1B.

1.6 Diffuse white matter injury (DWMI)

Over the past two decades the incidence of live preterm births within the United States has steadily increased, due in part to an increase in mothers giving birth past the age of 35 and the use of assisted reproductive technology (Salmaso et al. 2014). Over this same time period care of premature neonates has also improved leading to an increase in the survival of these infants, especially those that are born prior to 32 weeks of gestation and weighing less than 1500g (Deng 2010). Regardless of this improvement in survival premature neonates are still at a high risk for long-term neurological disabilities. These include motor, sensory, cognitive, and behavioral deficits in more than half of all premature infants and severe motor disabilities leading to diagnosis of cerebral palsy in 5-10% of surviving infants (Back 2015; Miller et al. 2005; Marlow et al. 2005; Roberts et al. 2009). Often these deficits persist into adulthood, even in cases with milder cognitive and motor deficits (Grunau, Whitfield, and Fay 2004; Hack et al. 2002; Lindström et al. 2007). The most common white matter lesion in premature neonates, thought to be the underlying cause of perturbed development of brain connectivity, is diffuse white matter injury (DWMI).

Table 1.1 Highlights the major myelin disorders with a known ISR/UPR role

Disease	Presence of UPR Markers	Effect of UPR Manipulation	References
Multiple Sclerosis	• *CHOP* mRNA in patients • *ATF4* mRNA in patients • Phosphorylated eIF2α in mouse models • CHOP protein in mouse models	• *Gadd34* deletion and pharmacological inhibition are protective in mouse models.	• Cunnea et al., 2011 • Way et al., 2015
Pelizaeus-Merzbacher Disease	• CHOP protein in patients • *Chop* mRNA in mouse models • *Atf4* mRNA in mouse models • *Bip* mRNA in mouse models	• *Chop* deletion exacerbates disease in mouse models.	• Southwood et al., 2002 • Southwood et al., 2013
Vanishing White Matter Disease	• *ATF4* mRNA and protein in patients • *CHOP* mRNA in patients • *GADD34* mRNA in patients • *BiP* mRNA in patients • XBP-1 splicing in patients • Phosphorylated PERK in patients • Phosphorylated eIF2α in patients	• Effects of UPR manipulation on disease outcome have not been studied.	• van Kollenburg et al., 2006 • van der Voorn et al., 2005
Charcot-Marie-Tooth	• BiP mRNA and protein in mouse models • CHOP mRNA and protein in mouse models • XBP-1 splicing in mouse models	• *Chop* deletion is protective in some mouse models. • *Gadd34* deletion and pharmacological inhibition are protective in some mouse models.	• Bai et al., 2013 • Pennuto et al., 2008 • D'Antonio et al., 2013

1.6.1 Pathogenesis of DWMI

DWMI is caused by hypoxic and/or ischemic events in combination with or independent of inflammation (Deng 2010). In previous decades the most common form of white matter injury in premature infants were focal cystic necrotic lesions with complete cell loss called periventricular leukomalacia, however, with improved care the prevalence of these lesions has declined significantly (Back 2015). Today the most common white matter lesion in premature infants is DWMI that is identified by MRI in approximately one-third of premature infants born prior to 32 weeks of gestation, although MRI likely underestimates the prevalence of DWMI

(Woodward et al. 2006). As previously mentioned, myelination in the CNS is performed by oligodendrocytes. The oligodendrocyte lineage is one of the best characterized in the body where OPCs are first specified from neural progenitor cells, followed by maturation into pre-myelinating oligodendrocytes, and final mature myelinating oligodendrocytes (Emery 2010). Specification and maturation along this lineage is controlled by a complex set of intrinsic and extrinsic signals that produce mature oligodendrocytes that myelinate axons (Emery 2010). Importantly, it is the immature OPCs that are the primary cells injured in DWMI and predominate the oligodendrocyte lineage during the time frame, 23-32 weeks of gestation, at which premature infants are most susceptible to DWMI (Buser et al. 2012). In addition, it has been shown that OPCs are highly sensitive to oxidative damage caused by hypoxia and/or ischemia (Back et al. 2007; Back et al. 2005; Riddle et al. 2006). This is in part due to decreased production of antioxidant enzymes in OPCs compared to mature oligodendrocytes (Folkerth et al. 2004). Although our previous understanding of the pathogenesis of DWMI focused on death of OPCs, our current understanding presents a more complicated story involving multiple cellular and molecular mechanisms. These include death of OPCs during the early phase of injury (Back et al. 1998), followed by robust regeneration of OPCs that are delayed or fail to mature completely (Jablonska et al. 2012; Buser et al. 2012), leading to disrupted myelination during critical developmental windows causing altered brain structure and connectivity (Mullen et al. 2011; Pandit et al. 2014; Counsell et al. 2008).

1.6.2 Current therapies for DWMI

Currently the only therapeutic intervention available to neonates with hypoxic and ischemic damage is mild hypothermia, where treatment begins within the first 6hrs following

birth with 48-72hrs of cooling to 34.5±0.5°C for the head alone and 33.5±0.5°C if cooling the whole body (Davidson et al. 2015). However, therapeutic hypothermia is only partially effective and importantly, has only become the standard of care for term neonates experiencing hypoxia and ischemia and not for premature neonates. While some groups have reported success in treatment of the premature neonate population with therapeutic hypothermia, questions of the effectiveness and safety of such interventions remain (Smit et al. 2015). The lack of interventional therapies for a disease that affects over fifty percent of premature neonates highlights the need for studies that further our understanding of the pathophysiology behind DWMI and providing novel therapeutic targets with the potential to reach the clinic.

1.7 Modeling DWMI with hypoxia

1.7.1 *In vitro* models of DWMI that involve hypoxia

DWMI is modeled *in vitro* with oxygen-glucose deprivation (OGD) to mimic hypoxic-ischemic events, and *in vitro* hypoxia to mimic neonatal hypoxia caused by poor lung development and immature cerebral vasculature. Importantly, *in vitro* OPCs have proven to be the most sensitive of the oligodendrocyte lineage to both the OGD and *in vitro* hypoxia models that recapitulate the susceptibility of OPCs to hypoxia and ischemic insults in DWMI (Back, Riddle, and McClure 2007; Deng et al. 2003).

Hypoxia and ischemia are modeled *in vitro* by OGD. Unfortunately, there is no consensus on the structure of the OGD paradigm. The similarity between disparate OGD models is decreased oxygen concentration and complete removal of glucose from the media. In addition, models of OGD require a return to oxygenated and glucose containing media in order to cause

cell death, suggesting that re-oxygenation plays a large role in the cytotoxicity of the OGD model. However, the level of oxygen used in OGD models varies significantly, ranging from anoxia to as high as 0.7% O_2. Moreover, while all models of OGD involve removal of glucose from the OGD media, models also vary in their accounting for acidity and concentrations of extracellular ions (Bondarenko and Chesler 2001a; Schmitz et al. 2012; Deng et al. 2003; Kraskiewicz and FitzGerald 2011). During hypoxic and ischemic brain injury tissue pH falls and there is a shift in the concentrations of extracellular ions. External potassium rises significantly in the hypoxic and ischemic brain while sodium, calcium, and chloride significantly fall (Bondarenko and Chesler 2001b; Bondarenko and Chesler 2001a; Hansen 1985). Therefore, OGD models that incorporate acidosis and ion shifts are preferred. Regardless of the specifics of the OGD model utilized, OGD leads to significant death of OPCs when measured 24hrs later. The mechanisms of OGD cytotoxicity involve oxidative stress and excitotoxity, and protection of OPCs from OGD in culture has been shown with the antioxidants minocycline and quercetin, and glutamate receptor antagonists that block calcium permeable AMPA and kainate receptors (Deng et al. 2003; Schmitz et al. 2012; Domercq et al. 2005; Wu et al. 2014). Interestingly, it has been shown that partial blockade of the IRE1 arm of the UPR has no effect on cytotoxicity caused by OGD (Kraskiewicz and FitzGerald 2011).

In vitro hypoxia has also been used as a model of DWMI. Although developed relatively recently, *in vitro* hypoxia has advantages over OGD in that it does not lead to cell death but instead causes arrested maturation of OPCs (Yuen et al. 2014). In this way, *in vitro* hypoxia better recapitulations the mechanism of maturational arrest that is thought to play a major role in today's more prevalent diffuse lesions. In addition, the effects of *in vitro* hypoxia are slower, requiring exposure on the order of days not hours and no re-oxygenation is needed to see an

effect. Again this may better model the hypoxic state caused by poor lung development and immature vascularization of the CNS that is a major contributor to DWMI. *In vitro* hypoxic experiments are performed by differentiating OPCs, or growing cerebellar slice cultures, under conditions of low oxygen. Using this model Yuen et al. showed that hypoxia activates Wnt signaling within OPCs that feed back in an autocrine fashion and inhibits OPC maturation. Inhibition of Wnt signaling in this study promoted myelination of slice cultures following hypoxia.

1.7.2 *In vivo* models of DWMI that involve hypoxia

In vivo models aimed at recapitulating the insults and phenotypical outcomes associated with DWMI that involves hypoxia include: the Rice-Vannucci model of rodent neonatal hypoxia and ischemic, rodent neonatal chronic intermittent hypoxia, and rodent neonatal chronic hypoxia. There is no one perfect model of DWMI with each model having strengths and weaknesses that will be discussed.

Neonatal hypoxia and ischemia, was first model in the rat by Rice and Vannucci and has become the most studied model of neonatal WMI. The Rice-Vannucci model is performed by first ligating the common carotid artery in postnatal day 6 to 7 rodent pups, followed by 4-8 hours of rest before exposure to 6-8% hypoxia for 0.5-4 hours (Rice, Vannucci, and Brierley 1981; Y. Shen, Plane, and Deng 2010). This model is widely used, well characterized, and results in gliosis, however, it produces variable lesions with low survival rate and requires considerable surgical skill to achieve success. In addition, the largest caveat to this model is the severity of lesion that it produces. The Rice-Vannucci model results in lesions that are severe and focal and most accurately represent lesions seen in patients with periventricular leukomalacia

(Salmaso et al. 2014). In the clinic this form of injury is decreasing and is no longer the most prevalent presentation, therefore the applicability of the Rice-Vannucci model is debatable.

Chronic intermittent hypoxia has previously been used to model the effects of sleep apnea in adults and has been established relatively recently as a model of DWMI (Cai et al. 2012). Chronic intermittent hypoxia best models infantile apnea, a common morbidity in newborn infants that causes brain damage including DWMI, with incidence of the condition inversely proportional to the maturity at birth (Cai et al. 2012). In fact, approximately 50% of premature infants suffer from infantile apnea and the incidence of infantile apnea in premature infants weighing less than 1000g is almost ubiquitous (Finer et al. 2006). The details of chronic intermittent hypoxia paradigms vary by study, however they all involve brief durations of hypoxic exposure on the order of minutes followed by re-oxygenation that are repeated over a number of hours for 1-2 weeks starting at P1 or P2 (Cai et al. 2012; Juliano et al. 2015). Chronic intermittent hypoxia models result in non-region specific hypomyelination of the brain, with thinner myelin sheaths and electrophysiological and sensorimotor deficits that persist into adult mice (Cai et al. 2012; Juliano et al. 2015). Many of these outcomes mimic the phenotype of DWMI in premature neonates and as such chronic intermittent hypoxia will be a model of significant utility in understanding the mechanism of disease and potential targets for therapy.

Chronic hypoxia during the neonatal period is a clinically relevant model of DWMI that mimics the hypoxic condition caused by underdeveloped lungs and vasculature of the CNS (Scafidi et al. 2014; Scafidi et al. 2009; Watzlawik et al. 2015). The paradigm is achieved by exposing neonatal mice from P3-P11 to 10±0.5% O_2 levels continuously, while control mice are kept at room-air (Fagel et al. 2006). In addition, both control and chronic hypoxia exposed mice are fostered to lactating CD1 female mice due to the fact that C57/Bl6 dams do not care for their

litters under hypoxic conditions (Fagel et al. 2006). This chronic hypoxia model has been well characterized and results in DWMI (Fagel et al. 2006; Scafidi et al. 2014). DWMI in this model is characterized by early transient decrease in levels of myelin enriched proteins, decreased staining for myelin, ventriculomelagy, decrease brain volume, and decreased numbers of mature oligodendrocytes without effecting total oligodendrocyte lineage cell numbers suggesting arrested maturation of OPCs (Scafidi et al. 2014; Yuen et al. 2014). These initial signs of DWMI recover by P60, however, similar to disrupted microstructure in human patients, mice exposed to chronic hypoxia have thinner myelin sheaths as adults compared to controls, which leads to deficits in sensorimotor behavior (Scafidi et al. 2014). Because this model is easy to implement and produces consistent DWMI that more closely mimics the most prevalent form of neurological injury in today's premature population, chronic hypoxia is becoming an increasingly popular model and has already been utilized in two important studies that point to potential mechanisms and therapeutic targets for DWMI (Scafidi et al. 2014; Yuen et al. 2014). Using the chronic hypoxia model Scafidi et al. demonstrated that endothelial growth factor (EGF) signaling plays a role in DWMI and that increasing EGF signaling by either overexpression of EGF receptor or administration of EGF protects oligodendrocytes and myelin, and promotes recovery from chronic hypoxia induced DWMI. Moreover, the Rowitch group has used the chronic hypoxia model to demonstrate that high-Wnt signaling tone, caused by chronic hypoxia, inhibits maturation of OPCs suggesting that targeted inhibition of Wnt signaling might protect OPCs from chronic hypoxia or promote recovery of oligodendrocytes and myelin following chronic hypoxia (Fancy et al. 2014; Yuen et al. 2014; Fancy et al. 2011).

1.8 The ISR and hypoxia

As previously mentioned hypoxia is a well-known activator of the ISR, and specifically of PERK. Hypoxia has been shown to increase peIF2α levels in a time and oxygen-dependent manner suggesting that cells may sense the severity of a hypoxic insult in part via the ISR (Koumenis et al. 2002). However, most work to date has focused on the role of the PERK arm of the ISR in tumor hypoxia where hypoxic insults are severe at less than 0.05% O_2 while in the mammalian brain interstitial oxygen levels range from 1-5% (Silver and Erecińska 1998; Koumenis et al. 2007; Sharp and Bernaudin 2004). Still, moderate hypoxia at 0.7-1.0% O_2 has been shown to increase levels of peIF2α in cell lines in a PERK dependent manner, although more slowly and to a lesser extent compared to anoxia or less than 0.1% O_2 (Y. Liu et al. 2010; Koumenis et al. 2002). In addition, studies have demonstrated that mouse embryonic fibroblasts (MEF) lacking PERK are more susceptible to both severe and mild hypoxia showing that PERK protects these cells under hypoxic conditions (Koumenis et al. 2002; Y. Liu et al. 2010). Other eIF2α kinases may also play a role in ISR activation caused by hypoxia, although they are not as well established as PERK. For example, removal of another eIF2α kinase GCN2 increases the susceptibility of MEFs to mild hypoxia (Y. Liu et al. 2010).

PERK dependent increases in levels of ATF4 protein and induction of ATF4 target genes has also been reported under severe hypoxic conditions of less than 0.01% O_2 (Blais et al. 2004; Rzymski et al. 2010). However, activation of ATF4 under moderate and mild hypoxia is more complex. In cancer cell lines ATF4 protein is not increased under moderate and mild hypoxia, while in mice treated with mild 10% O_2 ATF4 protein levels are increased in the liver along with induction of ATF4 target genes CHOP and GADD34 (Zhu et al. 2013; Ameri et al. 2004; Tagliavacca et al. 2012). In addition, ATF4 and its downstream target CHOP are both increased

at the protein level in neuronal cultures exposed to moderate hypoxia of 0.5% O_2 (Halterman et al. 2010). These differences in the effect of hypoxia on ATF4 levels suggest that while phosphorylation of eIF2α is a ubiquitous response to hypoxia, ATF4 induction is dependent on tissue, time, and severity of hypoxia exposure. This may be controlled by hypoxia-inducible factor 1-alpha (HIF1α). HIF1α is the master regulator of the adaptive response to hypoxia and it has been shown in cardiomyocytes that HIF1α negatively regulates expression of ATF4 and ATF4 targets (Guimarães-Camboa et al. 2015). This leads to an intriguing possibility that under moderate and mild hypoxia when HIF1α activity is at its highest ATF4 is repressed, potentially to avoid redundant induction of stress response genes. Nonetheless, the story of ATF4, and therefore downstream components of the ISR, in hypoxia is complex and requires further study.

1.9 The potential role of the ISR in DWMI

DWMI has a complex and varied etiology that involves hypoxic and/or ischemic damage to OPCs that causes DWMI and leads to behavioral, sensorimotor, and cognitive deficits. This disorder effects a growing population of premature infants and currently there are no approved therapies to treat DWMI. Because of this a better understanding of the pathophysiology of DWMI is crucial as a better understanding of the disease will ultimately lead to potential therapeutics. The ISR is a conserved stress response pathway that is activated by a variety of insults including, and most importantly for this work hypoxia. In addition, targeting the ISR can affect the outcome in a number of complex disorders of myelinating glia. This includes exacerbating disease in the case of ISR inhibition via deletion of the eIF2α kinase PERK, and ameliorating disease by enhancing the ISR via inhibition of GADD34 that in concert with PP1 dephosphorylates eIF2α and terminates the ISR. Given the important role the ISR, and

specifically the PERK pathway, plays in disorders of myelinating glia and that DWMI is caused by hypoxia, a known activator of the ISR via PERK, the question of whether the ISR via PERK plays a role in DWMI is important. Determining the role of the ISR in DWMI will give us a better understanding of the pathogenesis of this disorder, and it would also present the possibility for novel therapeutic targets to treat a disease that is growing in prevalence and at this point has no treatments.

This dissertation will address the hypothesis that: *The PERK arm of the ISR plays an active role in hypoxia induced DWMI and that inhibition of this pathway will exacerbate DWMI while enhancement of the PERK pathway will protect oligodendrocytes and myelin from hypoxia induced DWMI.*

Chapter 2. The integrated stress response in hypoxia induced diffuse white matter injury.

2.1 Abstract

There are currently no available treatments for preterm infants with diffuse white matter injury (DWMI) caused by hypoxia, a condition that results in neurodevelopmental deficits. Due to improved care of preterm neonates, the prevalence of DWMI is also increasing. A better understanding of the pathophysiology of DWMI and resulting novel therapeutic targets is therefore of critical importance. The integrated stress response (ISR), a highly conserved eukaryotic response to myriad stressors, has been shown to provide protection to oligodendrocytes and importantly is known to be activated by hypoxia. These findings indicate a potential role for the ISR in hypoxia-induced DWMI and may represent a target for much needed therapies. In this study we utilize *in vitro* and *in vivo* hypoxic models of DWMI to investigate whether the ISR is involved in DWMI. We demonstrate that *in vitro* hypoxia activates the ISR in primary OPCs and that genetically inhibiting the ISR in differentiating OPCs increases their susceptibility to *in vitro* hypoxia. We further show that a well-established *in vivo* mild chronic hypoxia (MCH) model of DWMI activates part of the ISR. Nonetheless, genetic inhibition of the ISR has no significant effect on MCH-induced DWMI, and moreover, genetic enhancement of the ISR exacerbates the negative effects of MCH. In addition, we establish a new severe acute hypoxia (SAH) model of DWMI and demonstrate that similar to MCH, SAH activates part of the ISR, although neither genetic inhibition nor genetic enhancement of the ISR appear to have a significant effect on SAH-induced DWMI. These studies suggest that while the ISR protects OPCs from hypoxia *in vitro*, it does not appear play a major role in the response to either MCH

or SAH-induced WMI and is therefore not a valid target for therapies aimed at improving neurological outcome in preterm neonates with hypoxia-induced DWMI.

2.2 Introduction

Diffuse white matter injury (DWMI), also known as periventricular leukomalacia or encephalopathy of prematurity, is a white matter disorder affecting low birth weight premature infants born between 23 and 32 weeks of gestation. Importantly, with improved care of premature neonates, the prevalence of DWMI is increasing as more low birth weight premature infants survive, approximately half of which manifest cognitive and learning disabilities by school age (Wilson-Costello et al. 2005; Back 2015; Deng 2010). Although the cellular and molecular mechanisms that cause DWMI are unknown, hypoxia, caused by underdeveloped neural vasculature and inefficient oxygenation from immature lungs, is known to play a major role (Volpe 2001; Volpe 2009; Scafidi et al. 2014). These hypoxic insults damage oligodendrocyte progenitor cells (OPCs), first causing death of OPCs and then inhibiting the maturation of replenishing OPCs, leading to decreased white matter (Back and Miller 2014). Currently there are no approved therapies for DWMI.

Hypoxia is also a known activator of the integrated stress response (ISR) (Koumenis et al. 2002). The ISR is a highly conserved eukaryotic response to a number of stressors. The ISR is activated by one of four stress-sensing kinases that phosphorylate the α subunit of eukaryotic translation initiation factor 2 alpha (eIF2α). Phosphorylation of eIF2α has been shown to occur in cells exposed to severe and mild hypoxia (Koumenis et al. 2002). Phosphorylated eIF2α (p-eIF2α) decreases global protein translation while increasing the translation efficiency of a subset of mRNAs including that of activating transcription factor 4 (ATF4), which upregulates

cytoprotective gene expression (Donnelly et al. 2013). ATF4 also increases the expression of the transcription factor CAAT enhancer binding protein homologous protein (CHOP; also known as *DDIT3*) (Harding et al. 2003). CHOP then increases growth and arrest DNA-damage 34 (GADD34; also known as protein phosphatase 1 regulatory unit [*PPP1R15A*]) expression, which forms a complex with protein phosphatase 1 (PP1) that dephosphorylates eIF2α (Novoa et al. 2001). In this way GADD34 acts in a negative feedback loop to terminate the ISR and restore global protein translation. The ISR is initially protective by decreasing metabolic load through translation inhibition and increased expression of cytoprotective genes. In the face of unresolved stress, however, CHOP accumulation becomes pro-apoptotic (Li et al. 2014; Marciniak et al. 2004; Zinszner et al. 1998). The ISR, especially via the stress-sensing eIF2α kinase PKR-like endoplasmic reticulum kinase (PERK; also known as eIF2α kinase 3 [*EIF2AK3]*) is protective in multiple disorders of oligodendrocytes and myelin (Clayton and Popko 2016; Hussien, Cavener, and Popko 2014). Importantly, PERK is also thought to be the main kinase responsible for eIF2α phosphorylation in response to hypoxia (Koumenis et al. 2002; Y. Liu et al. 2010; Fels and Koumenis 2006; Donnelly et al. 2013; Wouters et al. 2005). In addition, enhancing the ISR via genetic and pharmacological inhibition of GADD34, which prolongs phosphorylation of eIF2α, protects oligodendrocytes from inflammatory insults (Y. Lin, Huang, et al. 2014; W. Lin et al. 2008; W. Lin et al. 2005; W. Lin et al. 2007; W. Lin et al. 2013; Way et al. 2015). With the known protective role of the ISR and PERK in response to hypoxia and the ability to pharmacologically enhance the ISR to protect oligodendrocytes, the ISR is intriguing as a potential player and novel therapeutic target in DWMI.

2.3 Methods

2.3.1 Generation of OL-PERK-null and GADD34-null mice

All animals were housed under pathogen-free conditions and all animal procedures were approved by the Institutional Animal Care and Use Committees of the University of Chicago. All mice were on a C57BL/6 background and unless otherwise stated male and female mice were used.

OL-PERK-null mice were generated by crossing mice that are homozygous for the floxed *Perk* allele (P. Zhang et al. 2002) with mice that are hemyzigous for a transgene that expresses *Cre* recombinase under the transcriptional control of oligodendrocyte transcription factor 2 (Olig-2) (Schüller et al. 2008). These *Olig2-Cre* mice were kindly provided by Dr. David Rowitch and floxed PERK mice were provided by Dr. Douglas Cavener. Female mice homozygous for the floxed *Perk* allele were mated to mice homozygous for the floxed *Perk* allele and heterozygous for *Olig2-Cre* to generate *Olig2-Cre;Perk FL/FL* ("OL-PERK-null") and littermate controls homozygous for the floxed *Perk* allele but lacking *Cre* expression ("OL-PERK FL"). Recombination efficiency with *Olig2-Cre* mice is reported to be above 90% (Kucharova and Stallcup 2015). To determine the recombination efficiency *Olig2-Cre* mice were crossed to a *ROSA26-YFP* reporter line. Brain tissue was collected and stained for Olig2 and YFP that showed that 79.6±11.6% of Olig2+ cells were also YFP+ (Fig. 2.1A and 2.1B). In addition, oligodendrocytes isolated from OL-PERK-null mice showed a 94.4±1.6% reduction in PERK protein levels (Fig. 2.1C) and were more susceptible to ER stress induced by tunicamycin (Fig. 2.1D).

GADD34-null mice have been previously described (Novoa et al. 2001) and were bred in house. In order to increase the percentage of GADD34-WT and GADD34-null mice for the *in vivo* mild chronic and SAH experiments we undertook the following breeding strategy: female mice heterozygous for the *Gadd34* mutation were bred to either GADD34-WT or homozygous GADD34-null mice. The resulting litters were mixed at birth, and then genotyped and split between control and experimental groups at postnatal day 2 (P2). All mice used for mating were generated from breeding male and female mice heterozygous for the *Gadd34* mutation.

2.3.2 Oligodendrocyte progenitor cell isolation and culture

OPCs were isolated from P5-7 rat and mouse brains following a modified version of the immunopanning protocol first described by Barres et al. (1992) and subsequently improved upon and described elsewhere (Emery and Dugas 2013; Dugas and Emery 2013). Wild-type OPCs were generated from wild-type mice while PERK KO OPCs were generated from OL-PERK-Null mice. Rodent brains were removed and the cerebral cortices isolated and diced. Diced brains were then chemically dissociated at 34°C under 95%O_2/5%CO_2 gas for 60 minutes with papain (200U; Worthington Biochemical). Following chemical dissociation tissue was mechanically dissociated by trituration into a single cell suspension. The single cell suspension was then incubated sequentially on two negative selection plates coated with the antibodies RAN-2 and GC/O1 followed by a positive selection plate coated with the antibody O4. All antibodies came from hybridomal supernatant generated by the University of Chicago Monoclonal Facility. RAN-2 antibody binds astrocytes, allowing their removal from the cell suspension (Bartlett et al. 1981). GC/O1 antibody binds mature oligodendrocytes, removing them from the cell suspension (Sommer and Schachner 1981). Finally, O4 antibody binds OPCs

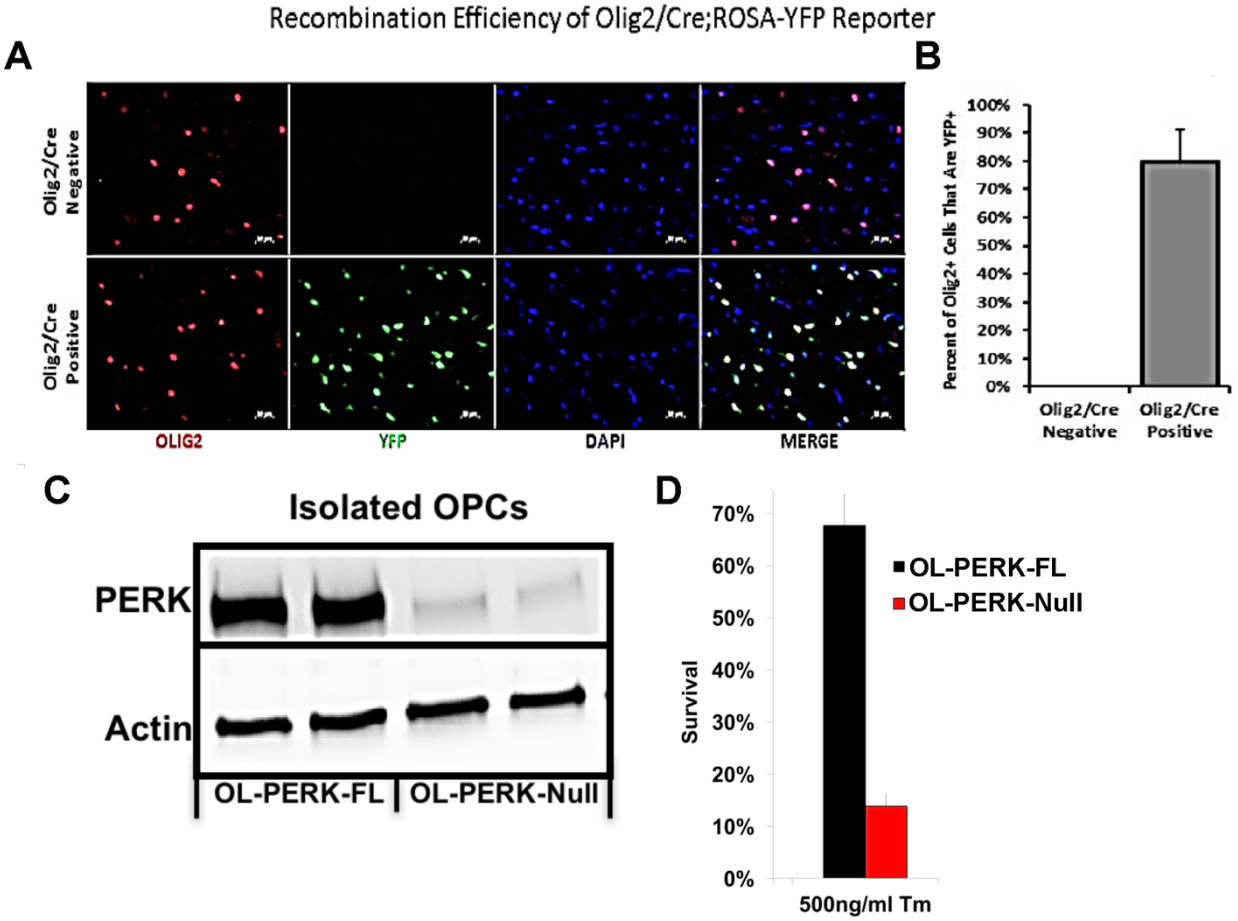

Figure 2.1. Recombination efficiency driven by Olig2/Cre is high and increases susceptibility of cells to ER stress. (a) Representative images of subcortical white matter from Olig2/Cre+ and Olig2/Cre- mice crossed to ROSA-YFP reporter and stained for Olig2 (red) and YFP (green). (b) The percentage of Olig2+ cells that were YFP+ were calculated to determine the recombination efficiency of the Olig2/Cre line. Data represents 3 mice per group. (c) OPCs isolated from P6 OL-PERK-null mice show significantly reduced levels of PERK protein compare to OPCs isolated from littermate OL-PERK-FL controls. (d) OL-PERK-null oligodendrocytes show higher vulnerability to the ER stress inducing chemical tunicamycin (Tm) compared to OL-PERK-FL controls. Data represents 3 independent cultures.

and was used for the positive selection plate (Sommer and Schachner 1981). Rodent OPCs bound to the O4 positive selection plate were treated with trypsin (2.5% Trypsin; Invitrogen) and mechanically blown off the dish, collected and pelleted at 1000xRPM for 15 minutes at room

temperature and finally resuspended in growth media and plated on 10cm culture treated dishes (BD Falcon) coated with poly-d-lysine (0.001mg/ml; Millipore).

OPCs were maintained at 10% CO_2 in a serum-free base growth media consisting of high glucose DMEM (4g/L glucose; Invitrogen) , insulin (5ug/mL; Roche), sodium pyruvate (1mM; Invitrogen), BSA (0.1mg/mL; Sigma), transferrin (0.1mg/mL; Sigma), putrescine (0.016mg/mL; Sigma), progesterone (0.006ug/mL; Sigma), sodium selenite (0.004ug/mL; Sigma), glutamate (2mM; Invitrogen), penicillin/streptomycin (100U/mL penicillin/100ug/mL streptomycin; Invitrogen), biotin (10ng/mL; Sigma), trace elements (1x; Mediatech), n-acetyl-cysteine (5ug/mL; Sigma), forskolin (0.0042mg/mL; Sigma), CNTF (0.01ug/mL; Peprotech), and NT-3 (0.001ug/mL; Peprotech). In addition, mouse OPC cultures were supplemented with B-27 (1x; Invitrogen) to improve survival. In order to maintain cultures in the OPC stage the mitogen PDGFAA (0.01ug/mL; Peprotech) was added to the culture media (Barres et al. 1993). Alternatively, OPCs can be terminally differentiated into mature oligodendrocytes by replacing the mitogen PDGFAA with the thyroid hormone T3 (2ug/mL; Sigma) (Barres, Lazar, and Raff 1994). The above immunopanning and culture protocol produces populations of OPCs from rat or mouse that are >95% pure (Fig. 2.2).

2.3.3 *In vitro* hypoxia

For *in vitro* hypoxia experiments, OPCs isolated from P5-P7 mouse brains were transferred from control proliferation media to identical proliferation media that was equilibrated to 0.1% O_2 for at least 2 hours in a ProOx C21 Biospherix. Cells were then cultured at 0.1% O_2 and 10% CO_2 for various time periods based on the experiment.

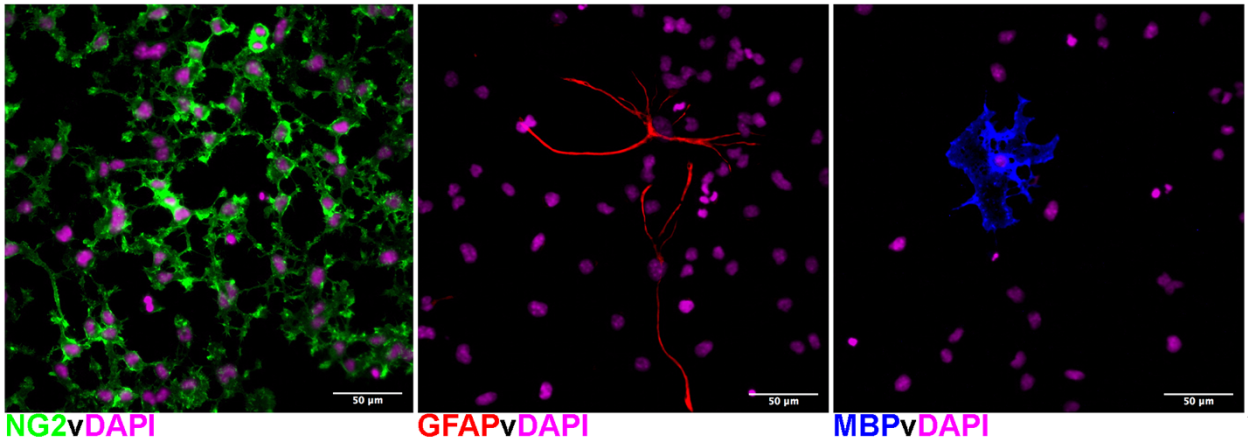

Figure 2.2. Purity of OPC cultures. Representative false color images and results from purity analysis of one OPC isolation. In this OPC isolation 97% of the cells were found to be NG2+ (green) OPCs, while only 2% of cells were GFAP+ (red) astrocytes and 1% of cells were MBP+ (blue) mature oligodendrocytes.

2.3.4 Immunocytochemistry and cell counts

Immediately following 48hrs of differentiation in either 0.1% O_2 or normoxia cells were fixed with ice-cold 4% paraformaldehyde for 15 minutes at room temperature. Cells were then washed with PBS, dried, and stored at -80°C until stained. Cells were blocked with 10% FCS/0.3% Triton in PBS and then incubated overnight in primary antibody in blocking solution. Cells were then washed with PBS, and incubated with AlexaFluor-conjugated secondary antibodies and mounted with Vectashield with DAPI mounting medium. The following primary antibodies were used: 1:250 MBP (808402, BioLegend) and 1:250 Olig2 (MABN50, Millipore). Stained cells were imaged with an Olympus IX81 inverted microscope with a Hamamatsu Orca Flash 4.0 Camera. Five non-overlapping fields of view were taken with a 20x objective and the percentage of Olig2+ cells that were also MBP+ were counted.

2.3.5 *In vivo* MCH and SAH models of DWMI

MCH is a well-described model of DWMI used by many labs and described in multiple publications (Scafidi et al. 2014; Scafidi et al. 2009; Yuen et al. 2014; Fancy et al. 2011). Mouse pups, both male and female, were genotyped and fostered to lactating CD1 dams at P2 and designated for either MCH or room air control (RA). Fostering is required for this protocol since C57BL/6 dams do not care for their litters under hypoxic conditions (Scafidi et al. 2014; Scafidi et al. 2009). At P3 pups assigned to MCH were placed into a Biospherix glove box maintained at 10±0.5% O_2 by displacement with nitrogen and controlled by a ProOx 360 from Biospherix. Pups were exposed to MCH for 8 days from P3-P11 at which point they were returned to room air until the end of the experiment. Room air control mice were also fostered to CD1 dams and kept at room air for the duration of the experiment.

To our knowledge, severe acute hypoxia (SAH) as a model of DWMI has not been previously described. Male and female mouse pups were fostered to lactating CD1 dams at P2 and designated for either SAH or RA control. Fostering was determined to be necessary experimentally. At P3 acute severe hypoxia pups were placed into a Biospherix glove box that was maintained at 7±0.5% O_2 by displacement with nitrogen under the control of a ProOx 360 from Biospherix. Pups were exposed to SAH for 24 hours from P3-P4, after that they were returned to room air until the end of the experiment. The duration of SAH was determined experimentally and was the maximum duration that lactating CD1 foster females could tolerate. Control mice in RA were also fostered to lactating CD1 dams and kept at room air for the duration of the experiment.

2.3.6 Total protein and RNA isolation

Protein was isolated from cells and snap frozen half-brain or frontal cortex rostral to the hippocampus using RIPA lysis buffer (Sigma, R0278) supplemented with protease inhibitor pills (cOmplete mini inhibitor cocktail, Roche, 11836170001), phosphatase inhibitor cocktail 2 (Sigma, P2850), phosphatase inhibitor cocktail 3 (Sigma, P5726), and 17.5mM β-glycerophosphate (Sigma, G9422). Protein lysates were then clarified by centrifugation and stored at -80°C. Protein concentration was determined using a BCA protein assay kit (ThermoScientific Pierce, 23255). The region of the frontal cortex rostral to the hippocampus was isolated to study myelin protein levels because subcortical white matter in this region is known to be susceptible to hypoxia induced DWMI (Fagel et al. 2006; Ment et al. 1998; Scafidi et al. 2014; Jablonska et al. 2012; Yuen et al. 2014). Additionally, this area was also analyzed by immunohistochemistry.

RNA was isolated from cells and snap frozen half-brain using the BioRad Aurum Total RNA Fatty and Fibrous Tissue Kit (BioRad, 732-6830) according to manufacturer's instructions. Total RNA concentration was measured by a NanoDrop (ThermoScientific) spectrophotometer and RNA quality was confirmed on an Agilent 2100 Bioanalyzer using an Agilent 6000 Nano Kit (Agilent Technologies, 5067-1511) according to the manufacturer's instructions. Only samples with an RNA integrity number above 7 were used.

2.3.7 Western blot

Protein extracts were denatured in Laemmli buffer with β-mercaptoethanol, separated by SDS-page and then transferred to nitrocellulose. Membranes were blocked with 5% non-fat milk in TBST and incubated overnight in primary antibody diluted in blocking buffer. Membranes

were then washed and incubated in horseradish peroxidase-conjugated secondary antibody in blocking buffer. Signal was detected by chemiluminescence (SuperSignal West Dura Extended Duration Substrate, Thermo Scientific Pierce, 34076). Western blot images have been cropped. All cropped images are designated by a black border. The following primary antibodies were used: 1:500 peIF2α (Abcam, AB32157), 1:1000 eIF2α (Cell Signaling, 9722S), 1:250 ATF4 (Aviva, ARP37017), 1:250 MAG (Invitrogen, 346200), 1:250 CNP (BioLegend, 836401), 1:1000 MBP (BioLegend, 808402), and 1:2000 actin (Sigma, A2066).

2.3.8 Quantitative real-time PCR

High quality RNA was reverse transcribed using the BioRad iScript cDNA Synthesis kit according to the manufacturer's instructions (BioRad, 1708891) and quantitative real-time polymerase chain reaction (PCR) was run on a BioRad CFX96 Real-Time PCR machine using SYBR Green detection. Results were analyzed using the ΔΔC(t) method with the Pfaffl correction for primer set specific PCR efficiency (Pfaffl 2001) on the BioRad CFX Manager software. RPL13A was used as the reference gene. The efficiency of each primer set was determined by running reactions with known dilutions of cDNA at 60C followed by calculation on the BioRad CFX Manager software. Primers and efficiencies can be found in Table 2.1.

Table 2.1 Primer Sequences and PCR Efficiencies

Gene of Interest	Primers	PCR Efficiency at 60°C
ATF4	Fwd: 5'-TGG ATG ATG GT TGG CCA GTG-3' Rev: 5'-GAG CTC ATC TGG CAT GGT TTC-3'	114.0%
CHOP	Fwd: 5'-CCA CCA CAC CTG AAA GCA GAA-3' Rev: 5'-AGG TGC CCC CAA TTT CAT CT-3'	106.8%
GADD34	Fwd: 5'-CCC TCC AAC TCT CCT TCT TCA G-3' Rev: 5'-CAG CCT CAG CAT TCC GAC AA-3'	87.4%
VEGF	Fwd: 5'-GCC TCC GAA ACC ATG AAC TTT-3' Rev: 5'-TGG GAC CAC TTG GCA TGG T-3'	93.2%
MBP	Fwd: 5'-GCT CCC TGC CCC AGA AGT-3' Rev: 5'-TGT CAC AAT GTT CTT GAA GAA ATG G-3'	102.7%
PLP	Fwd: 5'-CAC TTA CAA CTT CGC CGT CCt-3' Rev: 5'-GGG AGT TTC TAT GGG AGC TCA GA-3'	115.8%
MAG	Fwd: 5'-CTG CTC TGT GGG GCT GAC AG-3' Rev: 5'-AGG TAC AGG CTC TTG GCA ACT G-3'	109.5%
RPL13A	Fwd: 5'-TTC TCC TCC AGA GTG GCT GT-3' Rev: 5'-GGC TGA AGC CTA CCA GAA AG-3'	98.9%

2.3.9 Immunohistochemistry and cell counts

Mice were anaesthetized with 2.5% avertin and then transcardially perfused with 0.9% NaCl followed by cold 4% paraformaldehyde. Following perfusion, the brain was removed and post-fixed in cold 4% paraformaldehyde for 2hrs. Following post-fix brains were cryoprotected by immersion in 15% sucrose at 4°C overnight followed by immersion in 30% sucrose at 4°C overnight. Tissue was then embedded for sagittal sections in optimal temperature cutting compound (OCT), sectioned at 10µm, and then slides were stored at -80°C. Prior to staining sections were air dried and permeabilized at -20°C in acetone. Sections were blocked in 5% FBS/0.1% Triton-X in 1xTBS for an hour at room temperature then incubated overnight at 4°C in primary antibody diluted in blocking buffer. Sections were then incubated in secondary

fluorophore conjugated antibody and mounted with mounting medium containing 4',6-diamidino-2-phenylindole (DAPI) (Vectashield, H-1200). The following primary antibodies were used: 1:250 MBP (Biolegend, 808402), 1:50 Olig2 (Millipore, AB9610), and 1:50 CC1 (Calbiochem, OP80).

Images were acquired on an Olympus IX81 inverted microscope with a Hamamatsu Orca Flash 4.0 Camera. Images were acquired from the subcortical white matter in the frontal cortex rostral to the hippocampus and of anatomically similar sections. Approximately 100 Olig2+ cells were counted per mouse to calculate the percentage of CC1+/Olig2+ cells.

2.3.10 Statistics

Data are presented as mean±sem unless otherwise noted. Multiple comparisons were made using ANOVA with Tukey's post-test. Comparisons of two data points were made by a two-sided unpaired *t*-test. A P value of <0.05 was considered significant and all statistical analysis was run with GraphPad Prism software.

2.4 Results

2.4.1. Hypoxic activation of the ISR in isolated primary OPCs is partially PERK dependent

It has been shown in cell lines that *in vitro* hypoxia activates the ISR as indicated by increased phosphorylation of eIF2α (Koumenis et al. 2007). Nonetheless, whether hypoxia increases phosphorylation of eIF2α in primary OPCs *in vitro* has not been investigated. In addition, PERK has been shown to phosphorylate eIF2α in response to hypoxia, since PERK knockout mouse embryonic fibroblasts (MEFs) have decreased phosphorylation of eIF2α in

response to hypoxia compared to control wild-type MEFs (Koumenis et al. 2002; Blais et al. 2006; Y. Liu et al. 2010). Whether this role for PERK holds true in primary OPCs is not known. To investigate whether *in vitro* hypoxia increases phosphorylation of eIF2α and whether PERK plays a role in this activation we exposed primary isolated mouse OPCs to 0.1% O_2 for 0, 3, and 6hrs. Following hypoxic exposure levels of peIF2α were measured. We found that exposure of wild-type OPCs to 3 and 6hrs of hypoxia resulted in significantly increased levels of phosphorylated eIF2α compared to wild-type OPCs exposed to 0hr hypoxia (Fig. 2.3A and 2.3B). Moreover, when compared to time-matched PERK knockout OPCs, we found that wild-type OPCs had significantly higher peIF2α levels at 3 and 6hrs (Fig. 2.3A and 2.3B). This showed that hypoxia increases phosphorylated eIF2α in isolated OPCs and that PERK plays a role in these increased levels of peIF2α. However, although the majority of hypoxia-induced peIF2α expression is blocked in PERK KO OPCs, when compared to PERK KO OPCs exposed to 0hrs of hypoxia, PERK KO OPCs after 3 and 6hrs of hypoxia still had significantly higher levels of peIF2α (Fig. 2.3A and 2.3B). This suggests that PERK is not the sole kinase responsible for phosphorylating eIF2α in response to hypoxia.

We also examined levels of ATF4 protein in wild-type OPCs exposed to 0.1% O_2 and found that although there is increased phosphorylation of eIF2α in these cells there is no significant difference in ATF4 protein levels (Fig. 2.3C and 2.3D). These results show that *in vitro* hypoxia activates the ISR evident by increased phosphorylation of eIF2α, but without the corresponding increase in ATF4.

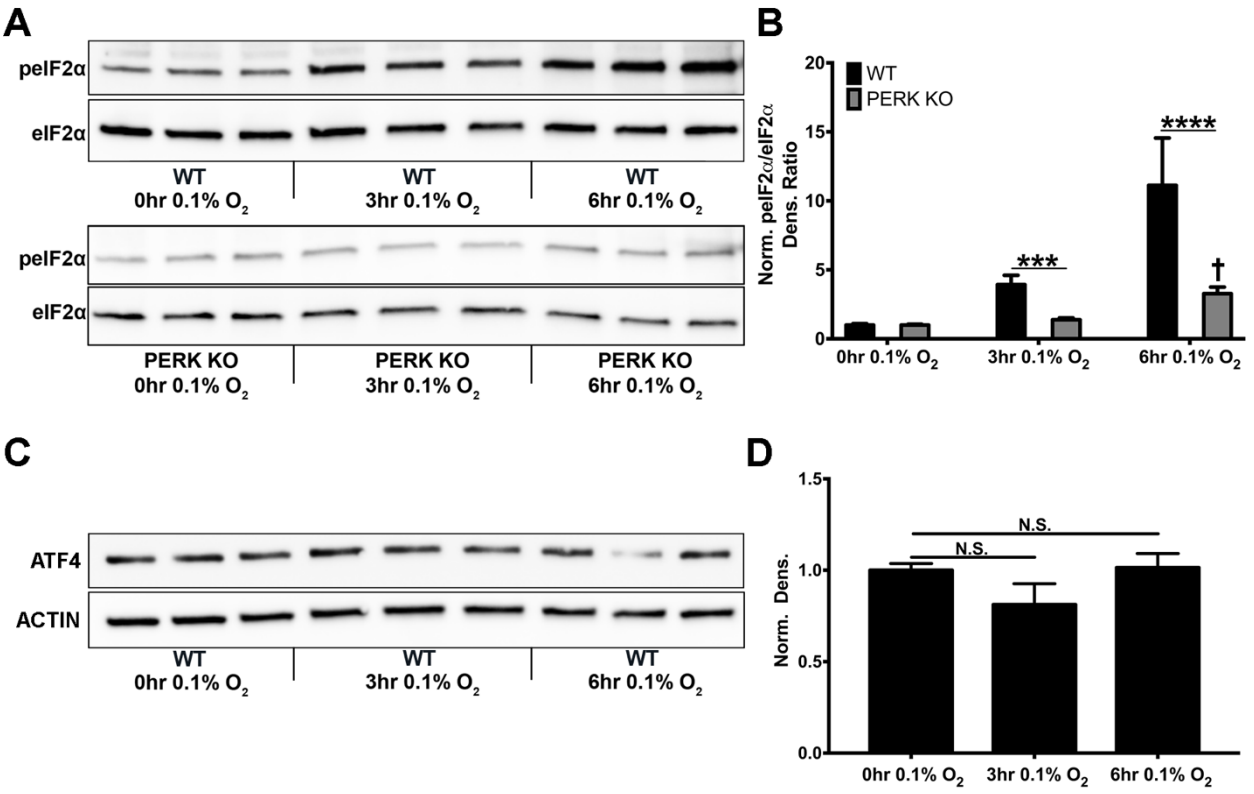

Figure 2.3. Hypoxia increases peIF2α in a PERK dependent manner but does not increase ATF4 protein levels in isolated primary OPCs. (a) Representative peIF2α/eIF2α blots of WT and PERK KO OPCs exposed to 0.1% O_2 for 0,3, or 6hrs. (b) Ratio of peIF2α/eIF2α normalized to 0hr strain matched controls for WT and PERK KO OPCs exposed to 0.1% O_2. (c) Representative ATF4 and Actin blots of WT exposed to 0.1% O_2 for 0,3, or 6hrs. (d) Densitometry of ATF4 normalized to 0hr control. Data presented as mean±sem for 3 independent cultures with 3 replicates each. ***P<0.005 and ****P<0.0001 by unpaired two-tailed *t*-test. †P<0.05 by ANOVA w/Tukey's post-test compared to PERK KO OPCs exposed to 0hrs of 0.1% O_2.

To determine whether the diminished capacity of PERK KO OPCs to phosphorylate eIF2α in response to hypoxia results in an enhanced susceptibility to hypoxia we exposed differentiating wild-type and PERK KO OPCs to 0.1% O_2 for 48hrs during differentiation. Hypoxia has been shown to inhibit differentiation of OPCs *in vitro* (Yuen et al. 2014). We found that as previously reported differentiating OPCs exposed to hypoxia during differentiation have a decrease in the percentage of MBP+ mature oligodendrocytes compared to cells differentiated

under normoxic conditions (Fig. 2.4A and 2.4B). In addition, we discovered that PERK KO cells were more vulnerable to *in vitro* hypoxia during differentiation and displayed significantly fewer MBP+ cells compared to wild-type cells exposed to hypoxia (Fig. 2.4A and 2.4B). This shows that, as expected given the protective role of the ISR, inhibition of ISR activation via PERK leads to an increased susceptibility of OPCs to hypoxia.

2.4.2 MCH causes DWMI in neonatal mice.

Brain injury from chronic hypoxia caused by immature lung development can be modeled by MCH in neonatal mice (Scafidi et al. 2009). To confirm that mice were experiencing hypoxia in this model we measured expression of the hypoxic response gene vascular endothelial growth factor (VEGF) and found that 4d of MCH significantly increased VEGF expression (Fig. 2.5A). We then examined the brains of MCH exposed mice to validate that MCH causes DWMI. MCH led to decreased expression of myelin enriched transcripts myelin-associated glycoprotein (MAG), proteolipid protein (PLP), and myelin basic protein (MBP) (Fig. 2.5B). Exposure to MCH also caused decreased MBP immunostaining and decreased numbers of mature CC1+ oligodendrocytes in the subcortical white matter (Fig. 2.6A and 2.6B). Importantly, the total number of oligodendrocyte lineage cells, marked by oligodendrocyte transcription factor (OLIG-2), was not significantly altered, suggesting that MCH caused decreased maturation of OPCs into mature CC1+ oligodendrocytes (Fig. 2.6B). In addition, MCH led to decreased levels of the mature myelin specific proteins (MAG), 2',3'-Cyclic-nucleotide 3'- phosphodiesterase (CNP), and MBP (Fig. 2.6C and 2.6D). This shows that as previously described, MCH is a valid model of DWMI.

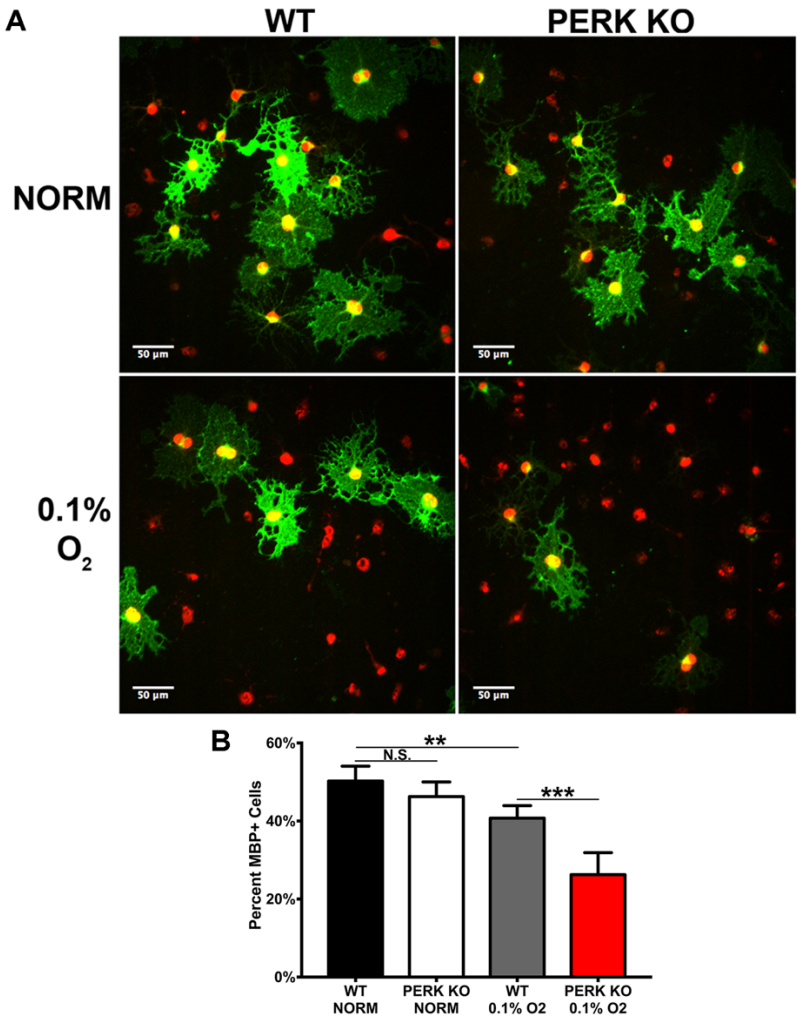

Figure 2.4. Oligodendrocyte specific *Perk* deletion sensitizes differentiating OPCs to hypoxia. (a) Representative images of WT and PERK KO OPCs differentiated for 48hrs under normoxia (NORM) or 0.1% O_2 and stained for the mature oligodendrocyte marker MBP (green) and the pan-oligodendrocyte lineage cell marker Olig2 (red). (e) Quantification of the percent MBP+ cells in panel d. Data represents four repeat experiments with ***P<0.005 and **P<0.01 by ANOVA with Tukey's post-test. All

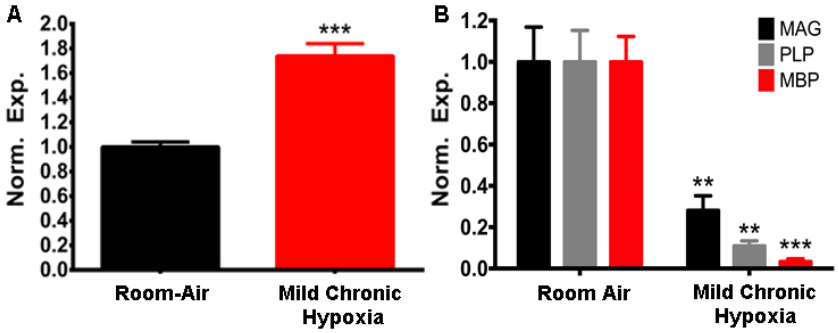

Figure 2.5 Mild Chronic hypoxia increases expression of VEGF and decreases expression of myelin transcripts. (a)Expression of the hypoxic response gene VEGF is increased in P7 mice by 4 days of mild chronic hypoxia. (b) Myelin transcripts MAG, PLP, and MBP are decreased in brain from P11 mice exposed to mild chronic hypoxia. Data presented as mean±sem for N=3-4, **P<0.01 and ***P<0.005 compared to room air control by unpaired two-tailed *t*-test.

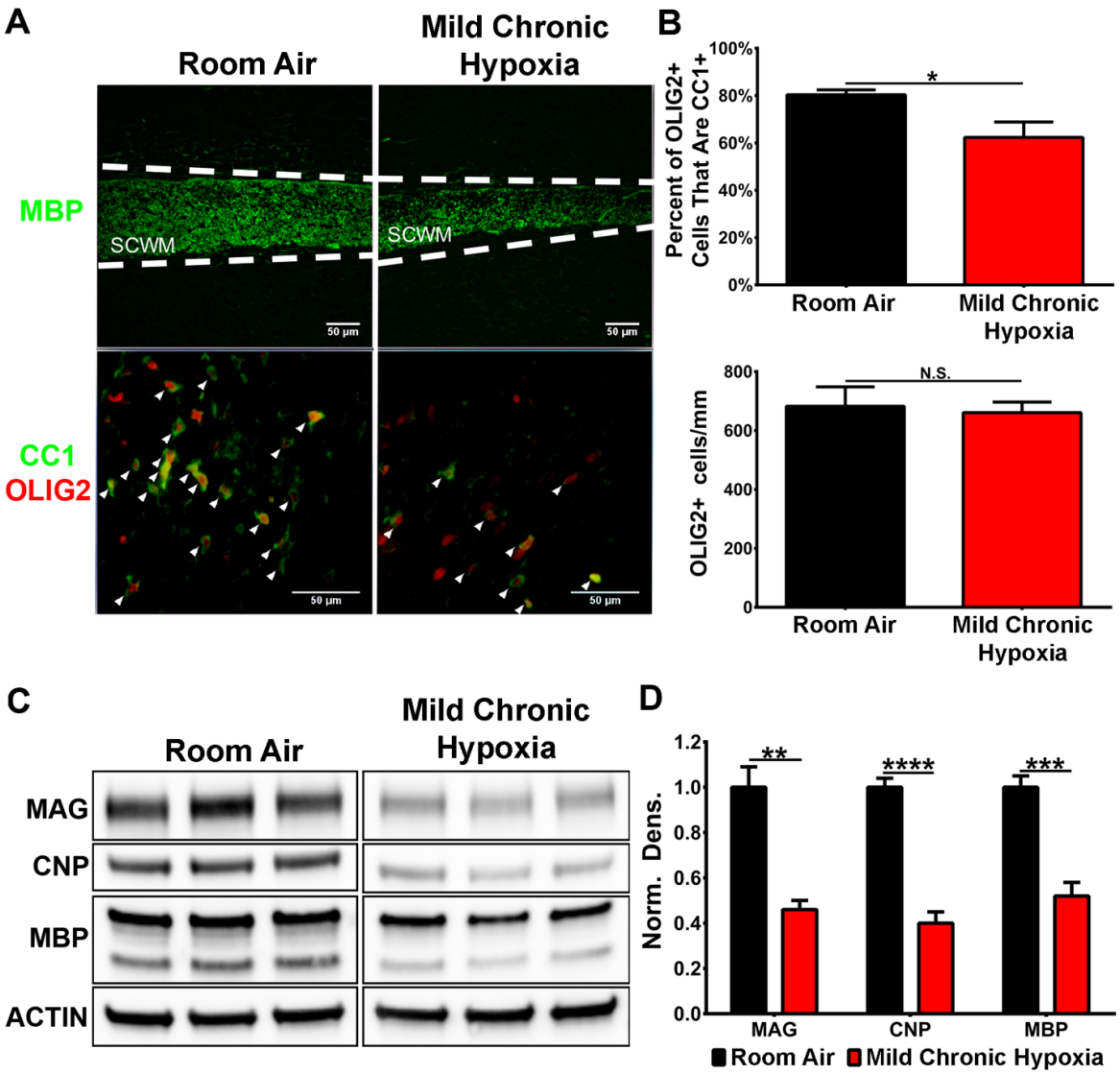

Figure 2.6. Mild chronic hypoxia causes diffuse white matter injury. (a) Top panels are representative images of MBP- (green) stained subcortical white matter (SCWM) from P18 mice exposed to mild chronic hypoxia or room air control. Bottom panels are representative images of mature CC1+ (green) oligodendrocytes and Olig2+ (red) oligodendrocyte lineage cells from P18. ((b) Quantification of the percent of Olig2+ oligodendrocyte lineage cells that are CC1+ mature oligodendrocytes and density of Olig2+ oligodendrocyte lineage cells in P18 mild chronic hypoxia and room air exposed mice. Data represents N≥3 mice per group with *P<0.05 by unpaired two-tailed *t*-test. (c) Representative blots of myelin-enriched proteins MAG, CNP, and MBP from P18 mice exposed to mild chronic hypoxia or room air. (d) Quantification of MAG, CNP, and MBP protein levels. Data represents N≥3 mice per group with **P<0.01, ***P<0.005, and ****P<0.0001 by unpaired two-tailed *t*-test. All data presented as mean±sem and scale bar equals 50µm.

2.4.3 MCH increases phosphorylation of eIF2α in brain

As shown *in vitro*, hypoxia increases phosphorylation of eIF2α that is indicative of activation of the ISR. To determine whether *in vivo* MCH activates the ISR in neonatal mouse brains we collected brain tissue at various time points throughout the MCH exposure. We found that at 4 and 6 days of MCH, levels of peIF2α were significantly higher compared to age-matched room air controls (Fig. 2.7A and 2.7B). Surprisingly however, increased phosphorylation of eIF2α was not accompanied by an increase in ATF4 protein levels. Instead, ATF4 protein levels were significantly decreased compared to age-matched room air controls (Fig. 2.7A and 2.7B). In agreement, we saw no evidence of CHOP and GADD34 induction (Fig. 2.7C), both components of the ISR that are activated by ATF4. Our results suggest that while increased phosphorylation of eIF2α in the brain is a consequence of hypoxia, the transcriptional response of the ISR through ATF4 does not appear to play a role.

As mentioned the PERK pathway plays a role in both the ISR and the UPR and phosphorylation of eIF2α occurs in both stress response pathways. Consequently, when studying the PERK pathway it is important to determine whether increased peIF2α is occurring with, or independent of, activation of the unfolded protein response. This can be done by examining the activation status of one of the other two arms of the unfolded protein response, the IRE1 arm and ATF6 arm. To determine whether phosphorylation of eIF2α in MCH is occurring in concert with activation of the UPR or independently as a component of the ISR we measured XBP1 splicing and in brains exposed to either MCH or RA control. MCH did not induce splicing of XBP1 at any time point suggesting that the IRE1 arm of the UPR is not activated and that MCH is not causing ER stress in neonatal brain (Fig. 2.8).

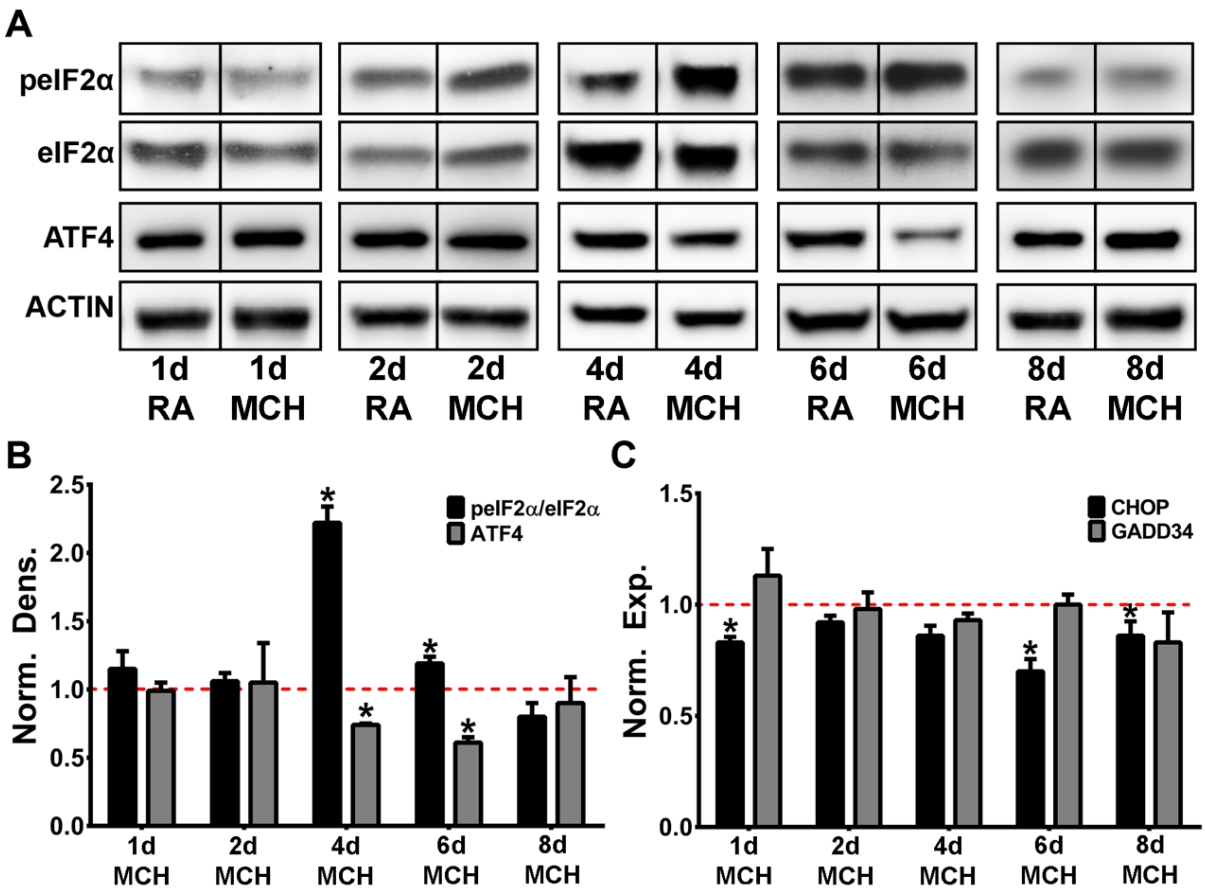

Figure 2.7. Mild chronic hypoxia increases phosphorylation of eIF2α, but decreases ATF4 protein levels and does not induce CHOP and GADD34 expression. (a) Representative peIF2α, eIF2α, and ATF4 blots from mice exposed to either 1, 2, 4, 6, or 8d of mild chronic hypoxia (MCH) or room air control (RA). (b) Quantification of peIF2α, eIF2α, and ATF4 protein levels. Data presented as peIF2α/eIF2α ratio normalized to time-matched RA-exposed control mice. Data represents N≥3 mice per group with *P<0.05 compared to time-matched control (red dashed line) by unpaired two-tailed *t*-test. (c) Expression of CHOP and GADD34 mRNA levels normalized to time-matched RA-exposed controls. Data represents N≥3 mice per group with *P<0.05 compared to time-matched control (red dashed line) by unpaired two-tailed *t*-test.

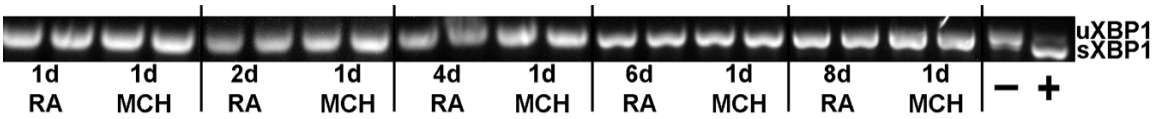

Figure 2.8. Mild chronic hypoxia does not lead to XBP1 splicing. XBP1 splicing was measured by PCR as a marker of activation of the IRE1 arm of the unfolded protein response. There is no evidence that mild chronic hypoxia (MCH) leads to production of spliced XBP1 (sXBP1), as evident by no shift from the unspliced XBP1 (uXBP1) band size in MCH samples compared to room air controls (RA). Compared to the clear shift in the XBP1 band when cells are exposed to the known ER stressor tunicamycin (+) compared to untreated (-) cells.

2.4.4 Genetic manipulation of the ISR and MCH-induced DWMI

Manipulation of the ISR has proven to be a valid strategy for protecting oligodendrocytes in mouse models of myelin disorders (Clayton and Popko 2016). To determine whether genetic manipulation of the ISR affects MCH-induced DWMI, we took advantage of OL-PERK-null and GADD34-null mice, two genetic mouse lines that are deficient in different ISR components and allow us to study the effects of diminishing or enhancing the pathway. Importantly, neither of these lines show any disruption in developmental myelination (Fig. 2.9). OL-PERK-null mice have PERK deleted specifically from oligodendrocyte lineage cells and therefore makes these cells incapable of activation the ISR in response to stress that targets PERK. Given the protective nature of the ISR, and specifically PERK, in oligodendrocyte lineage cells subject to stress (Hussien, Cavener, and Popko 2014) we would predict that inhibition of the ISR in OL-PERK-null mice would exacerbate MCH-induced DWMI. In contrast GADD34-null mice have a global mutation in GADD34 that makes it nonfunctional and unable to dephosphorylate eIF2α prolonging the ISR (Novoa et al. 2001). Again given the protective nature of the ISR and that inhibition of GADD34 has proven to protect oligodendrocyte lineage cells from other stresses (Way et al. 2015), we would predict that enhancement of the ISR in GADD34-null mice would ameliorate MCH-induced DWMI.

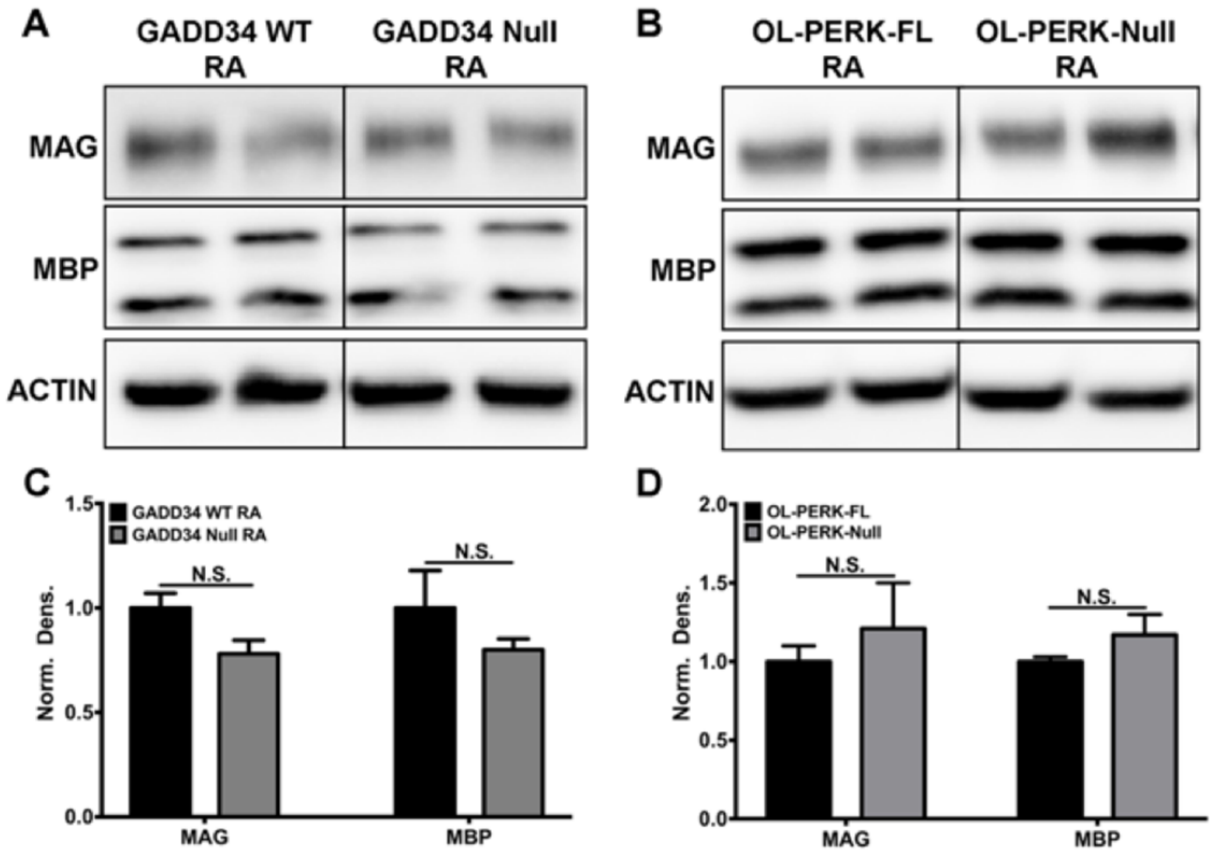

Figure 2.9 Neither oligodendrocyte-specific *Perk* deletion nor global GADD34 deletion has an effect on developmental myelination. (a,b) Representative blots of MAG and MBP protein levels in P18 GADD34 WT and GADD34-Null mice (a), and P18 OL-PERK-FL and OL-PERK-Null mice (b). (c,d) Quantification of MAG and MBP protein levels in P18 GADD34 WT and GADD34-Null mice (c), and P18 OL-PERK-FL and OL-PERK-Null mice (d). Data represents N≥3 mice per group. Data presented as mean±sem.

To determine whether oligodendrocyte-specific deletion of PERK exacerbated MCH-induced DWMI, we exposed OL-PERK-FL and OL-PERK-null mice to MCH. Again, *Perk* deletion from oligodendrocyte lineage cells was expected to be protective because of the known protective role of PERK in other cells, and because of the *in vitro* results where PERK KO OPCs were more susceptible to hypoxia (Fig. 2.4). Surprisingly though, we found that compared to OL-PERK-FL control mice exposed to MCH, OL-PERK-null mice exposed to MCH showed no

significant difference in expression levels of myelin-specific proteins MAG, CNP, and MBP (Fig. 2.10A and 2.10B). This was confirmed by immunostaining for MBP in the subcortical white matter where there was no difference in the level of MBP staining between OL-PERK-FL controls and OL-PERK-null mice challenged with MCH (Fig. 2.10C). Moreover, there was no difference between groups of MCH expose mice when the percentage of mature oligodendrocytes stained with CC1+ was analyzed (Fig. 2.10C and 2.10D). This shows that even though PERK protects OPCs from *in vitro* hypoxia, PERK signaling within oligodendrocytes lineage cells does not play a protective role in the *in vivo* MCH model of DWMI.

Inhibition of GADD34 both genetically and pharmacologically has been shown to protect oligodendrocytes from *in vitro* treatment with the inflammatory cytokine IFN-gamma and in mouse models of multiple sclerosis (Way et al. 2015). To test whether GADD34 inhibition protects oligodendrocytes and white matter from MCH-induced DWMI, we exposed GADD34-WT and GADD34-null mice to MCH. While we would predict that GADD34-null mice would be protected from MCH-induced DWMI, we surprisingly found that GADD34-null mice had significantly lower levels of MAG, CNP, and MBP compared to GADD34-WT mice (Fig. 2.11).

In addition to decreased levels of myelin-specific proteins, GADD34-null mice exposed to MCH exhibited decreased body weight and increased mortality compared to MCH-exposed GADD34-WT mice. GADD34-WT mice exposed to MCH weighed 7.8±0.3 grams compared to 5.0±0.3 grams for GADD34-null mice exposed to MCH, and while 85% of GADD34-WT mice survived MCH exposure, only 31% of GADD34-null mice survived. This data raises the possibility that the exacerbated effects of MCH on GADD34-null mice are systemic and not CNS-specific. In support of this interpretation we found no evidence of increased or prolonged phosphorylation of eIF2α in the brain of MCH-exposed GADD34-null mice (Fig. 2.12).

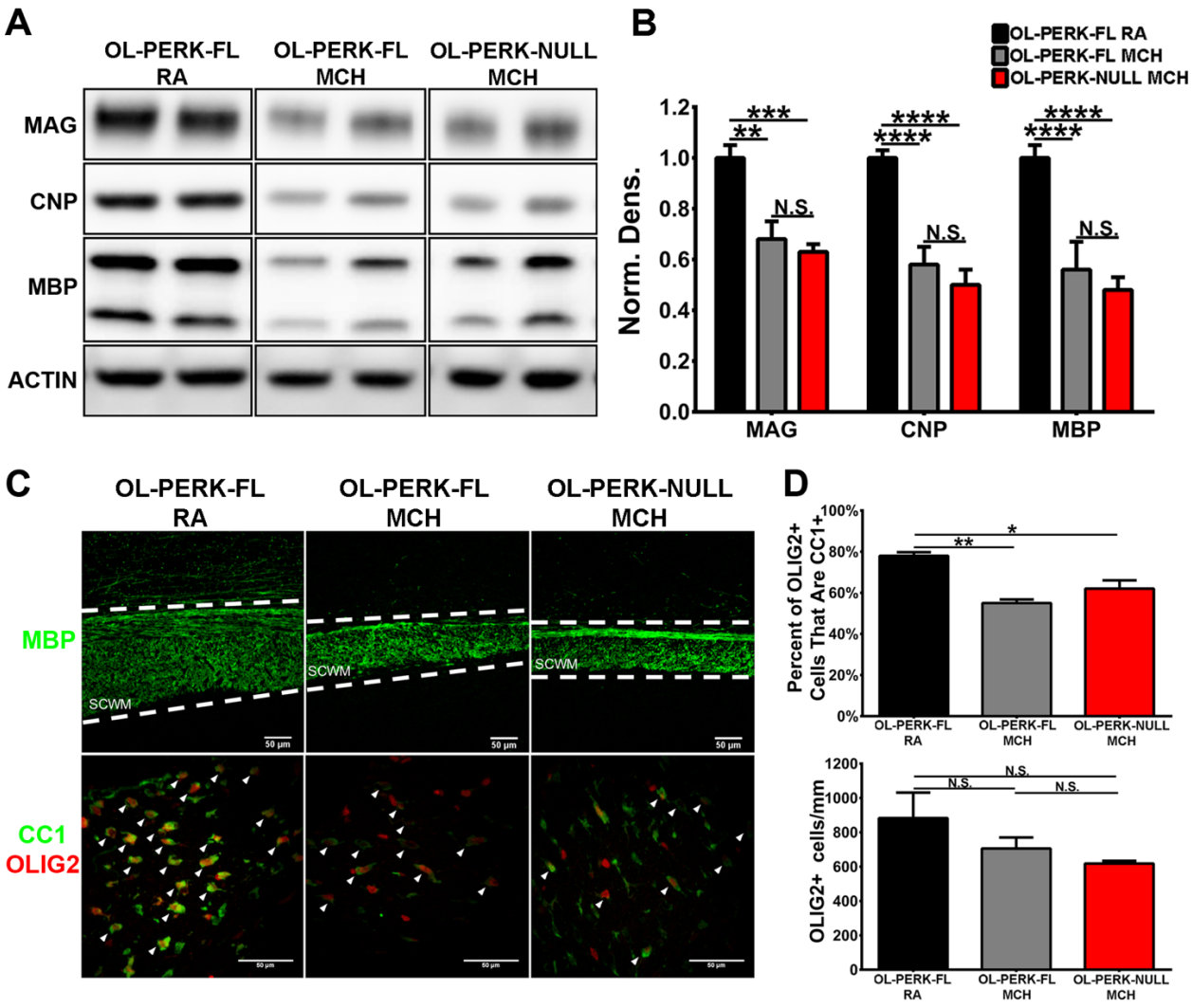

Figure 2.10 Oligodendrocyte-specific deletion of *Perk* has no effect on mild chronic hypoxia-induced diffuse white matter injury. (a) Representative blots of myelin-enriched proteins MAG, CNP, and MBP from P18 OL-PERK-FL and OL-PERK-Null mice exposed to mild chronic hypoxia (MCH) and room-air control (RA). (b) Quantification of MAG, CNP, and MBP protein levels. Data represents N≥3 mice per group with **P<0.01, ***P<0.005, and ****P<0.0001 by ANOVA with Tukey's post-test. (c) Representative images of subcortical white matter (SCWMI) from P18 OL-PERK-FL and OL-PERK-Null mice exposed to MCH and RA and stained with MBP (green, top panels) or CC1 (green, bottom panels) and Olig2 (red, bottom panels). (d) Quantification of the percent of Olig2+ oligodendrocyte lineage cells that are CC1+ mature oligodendrocytes and density of Olig2+ oligodendrocyte lineage cells in P18 OL-PERK-FL and OL-PERK-Null mice exposed to MCH and RA. Data represents N≥3 mice per group with **P<0.01 and *P<0.05 by ANOVA with Tukey's post-test. Data presented as mean±sem and scale bars equals 50µm.

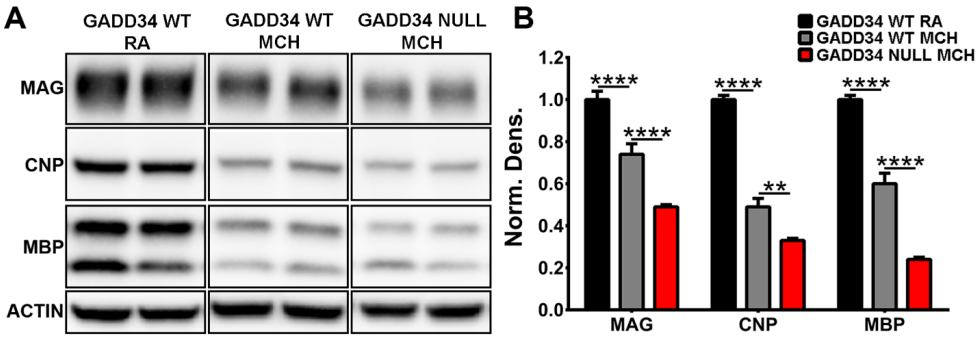

Figure 2.11. Global *Gadd34* deletion exacerbates mild chronic hypoxia-induced diffuse white matter injury. (a) Representative blots of MAG, CNP, and MBP from P18 GADD34 WT and GADD34-Null mild chronic hypoxia (MCH) and room air (RA) exposed mice. (b) Quantification of MAG, CNP, and MBP protein levels from P18 GADD34 WT and GADD34-Null mice exposed to MCH and RA. Data represents N≥3 mice per group with **P<0.01 and ****P<0.0001 by ANOVA with Tukey's post-test. Data presented as mean±sem.

In these same mice we found that MCH increases phosphorylation of eIF2α in the heart of GADD34-WT mice and measured phosphorylation of eIF2α in the hearts of GADD34-null mice to determine whether *Gadd34* deletion was having an effect in non-neuronal tissue. Interestingly, phosphorylation of eIF2α in the heart was increased in MCH exposed GADD34-null mice compared to GADD34-WT mice (Fig. 2.13) showing that *Gadd34* deletion is having the expected effect of prolonging phosphorylation of eIF2α in tissue distinct from the CNS. The lack of a CNS effect in the MCH exposed GADD34-null mice also agrees with absence of GADD34 induction in the CNS of MCH challenged mice (Fig 2.7C).

2.4.5 GADD34-null mice have a diminished hematopoietic response to MCH

Given that *Gadd34* deletion does not prolong or increase levels of peIF2α in brain from MCH exposed pups, it is unlikely that increased susceptibility of GADD34-null animals to MCH is a CNS specific event. Indeed, characterizing a distinct *Gadd34* mutant mouse another group

found that GADD34-null mice exhibit a mild deficit in hemoglobin production under normal conditions (Patterson et al. 2006). This deficit could decrease the ability of GADD34-null mice to mount an adaptive hematopoietic response to hypoxia and could explain why GADD34-null mice have worse outcomes when exposed to MCH compared to controls. To test this possibility, blood samples were collected from P7 GADD34 WT and GADD34-null mice exposed to 4 days of MCH and submitted the blood samples to IDEXX laboratories (IDEXX, Maine US) for a complete blood count. We found that, compared to GADD34 WT mice, GADD34-null pups have an apparent deficit in their hematopoietic response to MCH (Fig. 2.14). This included lower red blood cell concentration and hematocrit (Fig 2.14A and 2.14B) as well as, decreased total blood hemoglobin concentration and decreased mean corpuscular hemoglobin. Although further experiments are needed, these findings provide a potential mechanistic explanation for why GADD34-null mice are more vulnerable to MCH.

2.4.6 Severe acute hypoxia (SAH) an alternative model of DWMI

Premature neonates are also exposed to brief episodes of severe hypoxia (Martin et al. 2011). Since oligodendrocyte-specific *Perk* ablation had no significant effect on MCH-induced DWMI, and given that global deletion of GADD34 increased the deleterious effects of this chronic insult, we examined the role of the ISR in a severe acute hypoxic (SAH) model of DWMI to determine whether the ISR is better equipped for acute hypoxic stress. In order to address this question, we first had to determine whether SAH leads to DWMI in neonatal mice similar to the well-established MCH model. Therefore, we exposed neonatal mice to 7±0.5% O_2 for 24hrs from P3-P4. Similar to the MCH model, SAH led to increased expression of VEGF and decreased expression of myelin transcripts PLP and MBP (Fig. 2.15).

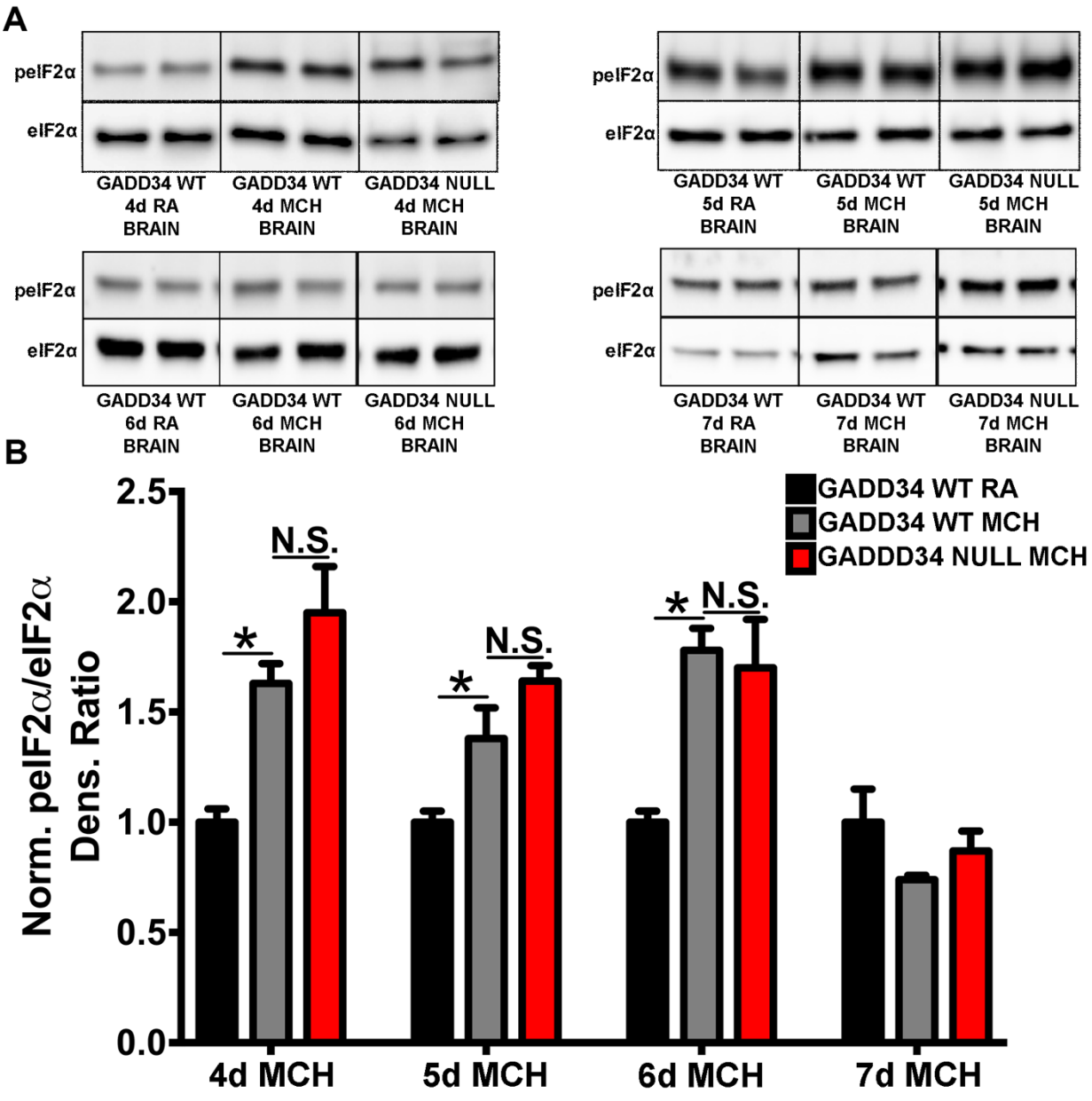

Figure 2.12 *Gadd34* deletion does not increase or prolong phosphorylation of eIF2α in mild chronic hypoxia exposed brain. (a) Representative blots of peIf2α and eIF2α in brain lysate from GADD34 WT and GADD34-Null mice exposed to either 4, 5, 6, or 7d of mild chronic hypoxia (MCH) or room-air (RA). (b) Quantification of peIF2α and eIF2α protein levels in brain lysate from GADD34 WT and GADD34-Null mice exposed to either 4, 5, 6, or 7d of MCH or RA. Data represents N≥3 mice per group and presented as peIF2α/eIF2α ratio normalized to time-matched GADD34 WT RA exposed control mice, with *P<0.05 by ANOVA with Tukey's post-test. Data presented as mean±sem.

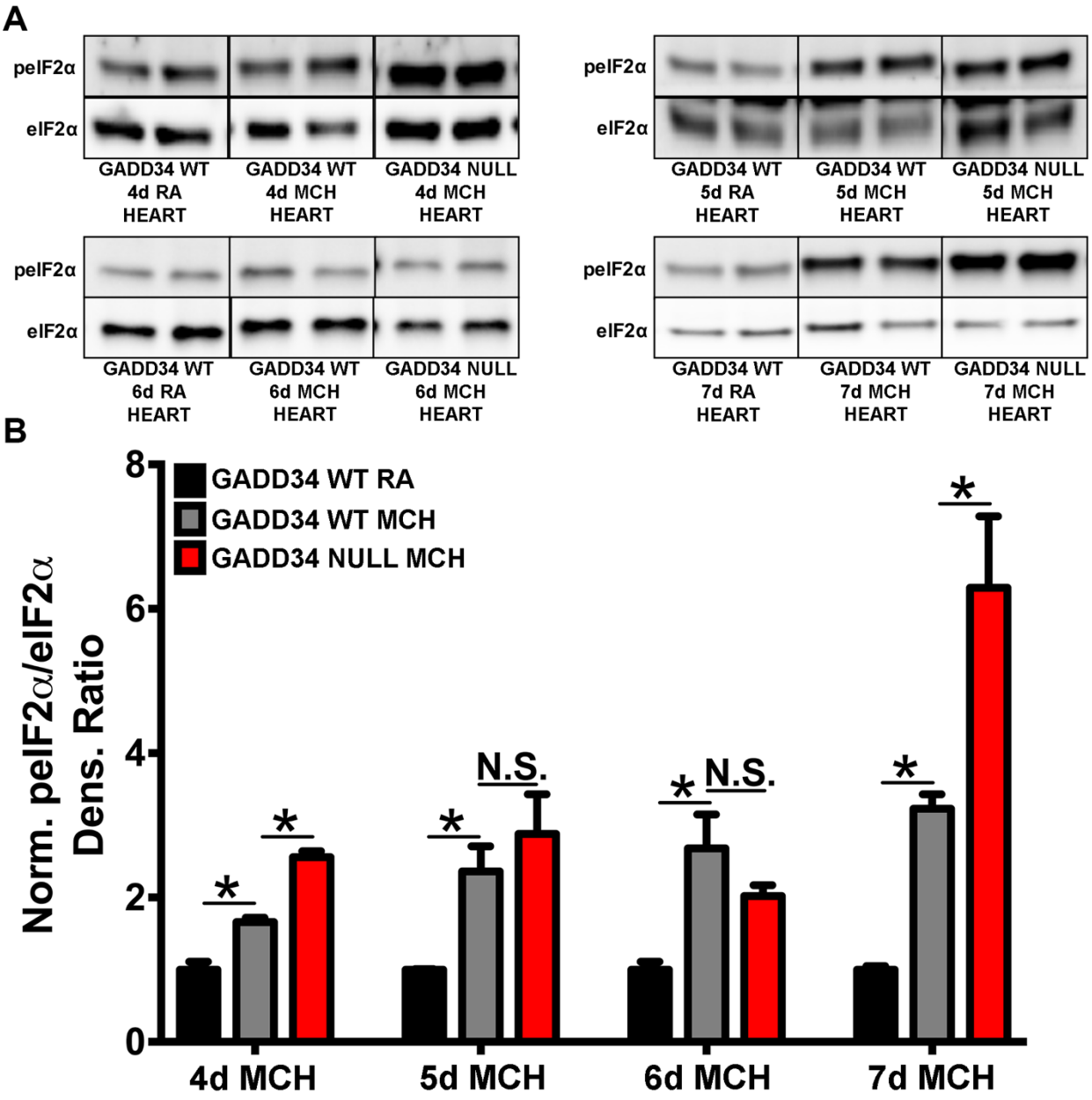

Figure 2.13. *Gadd34* deletion increases phosphorylation of eIF2α in mild chronic hypoxia exposed heart. (a) Representative blots of peIf2α and eiF2α in heart lysate from GADD34 WT and GADD34-Null mice exposed to either 4, 5, 6, or 7d of mild chronic hypoxia (MCH) or room-air control (RA). (b) Quantification of peIF2α and eIF2α protein levels in heart lysate from GADD34 WT and GADD34-Null mice exposed to either 4, 5, 6, or 7d of MCH or RA. Data represents N≥3 mice per group and presented as peIF2α/eIF2α ratio normalized to time-matched GADD34 WT RA exposed control mice, with *P<0.05 by ANOVA with Tukey's post-test. Data presented as mean±sem

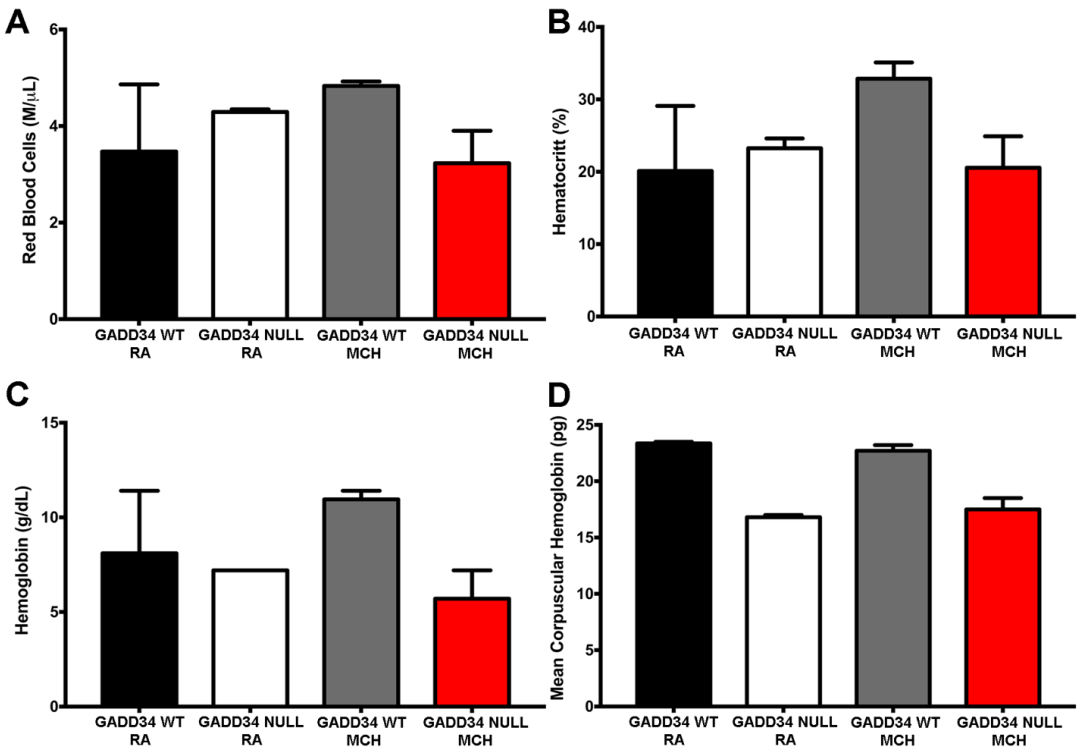

Figure 2.14 GADD34-null mice have a possible deficit in hematopoietic adaptation to hypoxia. (a) Red blood cell levels appear to increase during mild chronic hypoxia (MCH) exposure in GADD34 WT pups but not in GADD34-null mice. (b) Hematocrit levels seem increase in GADD34 WT pups during MCH exposure but not in GADD34-null mice. (c,d) Total blood hemoglobin concentration and mean corpuscular hemoglobin increase during MCH in GADD34 WT but not GADD34-null mice. Data presented as mean±sem for N=2 samples per group with blood pooled from 2 mice.

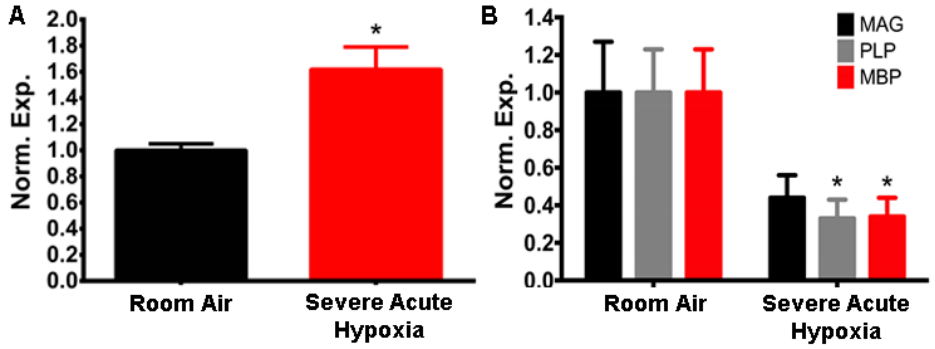

Figure 2.15 Severe acute hypoxia increases expression of VEGF and decreases expression of myelin transcripts. (a) Expression of VEGF is increased by 12hrs of severe acute hypoxia in P4 mice, while expression of PLP and MBP (d) is decreased by 24hrs of SAH in P4 mice. Data represents N≥3 mice per group with *P<0.05 by unpaired two-tailed *t*-test compared to experiment matched RA control. Data presented as mean±sem.

The SAH model also led to decreased MBP staining in the subcortical white matter and decreased mature CC1+ oligodendrocytes with no change in the number of total OLIG2+ cells (Fig. 216A and 2.16B). Moreover, SAH-exposed pups showed decreased levels of myelin enriched proteins MAG, CNP, and MBP (Fig. 2.16C and 2.16D). These experiments indicate that SAH is an alternative model of DWMI.

2.4.7 SAH increases phosphorylation of eIF2α in brain

Having established SAH as a model of DWMI we next examined whether SAH activates the ISR in the neonatal brain. Similar to MCH, SAH lead to increased phosphorylation of eIF2α during the hypoxic insult (Fig 2.17A and 2.17B). The heightened severity of SAH increased peIF2α levels within 12hrs, more rapidly than under conditions of mild hypoxic stress. This correlation between the kinetics of eIF2α phosphorylation with hypoxic severity has been previously found (Koumenis et al. 2002), suggesting that activation of the ISR is tuned to the severity of hypoxic insult. Phosphorylation of eIF2α was also transient in SAH, beginning to return to baseline by the end of the 24hr hypoxic exposure. In agreement with our results from the MCH experiments, SAH also did not increase levels of downstream ISR components. Like MCH, SAH caused a decrease in ATF4 protein levels (Fig. 2.17A and 2.17B), which may explain the subsequent lack of CHOP and GADD34 mRNA induction (Fig. 2.17C). These experiments suggest that while decreasing global protein translation through phosphorylation of eIF2α may be important, a full ISR response including the transcriptional response driven by ATF4 does not play a significant role in response to SAH.

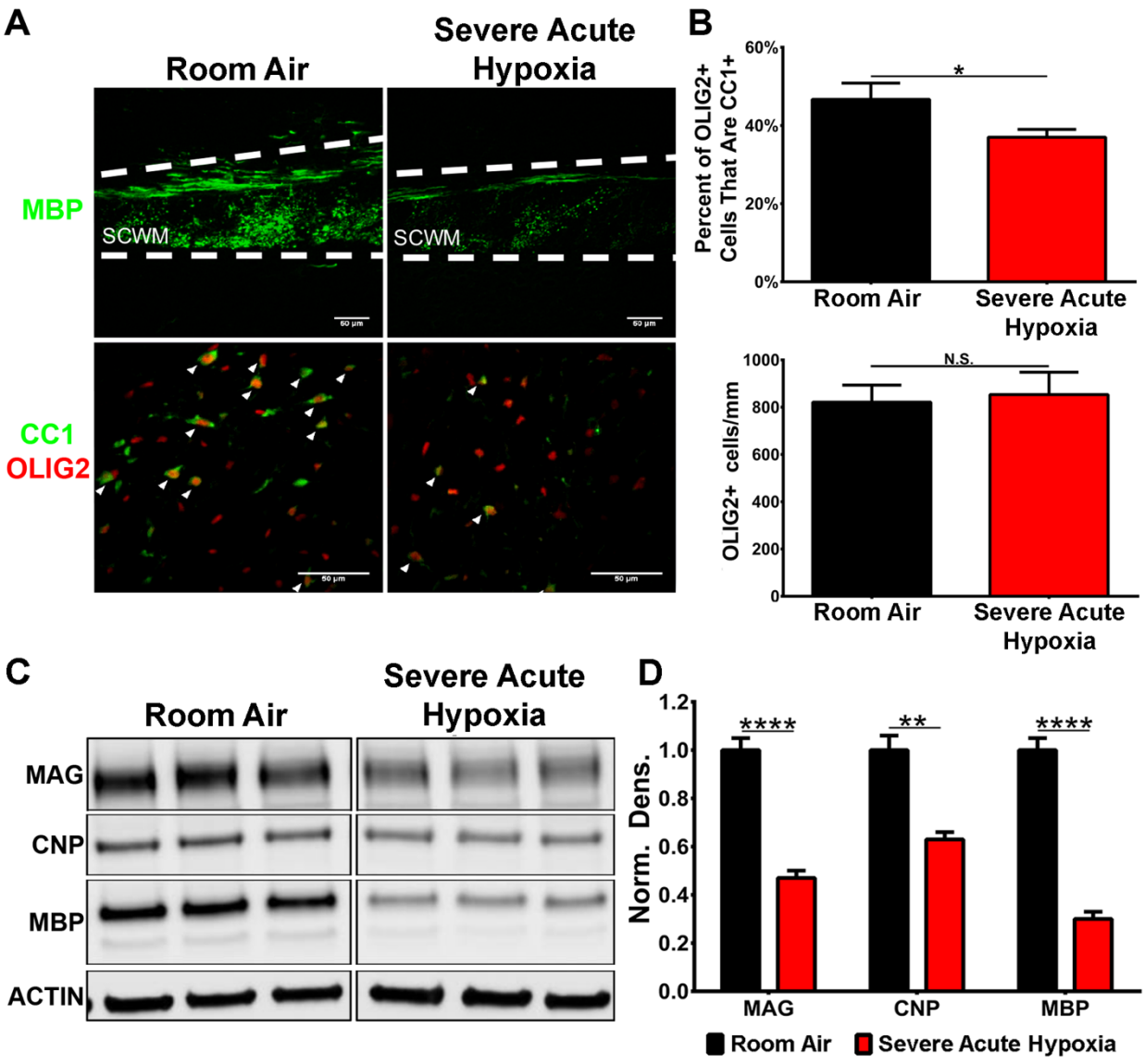

Figure 2.16 Severe acute hypoxia as an alternative model of diffuse white matter injury. (a) Top panels are representative images of MBP-(green) stained subcortical white matter (SCWM) from P11 mice exposed to severe acute hypoxia (SAH) or room-air control (RA). (a) Bottom panels are representative images of mature CC1+ (green) oligodendrocytes and Olig2+ (red) oligodendrocyte lineage cells from P11 mice exposed to SAH or RA. (b) Quantification of the percent of Olig2+ oligodendrocyte lineage cells that are CC1+ mature oligodendrocytes and density of Olig2+ oligodendrocyte lineage cells in P11 SAH and RA-exposed mice. Data represents N≥3 mice per group with *P<0.05 by unpaired two-tailed *t*-test. (c) Representative blots of myelin enriched proteins MAG, CNP, and MBP from P11 mice exposed to SAH or RA. (d) Quantification of MAG, CNP, and MBP protein levels from P11 mice exposed to SAH or RA. Data represents N≥3 mice per group with **P<0.01 and ****P<0.0001 by unpaired two-tailed *t*-test. All data presented as mean±sem and scale bars equals 50µm.

To determine whether SAH-induced phosphorylation of eIF2α was associated with ER stress and activation of the UPR we examine whether SAH caused splicing of XBP1, a marker for activation of the IRE1 arm of the UPR. Neither 12 nor 24 hours of SAH induced splicing of XBP1 suggesting that IRE1 is not activated and phosphorylation of eIF2α in SAH is not caused by ER stress (Fig 2.18).

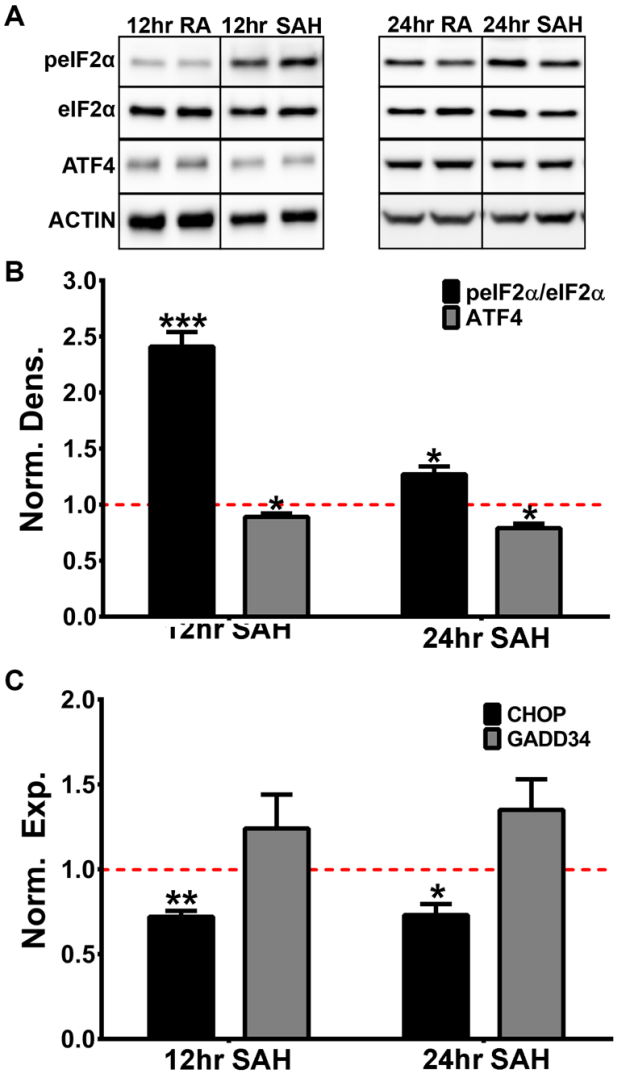

Figure 2.17. Severe acute hypoxia increases phosphorylation of eIF2α, but decreases ATF4 protein levels and does not induce CHOP and GADD34 expression. (a) Representative peIF2α, eIF2α, and ATF4 blots from mice exposed to either 12 or 24hr of severe acute hypoxia (SAH) or room air control (RA). (b) Quantification of peIF2α, eIF2α, and ATF4 protein levels. Data presented as peIF2α/eIF2α ratio normalized to time-matched RA-exposed control mice. Data represents N≥3 mice per group with *P<0.05 and ***P<0.005 compared to time-matched control (red dashed line) by unpaired two-tailed *t*-test. (c) Expression of CHOP and GADD34 mRNA levels normalized to time-matched RA-exposed controls. Data represents N≥3 mice per group with *P<0.05 and **P<0.01 compared to time-matched control (red dashed line) by unpaired two-tailed *t*-test.

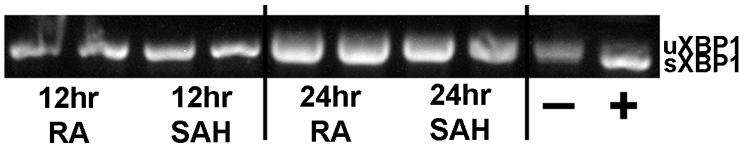

Figure 2.18 Severe acute hypoxia does not activate the IRE1 arm of the unfolded protein response. XBP1 splicing was measured by PCR as a marker of activation of IRE1. There is no evidence that severe acute hypoxia (SAH) leads to production of spliced XBP1 (sXBP1). Compared to XBP1 splicing when cells are exposed to the known ER stressor tunicamycin (+) compared to untreated (-) cells.

2.4.8 Genetic manipulation of the ISR and SAH-induced DWMI

We next examined the effect that genetic manipulation of the ISR has on SAH-induced DWMI. We exposed OL-PERK-null and OL-PERK-FL controls to SAH and did not find a significant difference in the level of myelin-enriched proteins MAG, CNP, and MBP between the two groups when measured at P11 (Fig. 2.19A and 2.19B). These results were validated by MBP immunohistochemistry and cell counts of the percentage of mature CC1+ oligodendrocytes. No significant difference was found in the percentage of mature CC1+ oligodendrocytes in OL-PERK-null and OL-PERK-FL pups exposed to SAH (Fig. 2.19C and 2.19D). These results indicate that the ISR via PERK does not play a significant role in SAH-induced DWMI.

We also exposed global GADD34-null pups to SAH. In contrast to our findings with MCH, GADD34-null pups did not show increased susceptibility to SAH. There was no significant difference in the body weight of SAH exposed GADD34-null mice versus controls, 6.6±0.2 grams versus 6.1±0.2 grams respectively. GADD34-null mice exposed to SAH did not exhibit a higher mortality rate and there was no significant difference in MAG, CNP, and MBP protein levels when comparing SAH challenged GADD34- null and GADD34-WT mice. These results demonstrate that GADD34-null mice are not susceptible to all hypoxic insults, but that the hypoxic stress has to be chronic in order for GADD34 deficiency to be detrimental.

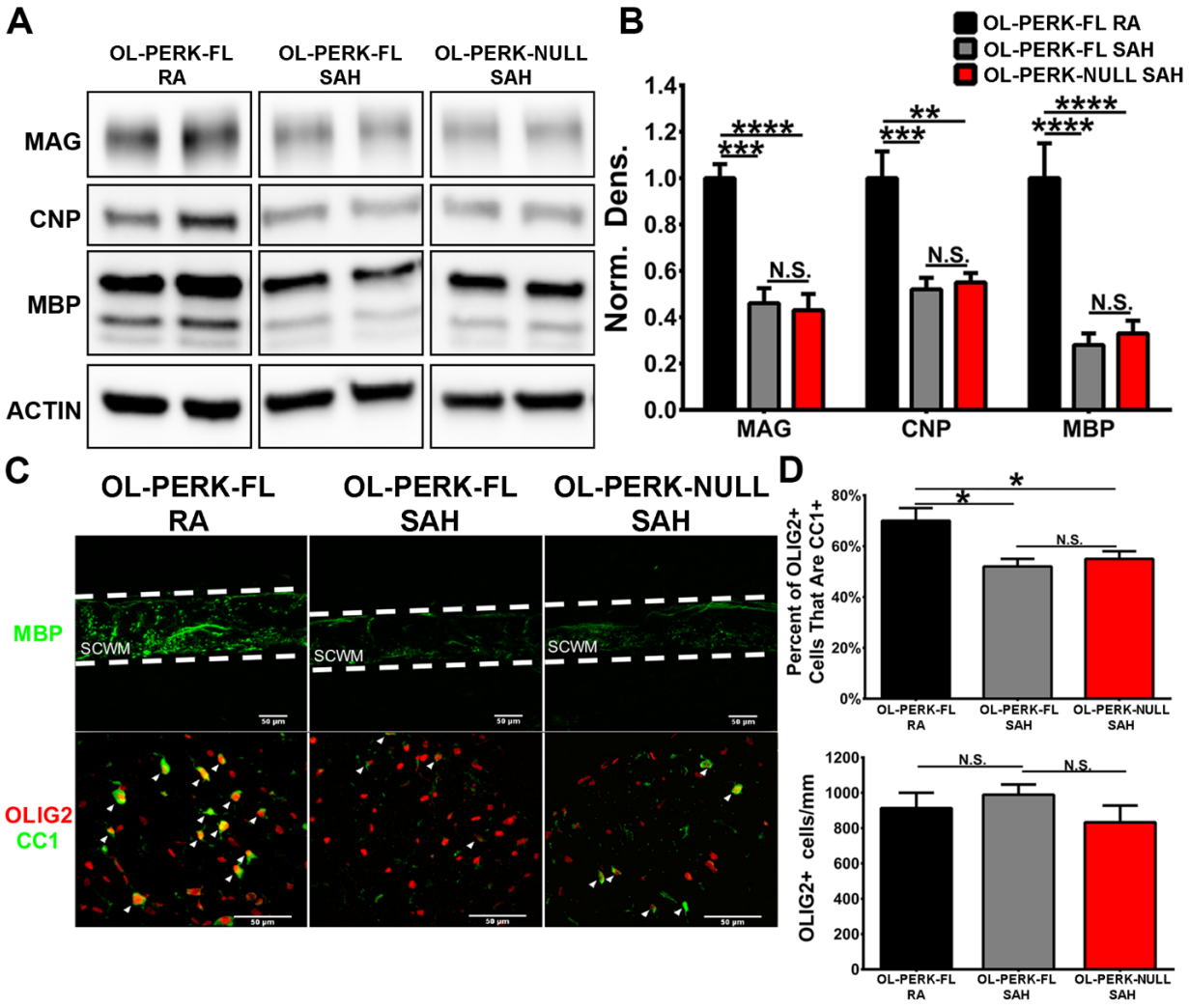

Figure 2.19. Oligodendrocyte-specific deletion of *Perk* has no effect on severe acute hypoxia-induced diffuse white matter injury. (a) Representative blots of MAG, CNP, and MBP from P11 OL-PERK-FL and OL-PERK-Null mice exposed to severe acute hypoxia (SAH) and room-air control (RA). (b) Quantification of MAG, CNP, and MBP protein levels from P11 OL-PERK-FL and OL-PERK-Null mice exposed to SAH and RA. Data represents N≥3 mice per group with **P<0.01, ***P<0.005, and ****P<0.0001 by ANOVA with Tukey's post-test. (c) Representative images of subcortical white matter (SCWMI) from P11 OL-PERK-FL and OL-PERK-Null mice exposed to SAH and RA and stained with MBP (green, top panels) or CC1 (green, bottom panels) and Olig2 (red, bottom panels). (d) Quantification of the percent of Olig2+ oligodendrocyte lineage cells that are CC1+ mature oligodendrocytes and density of Olig2+ oligodendrocyte lineage cells in P11 OL-PERK-FL and OL-PERK-Null mice exposed to SAH and RA. Data represents N≥3 mice per group with **P<0.01 and *P<0.05 by ANOVA with Tukey's post-test. Data presented as mean±sem and scale bars equal 50µm.

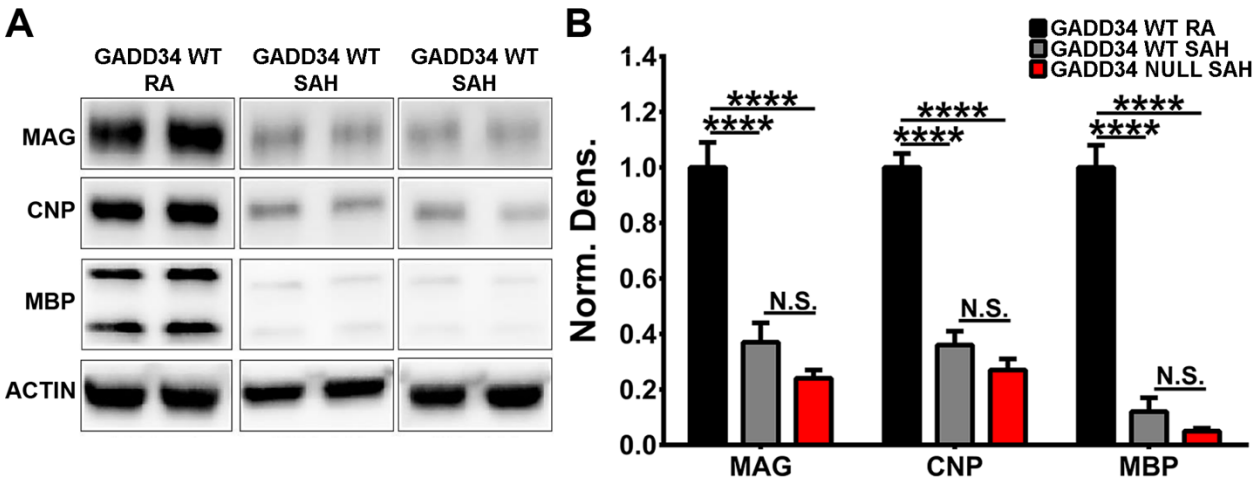

Figure 2.20. Global *Gadd34* deletion has no effect on severe acute hypoxia induced diffuse white matter injury. (a) Representative blots of MAG, CNP, and MBP from P11 GADD34 WT and GADD34-Null mice exposed to severe acute hypoxia (SAH) and room air control (RA). (b) Quantification of MAG, CNP, and MBP protein levels in P11 GADD34 WT and GADD34-Null mice exposed to SAH and RA. Data represents N≥3 mice per group with ****P<0.0001 by ANOVA with Tukey's post-test. Data presented as mean±sem and scale bars equal 50μm.

2.5 Discussion

We demonstrate that *in vitro* hypoxia increases phosphorylation of eIF2α in primary isolated OPCs and that this increase in peIF2α involves PERK. In PERK KO OPCs we show that *in* vitro hypoxia results in diminished peIF2α compared to wild-type cells that makes PERK KO OPCs more vulnerable to *in vitro* hypoxia. Moreover, we showed that in two models of hypoxia induced DWMI levels of peIF2α are transiently increased in the brain of neonatal mice, but that this increased peIF2α does not activate downstream ISR components. In fact, both MCH and SAH decreased ATF4 protein levels and did not lead to induction of CHOP and GADD34. Although both hypoxic models increased eIF2α phosphorylation, oligodendrocyte-specific deletion of PERK had no effect on either MCH or SAH-induced DWMI. Finally, we have shown that contradictory to other insults, global deletion of *Gadd34* increased susceptibility of mice to

MCH and had no detectable effect on mice exposed to SAH. Together, these studies show that although PERK plays a role in oligodendrocyte lineage cells exposed to *in vitro* hypoxia, PERK signaling within oligodendrocytes lineage cells does not appear to play a crucial role in either *in vivo* MCH or SAH-induced DWMI. Moreover, we found that inhibition of GADD34 is detrimental in the presence of a chronic hypoxic insult and ineffective in an acute hypoxic insult.

PERK-mediated phosphorylation of eIF2α in response to hypoxia occurs in cell lines *in vitro* (Koumenis et al. 2002). We have shown that in primary isolated OPCs, *in vitro* hypoxia also increases phosphorylation of eIF2α in a mostly PERK-dependent manner. Nonetheless, some increase in phosphorylation of eIF2α is still seen in PERK KO OPCs exposed to *in vitro* hypoxia (Fig. 2.3A and 2.3B). This is most likely due to redundancy between stress-sensing eIF2α kinases. In fact, GCN2 has also been shown to respond to *in vitro* hypoxia (Y. Liu et al. 2010) and it is possible that the response of PERK KO OPCs to hypoxia is driven by this alternative eIF2a kinase. Regardless of the potential activation of redundant eIF2α kinases, PERK KO OPCs still show a significantly increased susceptibility to *in vitro* hypoxia, demonstrating that PERK activity is important for OPC survival in response to hypoxia.

Although *in vivo* MCH increases eIF2α phosphorylation in neonatal mouse brains, oligodendrocyte-specific deletion of *Perk* had no effect on MCH-induced DWMI (Fig. 2.10). The disparate results generated by *in vitro* and *in vivo* hypoxia could be due to the severity of the hypoxic stress. Although we were unable to directly measure the percentage of oxygen available to oligodendrocyte lineage cells during MCH *in vivo*, it is unlikely to reach the degree of oxygen depletion that we are able to obtain with isolated oligodendrocyte lineage cells *in vitro*. *In vitro* hypoxia allows for a much more severe level of hypoxia without the confounding factor of the

systemic effects hypoxia has on survival of the subject *in vivo*. To address this, we developed a new SAH model of DWMI where we exposed pups to 7±0.5% O_2 for 24hrs. The 7±0.5% O_2 set point was used as it was the lowest percentage of oxygen tolerated by the lactating females over a 24hr period. This new SAH model leads to decreased levels of myelin transcripts and proteins, and inhibits OPC maturation decreasing the number of mature oligodendrocytes in the CNS (Fig 2.16) To determine whether the ISR plays a differential role in a severe acute hypoxic stress versus a mild chronic hypoxic stress. However, even with the increased severity of hypoxia, oligodendrocyte-specific deletion of *Perk* did not have a significant effect on SAH-induced DWMI (Fig 2.19). Taken together, these results suggest that oligodendrocyte lineage cell specific PERK signaling does not appear to play a pivotal role in hypoxia-induced DWMI.

Both MCH and SAH lead to a transient increase in peIF2α that returns to baseline during the hypoxic exposure (Fig. 2.7 and 2.17). However, neither MCH nor SAH increase expression of GADD34 suggesting that dephosphorylation of eIF2α occurs through a GADD34 independent mechanism. A second constitutively active regulator of PP1 dephosphorylation of eIF2α known as constitutive repressor of eIF2α phosphorylation (CreP; also known as protein phosphatase 1 regulator subunit 15B [PP1R15B]) exists and is responsible for maintaining low levels of peIF2α under non-stressed conditions (Jousse et al. 2003; Harding et al. 2009). Although considered to be non-stress induced, it is possible that in the absence of GADD34, CreP levels increase and cause dephosphorylation of MCH and SAH induced peIF2α (Reid et al. 2016). It is also possible that a hypoxia induced negative feedback loop exists that inhibits PERK, the eIF2α kinase responsible for increased peIF2α under hypoxia, allowing low levels of CreP to dephosphorylate eIF2α over time. One potential mechanism is through the Akt pathway. The

Akt pathway is activated by hypoxia and has been shown to inhibit activation of PERK, the putative eIF2α kinase that responds to hypoxia (Beitner-Johnson et al. 2001; Deguchi et al. 2009; Mounir et al. 2011).

It is interesting that while both MCH and SAH lead to increased levels of peIF2α, neither hypoxic insult causes induction of a full ISR response. This may be due to hypoxia-driven decrease in ATF4 protein levels (Fig. 2.7 and 2.17). The decrease in ATF4 protein levels corresponded to the duration of hypoxia in which peIF2α levels were increased, and no increase in CHOP or GADD34 mRNA was found. To validate that CHOP does not play a role in either MCH or SAH-induced DWMI we exposed CHOP-null mice to MCH and SAH and found that no apparent difference between CHOP-null and control mice in either model (Fig. 2.21). As mentioned, this truncated ISR is not unprecedented, however no one has before shown that hypoxia activates an incomplete ISR in neonatal mouse brain. It is possible that while the survival response to hypoxia requires phosphorylation of eIF2α and energy conservation via decreased protein translation, an adaptive transcriptional response driven by ATF4 is expendable due to adaptive HIF1a signaling. In fact, HIF1α was shown to be a repressor of ATF4 expression and expression of numerous ATF4 targets (Guimarães-Camboa et al. 2015). This suggest a complex interplay between transcriptional responses to hypoxia driven by Hif1α and ATF4, the outcome of which is most likely cell and context specific.

Another interesting result from our study is the effect of global *Gadd34* deletion on the susceptibility of neonatal mice to MCH. Previous studies have shown that targeting inhibition of GADD34 is a promising strategy for protecting oligodendrocyte lineage cells and myelination from inflammation (Way et al. 2015). Similarly, we predicted that *Gadd34* deletion would

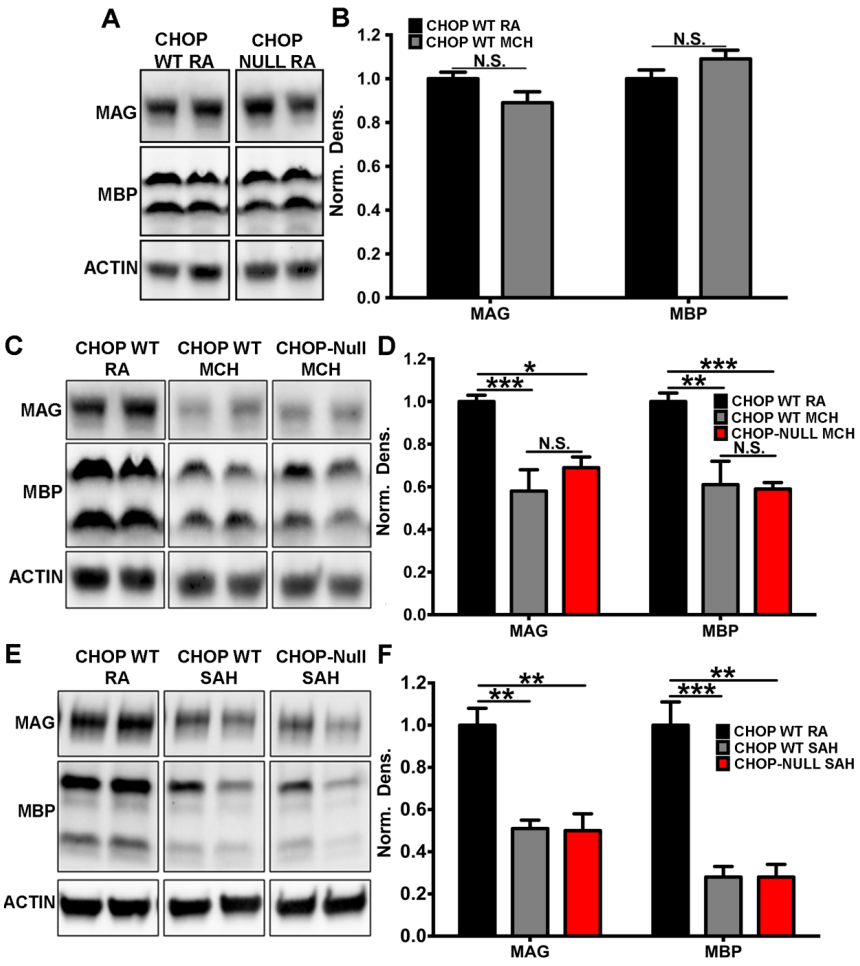

Figure 2.21. CHOP does not participate in either MCH or SAH-induced DWMI. (a,b) *Chop* deletion has no effect on developmental myelination in P18 mice. (c,d) No significant difference is seen in MAG and MBP protein levels between CHOP WT and CHOP-Null mice that were exposed to MCH. (e,f) There is no significant difference in MAG and MBP protein levels between CHOP WT and CHOP-Null mice exposed to SAH. Data presented as mean±sem for N=5. *P<0.05, **P<0.01, ***P<0.005 by ANOVA with Tukey's post-test.protect mice from MCH-induced DWMI.

Surprisingly, however, *Gadd34* deletion exacerbated the effects of MCH-induced DWMI (Fig. 2.11) as well as, causing decreased body weight and increased mortality of GADD34-null mice exposed to MCH. Systemic effects and increased peIF2α in MCH exposed GADD34-null heart and not in MCH exposed GADD34-null brain suggests that the detrimental effects of *Gadd34* deletion are not CNS specific (Fig. 2.12 and 2.13). Interestingly, it has been shown in a

different mouse line that *Gadd34* deletion diminishes hemoglobin production (Patterson et al. 2006). This perturbation in normal hematopoiesis could explain the increased mortality of GADD34-null mice exposed to MCH. In fact, our preliminary studies suggest that GADD34-null mice have a diminished capacity to mount a hematopoietic response to MCH (Fig. 2.14). This includes a lack of increased hemoglobin and red blood cell production in GADD34-null mice exposed to hypoxia compared to GADD34 WT mice. In addition, we were unable to detect any effect of *Gadd34* deletion on MCH-driven phosphorylation of eIF2α in the brain. These data suggest that the detrimental effects of *Gadd34* deletion in MCH are global and not CNS-specific. Moreover, *Gadd34* deletion had no effect in our SAH model of DWMI. This is perhaps not surprising given an adaptive hematopoietic response is more important under chronic hypoxia and not acute hypoxia (Sharp and Bernaudin 2004).

In conclusion our studies have shown that targeting the ISR is not an effective strategy for DWMI therapy. Although effective *in vitro*, oligodendrocyte-specific deletion of *Perk* and global deletion of *Gadd34* were either ineffective or detrimental in two *in vivo* models of hypoxia-induced DWMI.

Chapter 3. Neonatal hypoxia results in hypomyelination of the peripheral nervous system

3.1 Abstract

Though the consequences neonatal hypoxia, caused by premature birth, on central nervous system (CNS) myelination are well established, the effects of neonatal hypoxia on peripheral nervous system (PNS) myelination are less well known. We hypothesized that similar to the CNS neonatal hypoxia would lead to hypomyelination of the PNS with sustained motor deficits. Here we demonstrate that neonatal hypoxia results in thinner myelin and delayed development of axon bundles in the PNS of mice leading to electrophysiological and motor deficits that persist thru adulthood. These findings provide support for a role of hypoxic damage to the PNS in persistent motor deficits commonly experienced by premature infants and suggest that therapies designed to protect PNS myelin may improve clinical outcomes in premature infants.

3.2 Introduction

Premature birth as a percentage of total births in the United States continues to rise with an estimated 500,000 babies porn premature each year (Salmaso et al. 2014). In addition, improved care is increasing the number of neonates that survive prematurity, including those infants born at low birth weight (<1500g) (Back 2015; Back and Miller 2014; Deng 2010). Unfortunately, neurodevelopmental disabilities caused by premature birth have not decreased leading to over half of preterm survivors experiencing motor, sensory, behavioral, and/or cognitive deficits (de Kieviet et al. 2009; Hack et al. 2002; Marlow et al. 2005; Miller et al. 2005). Because of damage suffered during critical developmental windows these deficits persist

at high rates into adolescence and adulthood. With the prevalence and persistence of these disabilities it is crucial to gain a better understanding of the pathophysiology of premature birth that results in neurological deficits.

To date, most studies have focused on the central nervous system (CNS) specific effects of premature birth. Because hypoxia is a common and clinically relevant insult many groups have used mouse models of neonatal hypoxia to show that hypoxia damages OPCs leading to diffuse white matter injury in the CNS that contributes to sensorimotor deficits (Scafidi et al. 2014; Back et al. 2006; Yuen et al. 2014). However, little is known about the effects of neonatal hypoxia on Schwann cells and myelination during development of the peripheral nervous system (PNS). This represents a gap in our understanding of neural morbidities caused by hypoxia during premature birth. A better understanding of the effect of neonatal hypoxia on PNS myelination could provide novel opportunities for therapeutic intervention.

In this study we have utilized a well-established mouse model to examine the effect of neonatal hypoxia on PNS myelination during development (Scafidi et al. 2009). We demonstrate that neonatal hypoxia results in hypomyelination characterized by thinner myelin sheets that persist into adulthood. Mice exposed to neonatal hypoxia also demonstrate transient delay in development of axonal bundles that recover when mice are returned to room air. Importantly, neonatal hypoxia also causes electrophysiological and motor behavior deficits in adult mice. These results suggest that deficits in PNS myelin may be an underappreciated component of neurodevelopmental disabilities caused by premature birth, and that therapies designed to protect PNS myelin may improve clinical outcomes in premature infants.

3.3 Methods

3.3.1 Animals and neonatal hypoxia

All animals were housed under pathogen-free conditions and all animal procedures were approved by the Institutional Animal Care and Use Committees of the University of Chicago. C57BL/6 mice were bred in house and unless otherwise noted both male and female pups were used.

Neonatal hypoxia is a well-described model of diffuse white matter injury (DWMI) caused by neonatal hypoxia (Scafidi et al. 2014; Yuen et al. 2014; Fancy et al. 2011). Male and female mouse pups were fostered to lactating CD1 dams at postnatal day 2 (P2) and exposed to either chronic mild hypoxia or room air control. Fostering is required for this protocol since C57BL/6 dams do not care for their litters under hypoxic conditions. At P3 chronic mild hypoxia pups were placed into a Biospherix glove box maintained at 10±0.5% O_2 by displacement with nitrogen and controlled by a ProOx 360 from Biospherix. Pups were exposed to chronic mild hypoxia for 8 days from P3-P11 after which they were returned to room air until the end of the experiment. Room air control mice were also fostered to CD1 dams and kept at room air for the duration of the experiment. For histological studies samples were collected at P7, P11, P18, and P60 (Fig 3.1)

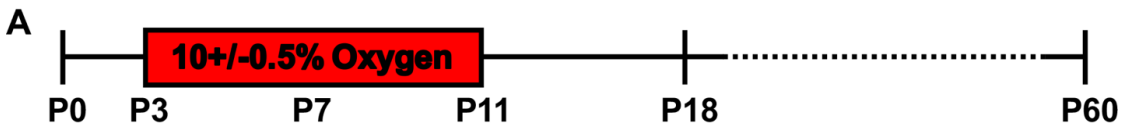

Figure 3.1. Neonatal hypoxia. To execute the neonatal hypoxia model mice were exposed to 10±0.5% O_2 from P3-P11 and tissue for histological analysis was collected at P7, P11, P18, and P60.

3.3.2 Electron Microscopy

Mice were anesthetized and perfused with buffer containing 4% paraformaldehyde and 2.5% glutaraldehyde in 0.1M sodium cacodylate buffer. Sciatic nerve tissue was then dissected and stored in perfusion buffer until processing. Sciatic nerves were fixed in 0.1M sodium cacodylate buffered 1% osmium tetroxide, dehydrated in ascending series of alcohols, and embedded in epoxy resin. Ultrathin sections were then imaged with a Tecnai Spirit electron microscope at the University of Chicago Electron Microscopy Facility. Greater than 10 non-overlapping images were taken at 1200X magnification from 4-6 mice per group. For g-ratio measurements greater than 200 total axons were counted per group and calculated using NIH ImageJ Software similar to the method previously described (Auer 1994).

3.3.3 Immunohistochemistry

P11 mice were taken directly from hypoxia or room air and anesthetized by intraperitoneal injection with avertin (0.5mg/g). Then the sciatic nerves were removed and embedded in OCT and snap-froze in isopentane with dry-ice. Cross sections were cut from fresh frozen tissue, fixed for 10 minutes in 4% paraformaldehyde, washed in PBS and stained with 1:250 KROX20 antibody (Covance, PRB-236P).

3.3.4 Total RNA Isolation and qPCR

RNA was isolated from snap-frozen pooled sciatic nerves using the BioRad Aurum Total RNA Fatty and Fibrous Tissue Kit (BioRad, 732-6830) according to manufacturer's instructions. Total RNA concentration was measured by a NanoDrop (ThermoScientific) spectrophotometer

and RNA quality was confirmed on an Agilent 2100 Bioanalyzer using an Agilent 6000 Nano Kit (Agilent Technologies, 5067-1511) according to manufacturer's instructions. Only samples with an RNA integrity number above 7 were used.

High quality RNA was reverse transcribed using the BioRad iScript cDNA Synthesis kit according to manufacturer's instructions (BioRad, 1708891) and quantitative real-time PCR was run on a BioRad CFX96 Real-Time PCR machine using SYBR Green detection. Results were analyzed using the ΔΔC(t) method on the BioRad CFX Manager software. RPL13A was used as the reference gene. Primers sequences can be found in Table 3.1.

Table 3.1. Primer Sequences for Wnt and Schwann Cell Transcripts

Gene of Interest	Primers
Lef1	**Fwd: 5'-ATGCACGTGAAGCCTCAACA-3'** **Rev: 5'-AGCTGCACTCTCCTTTAGCG-3'**
Axin2	**Fwd: 5'-AAGCCCCATAGTGCCCAAAG-3'** **Rev: 5'-GGGTCCTGGGTAAATGGGTG-3'**
cMyc	**Fwd: 5'-TTGGAAACCCCGCAGACAG-3'** **Rev: 5'-GCTGTACGGAGTCGTAGTCG-3'**
SCIP	**Fwd: 5'-GGAGAAGCGCATGACCCC-3'** **Rev: 5'-TGAGTTGGCGCATTCTGGAT-3'**
SOX2	**Fwd: 5'-ATGGGCTCTGTGGTCAAGTC-3'** **Rev: 5'-CCCTCCCAATTCCCTTGTAT-5'**
GalC	**Fwd: 5'-GCCTACGTGCTAGACGACTC-3'** **Rev: 5'-AGAACGATAGGGCTCTGGGT-3'**
KROX20	**Fwd: 5'-AATAGCTGGGCGAGGGG-3'** **Rev: 5'-ATGTTGATTCATGCCATCTCCC-3'**
P0	**Fwd: 5'-ACCTCTCAGGTCACGCTCTA-3'** **Rev: 5'-CATGGCACTGAGCCTTCTCTG-3'**
MBP	**Fwd: 5'-GCT CCC TGC CCC AGA AGT-3'** **Rev: 5'-TGT CAC AAT GTT CTT GAA GAA ATG G-3'**
MAG	**Fwd: 5'-CTG CTC TGT GGG GCT GAC AG-3'** **Rev: 5'-AGG TAC AGG CTC TTG GCA ACT G-3'**
RPL13A	**Fwd: 5'-TTC TCC TCC AGA GTG GCT GT-3'** **Rev: 5'-GGC TGA AGC CTA CCA GAA AG-3'**

3.3.5 Motor behavior analysis

Control and neonatal hypoxia exposed mice were tested for motor coordination and balance using the accelerating rotarod (Columbus Instruments). Control and neonatal hypoxia exposed mice were trained to remain on the rotarod at the constant speed of 5 rpm, and were tested once a week with four trials per test at 4, 6, and 8 weeks of age. Time to fall was measured by a blind investigator for each mouse on the rotarod as it accelerated from 5-45 rpm during a 300 second trial session. Mice were allowed 5 minutes of rest between each trial.

Similarly to previously described methods forelimb and hindlimb grip strength were measured using a computerized grip strength meter (Columbus Instruments, 0167-005L) (Elbaz et al. 2016). Mice were tested twice a week with 10 trials per test at 4, 6, and 8 weeks of age. Grip strength was measured by a blinded investigator.

Grid test measurements were performed by suspending mice inverted on a one-inch mesh grid. Mice use all four limbs to hang from the mesh grid and latency to fall is measured for each mouse up to 60 seconds. At 60 seconds the mouse is returned to the test cage and given 5 minutes of rest. Each mouse underwent 4 trials per test, once a week at 4, 6, and 8 weeks of age. The average of 4 trials was calculated and presented. Grid test measurements were performed by an investigator blind to experimental and control groups.

3.3.6 Electrophysiology

Electrophysiology was performed in P60 mice with a Nicolet Viking Quest Laptop System (VikingQuest). Recording electrodes were placed subcutaneously in the footpad with supramaximal stimulations performed with a 0.1-0.2ms pulse. Stimulation of the sciatic nerve was performed distally at the ankles and proximally at the sciatic notch. For each animal latency,

conduction velocity and amplitude of the compound action potential was measured and results for both sciatic nerves were averaged.

3.3.7 Statistics

Data are presented as mean±sem unless otherwise noted. Multiple comparisons were made using ANOVA with Tukey's post-test. Comparisons of two data points were made by a two-sided unpaired *t*-test. A P value of <0.05 was considered significant and all statistical analysis was run with GraphPad Prism software.

3.4 Results

3.4.1 Neonatal hypoxia leads to hypomyelination characterized by reduced myelin thickness in the PNS.

Since the effect of chronic hypoxic rearing on PNS myelination has not been studied we began by measuring myelin thickness of the sciatic nerve in control and hypoxia exposed mice. We found that g-ratios, a measure of myelin thickness where larger g-ratio values correlate to thinner myelin sheaths, were increased in hypoxia exposed pups at P7 after 4 days of hypoxia, at P11 after 8 days of hypoxia, and P18 after 8 days of hypoxia and 7 days of recovery at room air (Fig. 3.2A, 3.2B, and 3.2C). Moreover, thinner myelin in the PNS of neonatal hypoxia exposed pups persisted up to P60 (Fig. 3.2A, 3.2B, and 3.2C). This chronic myelination deficit is similar to the sustained effects of neonatal hypoxia on CNS myelin thickness that lead to sensorimotor deficits. Nonetheless, the percent of myelinated fibers did not differ between control and neonatal hypoxia exposed pups at any age examined (Fig. 3.2D). These results show that

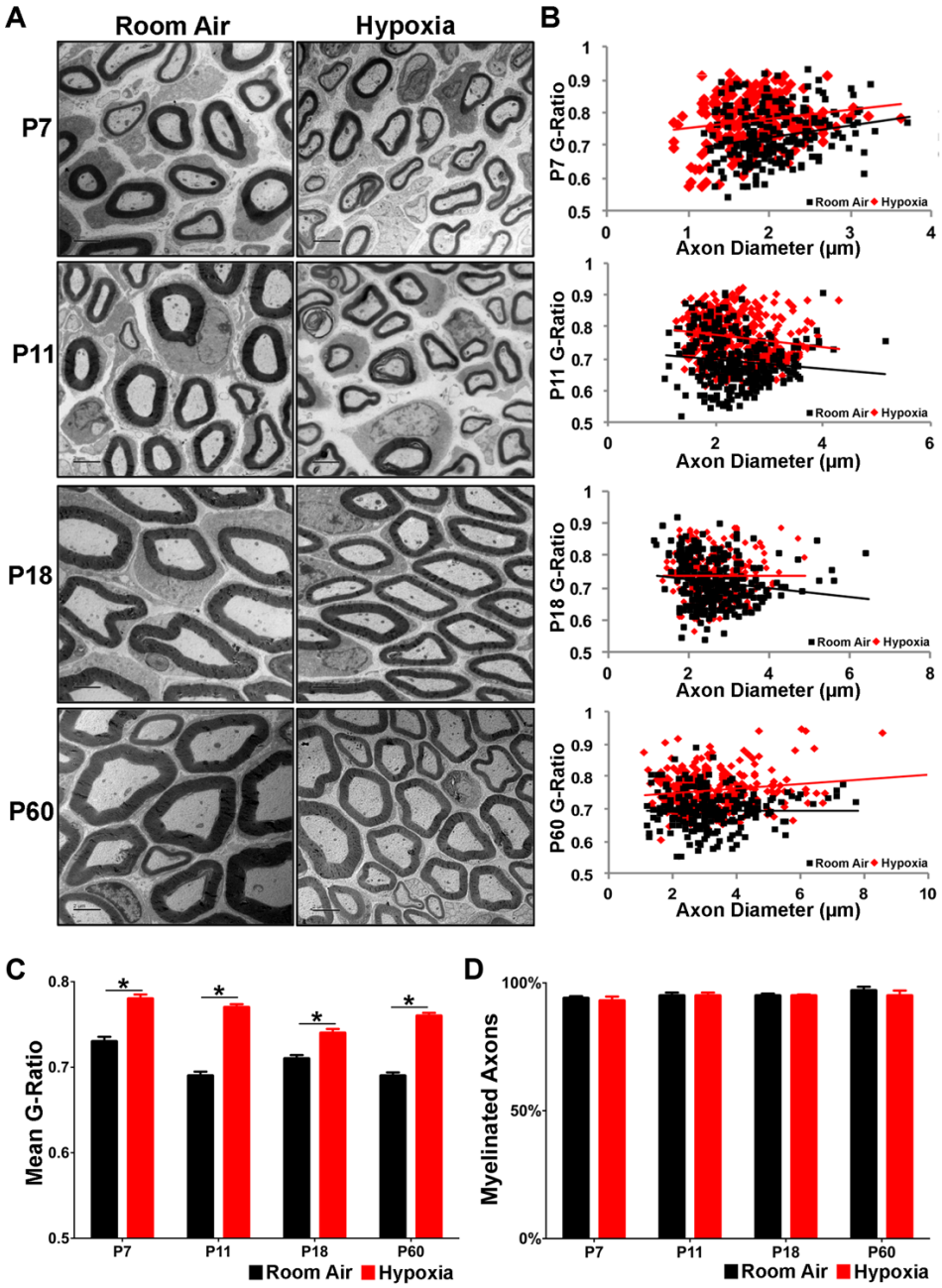

Figure 3.2. Neonatal hypoxia leads to thinner myelin in the PNS. Myelination in the sciatic nerve of hypoxia and room air exposed mice was analyzed using electron microscopy. (a) Representative electron microscope images from the sciatic nerve of room air control and hypoxia exposed pups. (b) Scatter plots of g-ratio versus axon diameter. (c) Myelin thickness measured by g-ratio was significantly thinner in hypoxia exposed pups compared to room air controls. (d) Hypoxia had no effect on the percentage of myelinated axons in the sciatic nerve. Data presented as mean±sem, for g-ratio calculations >200 axons were counted per group from 4-6 mice, for percent myelination N=4-6 mice. *P<0.05 by two-tailed *t*-Test. Scale bar represents 2µm in all images.

neonatal hypoxia leads to hypomyelination in the PNS that persists into adulthood with no apparent loss in the percent or total number of myelinated axons suggesting a mild deficit in myelin production rather than a robust phenotype caused by death of Schwann cells.

3.4.2 Neonatal hypoxia increases the size of PNS nerve bundles and the number of axons per bundle

During development of the PNS axons are removed from nerve bundles and myelinated by Schwann cells as they increase in diameter, an event called axonal sorting (Feltri, Poitelon, and Previtali 2016). Because of this dual role of Schwann cells, disruption in normal PNS development can affect myelination, axonal sorting, or both (Elbaz et al. 2016; Grigoryan et al. 2013). To determine whether neonatal hypoxia disrupts axonal sorting we analyzed axon bundles in the developing sciatic nerve of control and neonatal hypoxia exposed pups. We found that at P7 and P11, after 4 and 8 days of hypoxia respectively, the size of axonal bundles in hypoxia exposed pups were significantly larger than controls (Fig. 3.3A). This increase in the size of axonal bundles is driven by a significant increase in the number of axons within each bundle, and not an increase in the diameter of bundle axons (Fig. 3.3B and 3.3C). We also measured the size of myelinated axons to determine whether neonatal hypoxia may be delaying axonal growth. We found that there was no difference in the diameter of myelinated axons at any time point (Fig. 3.3D). This data suggests that neonatal hypoxia perturbs the early steps of the radial sorting process resulting in larger bundles with increased numbers of axons in the PNS.

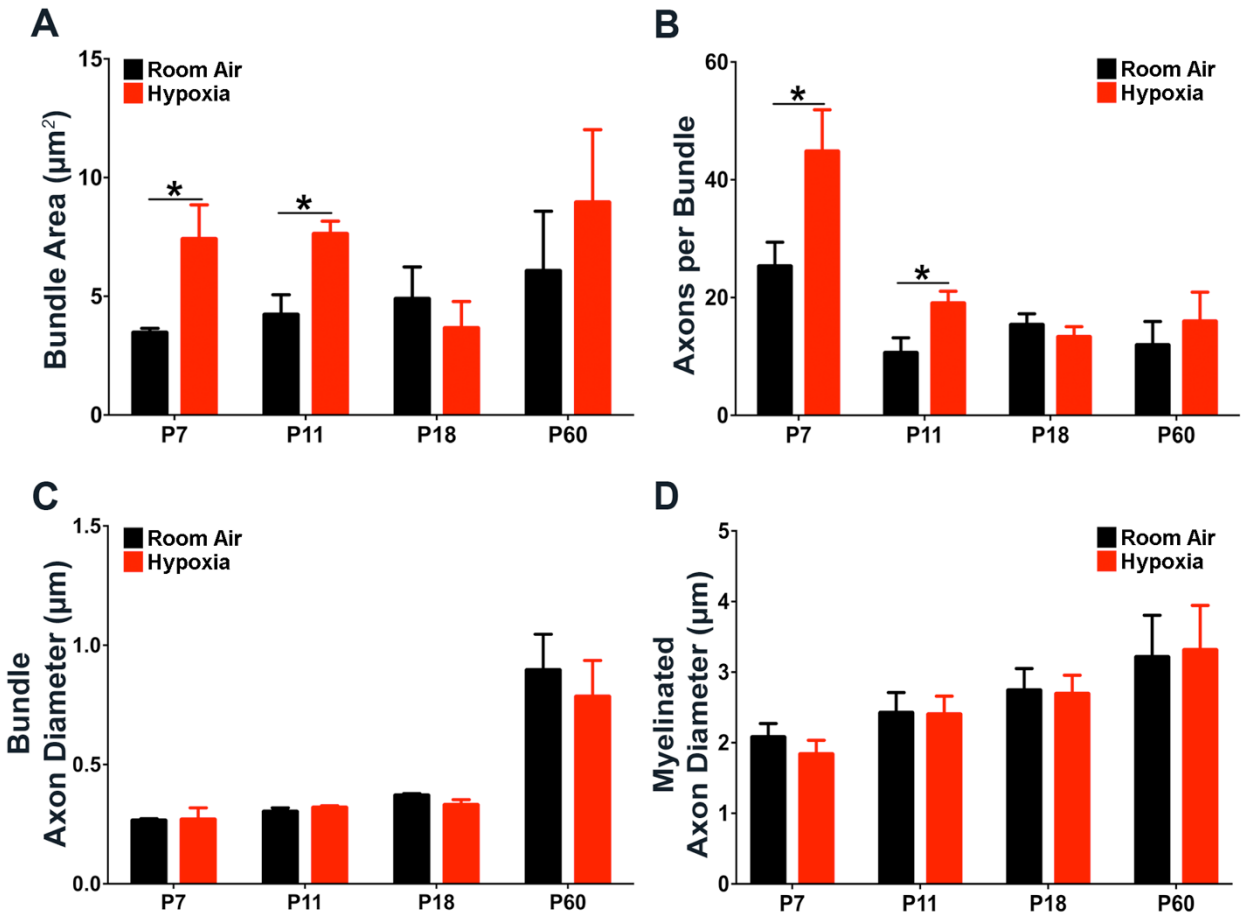

Figure 3.3 Neonatal hypoxia leads to disrupted maturation of axon bundles in the PNS. Axon bundles in neonatal hypoxia exposed and room air control mice were analyzed at P7, P11, P18, and P60 using electron microscopy. At P7 and P11, during hypoxic exposure, pups had significantly larger axon bundles in the PNS compared to RA controls (a) Bundle size recovered to control levels after 7 days of recovery at P18, and no long-term changes in axon bundle size were found at P60 (a). Increased bundle size corresponded with increased number of axons per bundle in NH exposed mice at P7 and P11, with no difference at P18 and P60 (b). There was no significant difference in the size of either bundle axons (c) or myelinated axons (d) in the PNS of NH and RA control mice. Data presented as mean±sem for N=4-6 mice per group, *P<0.05 by two-tailed *t*-Test.

3.4.3 Neonatal hypoxia does not affect the number of mature KROX20+ cells

Early growth response protein 2 or KROX20 is a zinc-finger transcription factor that is essential for the expression of myelin structural proteins and necessary components for myelin lipid synthesis (Salzer 2015; Topilko et al. 1994). Defects in KROX20 cause peripheral neuropathies like congenital hypomyelination neuropathy and Charcot-Marie-Tooth disease type 1D. To examine whether neonatal hypoxia inhibits maturation of Schwann cells in the PNS, P11sciatic nerves were stained for KROX20 in order to count the number of mature Schwann cells in the PNS of control and neonatal hypoxia exposed mice. We found that neonatal hypoxia exposed mice had significantly smaller sciatic nerves at P11, the end of the 8 days of neonatal hypoxic exposure, compared to control (Fig. 3.5). Nevertheless, this decrease in sciatic nerve size correlated with a decrease in overall size of mice exposed to neonatal hypoxia and when total body weight was controlled for there was no significant difference in normalized sciatic nerve size between room air and neonatal hypoxia mice at P11. It has been shown before that mice reared under hypoxic conditions are smaller, most likely due to deficient energy production, and this has led to the hypothesis that neonatal hypoxia leads to global dysmaturation. Because the sciatic nerves from neonatal hypoxia exposed mice are smaller we found that the density of KROX20+ cells was higher in neonatal hypoxia exposed mice compared to room air controls (Fig. 3.5). However, when the total number of KROX20+ cells was calculated per nerve there was no difference between hypoxia and control mice, which corresponds with there being no difference in KROX20 expression level (Fig. 3.5). These results suggest that PNS hypomyelination caused by neonatal hypoxia is not a result of decreased Schwann cell maturation.

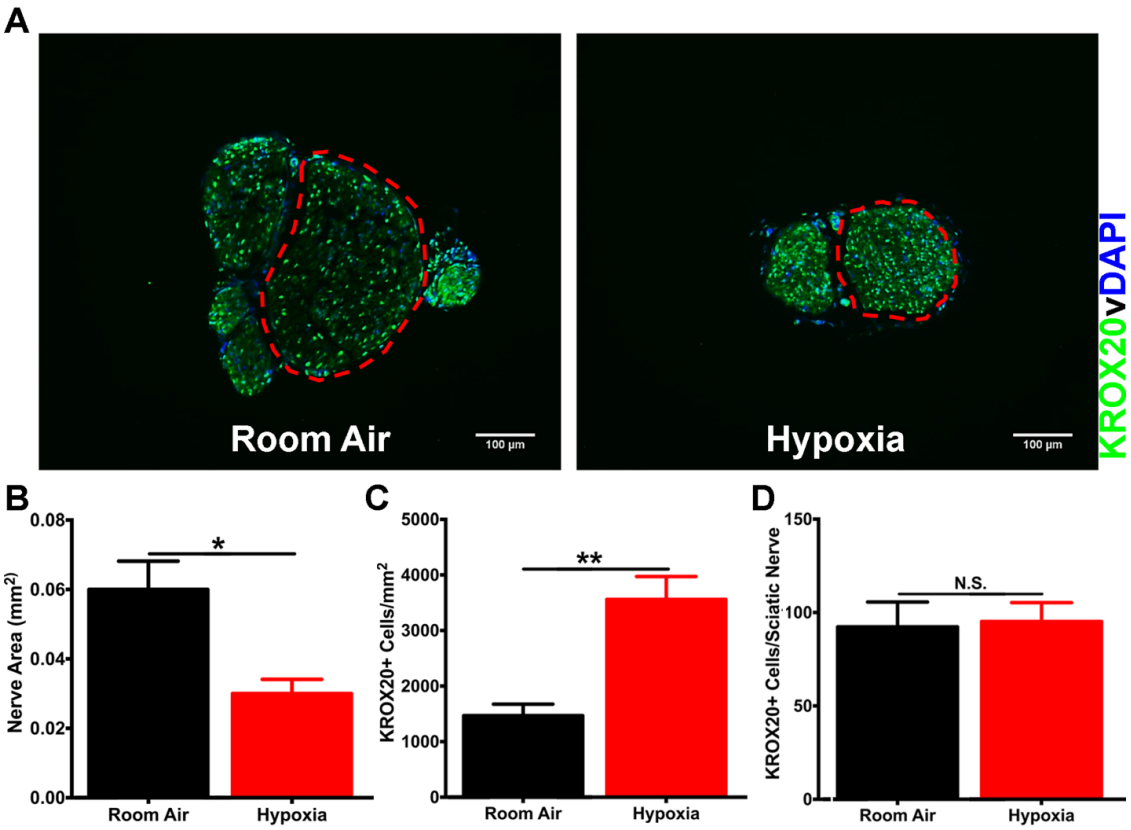

Figure 3.4. Neonatal hypoxia leads to increased KROX20+ cell density due to decreased tissue growth and no loss in total KROX20+ cells. Numbers of mature Schwann cells was measured using KROX20 staining in sciatic nerves from P11 mice exposed to hypoxia or room air. (a) Representative images of sciatic nerves stained with KROX20 (green) and DAPI (blue). (b) Area of the largest nerve segment (circled in red) was greater in room air mice compared to hypoxia. This most likely represents delayed maturation and not tissue atrophy. (c) Due to decreased nerve size the density of KROX20+ cells is increased in hypoxia exposed mice. (d) When controlled for sciatic nerve size the total number of KROX20+ cells is not significantly different between hypoxia and room air exposed mice at P11. Data presented as mean±sem for N=5-6, *P<0.05 and **P<0.01 by unpaired two-tailed *t*-test. Scale bar represents 100µm.

3.4.4 Neonatal hypoxia does not affect expression of Schwann cell markers

Inhibited maturation of Schwann cells in the PNS can lead to deficits in myelination and axonal sorting (Elbaz et al. 2016; Grigoryan et al. 2013) . To further examine whether neonatal hypoxia is effecting the maturation of Schwann cells total RNA was collected from pooled sciatic nerves and expression levels of immature Schwann cell markers SRY-Box 2 (Sox2) and galactosylceramidase (GalC), as well as, mature Schwann cell markers early growth response 2 also known as KROX20, myelin protein zero (P0), and MBP were measured by quantitative real-time PCR (Elbaz et al. 2016). I found that there was no increase in the expression of immature Schwann cell markers and correspondingly no decreased in mature Schwann cell markers (Fig. 3.4). These results combined with no apparent difference in KROX20+ cell numbers strongly suggest that the adverse PNS phenotypes caused by neonatal hypoxia are not due to decreased maturation of Schwann cells.

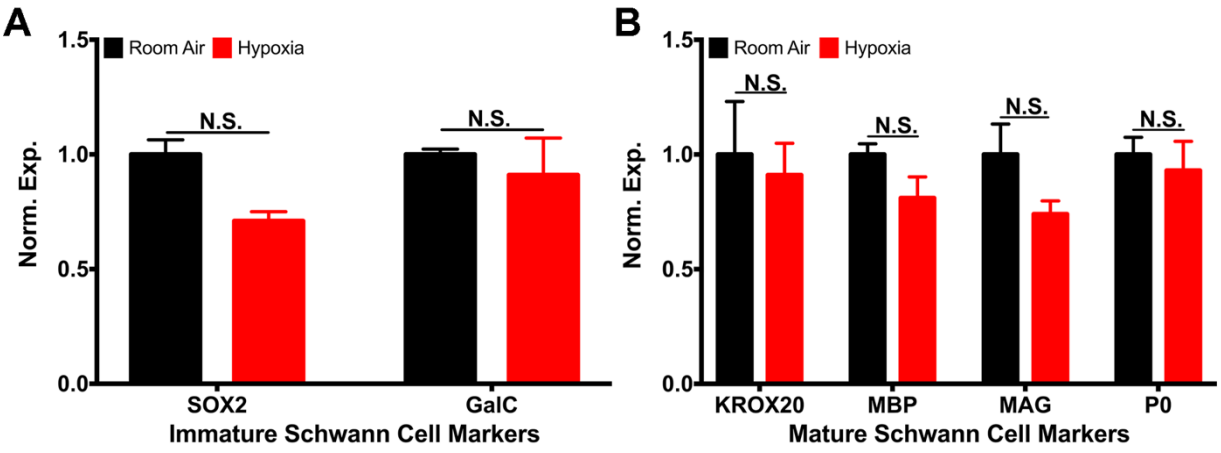

Figure 3.5. Neonatal hypoxia does not inhibit Schwann cell maturation. Schwann cell maturation was analyzed by qPCR in sciatic nerves from P7 mice exposed to 4 days of hypoxia. (a) There was no significant difference in expression of immature Schwann cell markers Sox2 and GalC. (b) There was no significant difference in expression of mature Schwann cell markers KROX20, MBP, MAG, and P0. Data presented as mean±sem for N=3 samples with 16 sciatic nerves pooled per sample.

3.4.5 Neonatal hypoxia does not activate Wnt signaling in sciatic nerve.

Wnt signaling in OPCs is activated by Wnt7a/7b in an autocrine fashion by neonatal hypoxia and has been shown to inhibit differentiation of OPCs into mature myelinating OLs (Yuen et al. 2014). Similarly, it has been shown that Wnt signaling in Schwann cells in the PNS inhibits proper PNS myelination and axonal sorting (Elbaz et al. 2016; Grigoryan et al. 2013). However, activation of Wnt signaling by hypoxia in the PNS has not been studied. Given that neonatal hypoxia perturbs proper PNS myelination we examined whether neonatal hypoxia activates Wnt signaling in the PNS, whicht would suggest that Wnt signaling is playing a similar role in the PNS as in the CNS. To examine activation of Wnt signaling total RNA was collected from sciatic nerve of WT P7 mice exposed to either 4 days of 10±0.5% O_2 or room-air controls and examined induction of Wnt target genes Lef1, Axin2, and cMyc. We determined at 4 days of neonatal hypoxia, instead of the full 8-day protocol because at 4 days PNS myelin deficits are already present and therefore if Wnt signaling was causative in the deficits it would be activated. There was no difference in the expression of Lef1, Axin2, or cMcy between neonatal hypoxia exposed and control mice (Fig. 3.6). This suggests that neonatal hypoxia does not activate WNT signaling in the PNS, and that the PNS myelin deficit caused by neonatal hypoxia is likely working through a different mechanism.

3.4.6 Neonatal hypoxia results in PNS electrophysiological and motor deficits that persist into adulthood.

As previously described, we found that mice exposed to neonatal hypoxia have thinner myelin at P60 compared to controls. One of the primary functions of myelin is to increase the

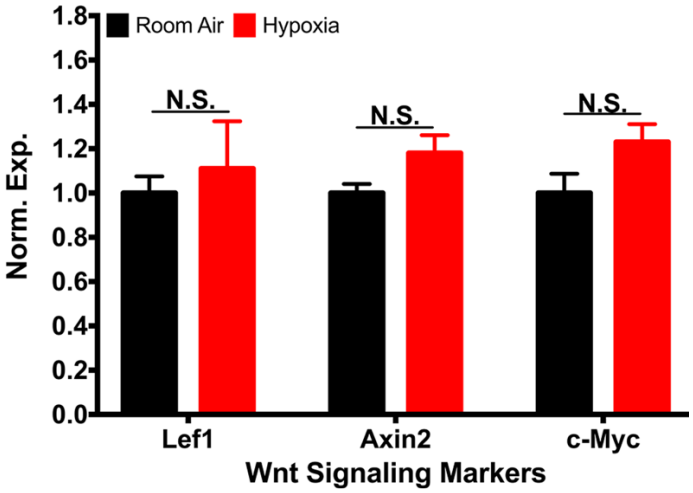

Figure 3.6. Neonatal hypoxia does not activate Wnt signaling in the PNS. Active Wnt signaling markers Lef1, Axin2, and c-Myc were measured by qPCR in sciatic nerves from P7 mice exposed to 4 days of hypoxia. No significant difference was found in any of the Wnt signaling markers. Data presented as mean±sem for N=3 samples with 16 sciatic nerves pooled per sample.

speed and fidelity of action potentials propagation along the axon, and disruptions in PNS myelination lead to motor deficits (Bercury and Macklin 2015; Hoyle et al. 2015). Given the decrease in PNS myelin thickness caused by neonatal hypoxia, we next wanted to determine whether this disturbance led to PNS motor deficits in older mice. To test these, we ran control and hypoxia exposed mice through a battery of motor tests at 4, 6, and 8 weeks of age. We found that on the rotarod, which tests balance and coordination, there was no deficit in hypoxia exposed pups (Fig. 3.7A). Nevertheless, when testing strength of all limbs with the grid test we found a mild deficit at 4 weeks of age that recovered by 6 and 8 weeks of age even though at P60 neonatal hypoxia exposed animals had thinner myelin (Fig. 3.7B). However, the rotarod and grid tests are crude measures that lack sensitivity. Therefore, we performed more sensitive grip strength measures using a dynamometer. Both forelimb and hindlimbs were tested and we found that neonatal hypoxia reared pups had significantly weaker forelimbs and hindlimbs at 4, 6, and 8 weeks (Fig. 3.7C and 3.7D). Importantly, the decreased strength of forelimbs and hindlimbs remained even after the weight of neonatal hypoxia reared pups recovered (Fig. 3.7F). Finally, to determine whether neonatal hypoxia leads to electrophysiological deficits that could cause the

observed motor deficits we measured latency, conduction velocity, and amplitude while artificially stimulating the sciatic nerve. We discovered that hypoxia exposed mice had slower conduction velocity when stimulating the sciatic nerve that correlates with the thinner myelin sheaths seen at P60 in mice exposed to neonatal hypoxia (Fig. 3.7E). These results show that the effects of neonatal hypoxia lead to PNS motor and electrophysiological deficits that persist in adult animals.

3.5 Discussion

In this study we demonstrate that neonatal hypoxia leads to hypomyelination characterized by decreased myelin thickness and delayed development of axon bundles in the PNS of mice. Moreover, we show that neonatal hypoxia causes sustained electrophysiological and motor deficits. These studies indicate that neonatal hypoxia has similar effects on the PNS as on the CNS and suggests that more attention be paid to potential PNS myelin damage in premature infants exposed to hypoxic insults.

A large body of clinical research has established that preterm infants, especially those with low birth weight, have significant motor impairment (Hemgren and Persson 2009; de Kieviet et al. 2009; Poole et al. 2015; Cooke and Foulder-Hughes 2003; Salt and Redshaw 2006). Importantly, these motor deficits are a risk factor for poor cognitive performance, behavioral problems, and learning disabilities due to their effect on a child's ability to explore the world and involvement in social activities (Losch and Dammann 2004; Piek et al. 2008; Diamond 2000). This highlights the importance of motor consequences in premature infants and the potential positive impacts of preventing motor deficits. This study shows that part of those motor deficits may be a result of perturbed PNS myelination.

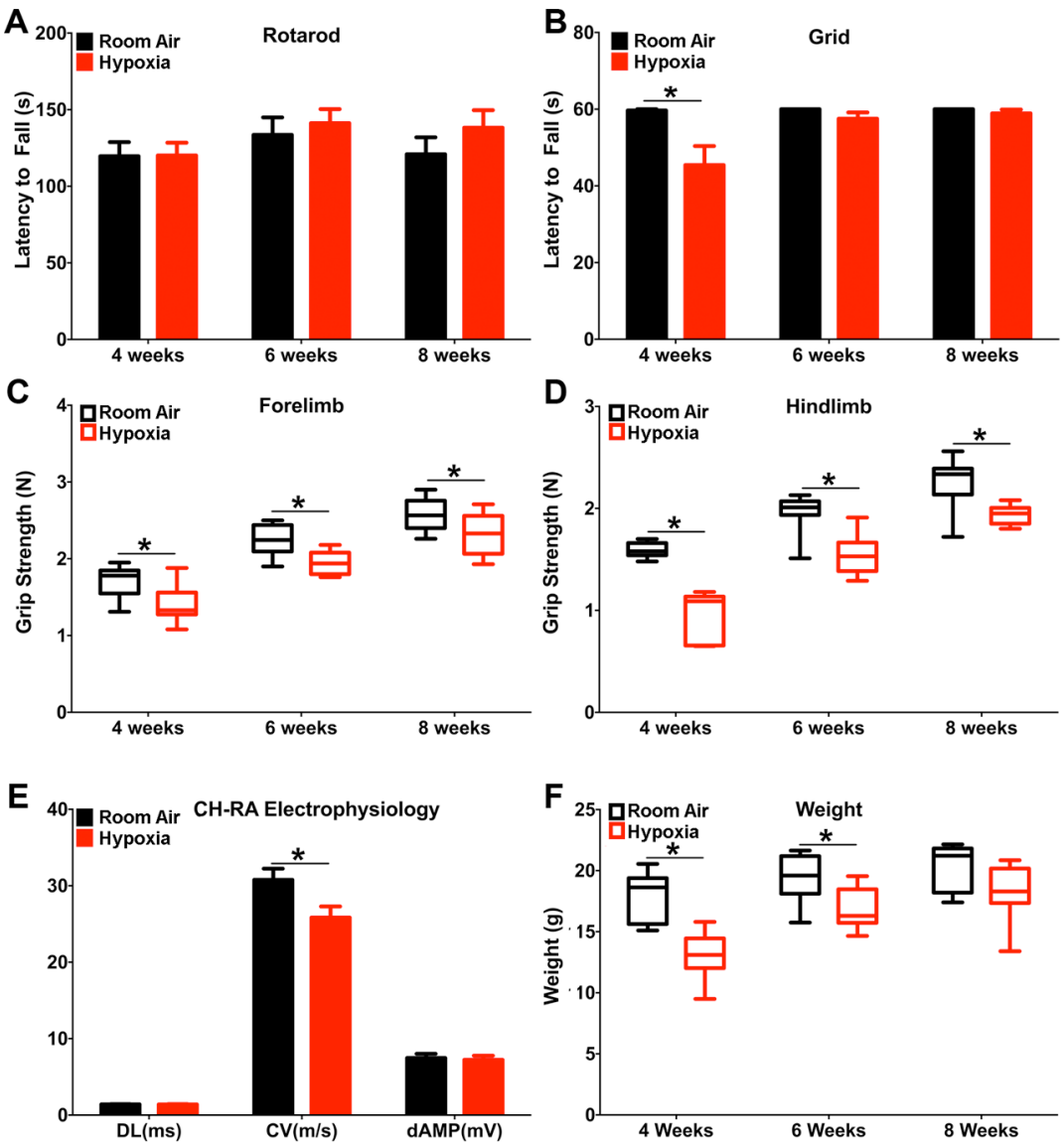

Figure 3.7. Neonatal hypoxia causes long-term motor and electrophysiological deficits. Motor deficits in mice previously exposed to hypoxia was measured in multiple motor tests at 4, 6, and 8 weeks of age. (a) Hypoxia had no effect on motor balance and coordination measured by rotarod. (b) Compared to room air controls, hypoxia exposed mice exhibited a decreased latency to fall in the grid test at 4 weeks of age that recovered by 6 weeks of age. (c) Forelimb and (d) hindlimb grip strength were significantly weaker in NH exposed mice at all time points measured. (e) In agreement with PNS myelin deficits hypoxia exposed pups had significantly slower conduction velocity at P60. (f) Hypoxia exposed animals weighed less than control animals at 4 and 6 weeks of age but recover to control levels at 8 weeks. Data presented as mean±sem for N=8-9 mice, *P<0.05 by two-tailed *t*-Test. For box and whisker plots the box represents the 25th to 75th percentile with the median designated by a line and the whiskers representing the minimum and maximum values.

We found that neonatal hypoxia caused decreased myelin thickness in the PNS. This decrease in myelin thickness was evident at all time points investigated, from P7 and P11 when the hypoxic insult was still ongoing, persisting at P18 after 7 days of recovery and even into adulthood at P60. This sustained hypomyelination likely underlies the decreased sciatic nerve conduction velocity in P60 mice previously exposed to neonatal hypoxia and the decreased forelimb and hindlimb strength found at 4, 6, and 8 weeks of age. However, the mechanism behind neonatal hypoxia induced hypomyelination of the PNS remains elusive. In the CNS neonatal hypoxia leads to death of OPCs that are quickly replenished by proliferating OPCs that fail to differentiate into myelinating oligodendrocytes (Salmaso et al. 2014). It is the failed maturation of replenishing OPCs, possibly due to hypoxia driven increased Wnt signaling, that is thought to underlie the behavioral deficits seen in adult mice previously exposed to neonatal hypoxia (Scafidi et al. 2014; Salmaso et al. 2014; Yuen et al. 2014). In the PNS we report decreased myelin thickness resulting from neonatal hypoxia, similar to the thinner myelin phenotype seen in the CNS of mice exposed to neonatal hypoxia. Therefore, we explored the possibility that hypoxia driven PNS hypomyelination is a result of fewer mature Schwann cells caused by death and/or inhibited maturation of Schwann cells due to hypoxia activated Wnt signaling. Unlike other reports of PNS hypomyelination we found no evidence that hypoxia decreases expression of mature Schwann cell markers KROX20, MAG, P0, and MBP (Fig. 3.4B) (Elbaz et al. 2016; Grigoryan et al. 2013). In addition, neonatal hypoxia did not increase in immature Schwann cell markers SOX2 and GalC, as one would predict when Schwann cell maturation is blocked (Elbaz et al. 2016; Grigoryan et al. 2013). Furthermore, while the density of KROX20+ cells was increased in neonatal hypoxia exposed P11 mice, this was caused by decreased tissue volume and not an effect on the number of KROX20+ cells. These results

strongly suggest that in the PNS neonatal hypoxia is causing hypomyelination through a mechanism that is distinct from those known to play a role in the CNS. Further studies are needed to understand the mechanism behind neonatal hypoxia induced PNS hypomyelination.

In conclusion, our studies have established that neonatal hypoxia causes sustained hypomyelination in the PNS and leads to long-term electrophysiological and motor deficits. These results suggest that the effects of neonatal hypoxia on PNS myelination may be an undervalued contributor to neurodevelopmental disabilities caused by premature birth, and warrant greater attention.

Chapter 4. Discussion

4.1 Summary

Myelin and myelinating glia are crucial to the proper function of the mammalian nervous system. Disruption in oligodendrocytes and Schwann cells cause a variety of diseases, some mild and others severe in their phenotypes and clinical outcomes (Clayton and Popko 2016). One such disorder of myelin and myelinating glia is DWMI. DWMI is a white matter disorder that affects premature infants born between 23-32 weeks of gestation with higher prevalence and severity in very low birthweight preterm infants (<1500g). A significant cause of DWMI is hypoxia caused by immature lung development. In the premature infant hypoxia preferentially damages OPCs leading first to cell death followed by arrested maturation of replenishing OPCs that results in impaired myelinogenesis during a critical developmental time window and leads to altered microstructure and connectivity in the developing brain. This neurological damage is thought to underlie the sensory, motor, behavioral, and cognitive deficits experienced by over 50% of individuals who survive prematurity, including the 5-10% of premature infants with severe white matter damage resulting in cerebral palsy (Back et al. 2015). Unfortunately, there are currently no clinically approved therapies to prevent DWMI. In addition, the incidence of DWMI is increasing as the percentage of preterm births increases and survival of preterm infants, especially very low birthweight infants, improves due to improved neonatal care. This precipitates a critical need for an increased understanding of the pathophysiology of DWMI with the goal of uncovering novel therapeutic targets, and developing new therapies for this growing patient population.

The ISR is a conserved stress response in all eukaryotic cells that is activated by, and provides protection from, various cellular stresses, including hypoxia. The ISR is initiated by one of four stress sensing kinases, of which PERK is the putative responder to hypoxia, which phosphorylates eIF2α (Donnelly et al. 2013). Phosphorylation of eIF2α leads to inhibition of global protein translation and upregulation of cytoprotective genes through ATF4, a transcription factor that along with a host of other transcripts contains appropriate regulatory elements that allow for increased translation under conditions of eIF2α phosphorylation (Pavitt et al. 2012). ATF4 also induces expression of CHOP, CHOP in turn increases GADD34 expression. GADD34 then forms a complex with PP1 and dephosphorylates eIF2α terminating the ISR. While initially protective, in the face of unresolved stress the ISR can become pro-apoptotic through accumulation of CHOP. The PERK arm of the ISR is a proven cytoprotective pathway in oligodendrocyte lineage cells (Way et al. 2015). Inhibiting the ISR through removal of PERK from oligodendrocytes exacerbates myelin loss and oligodendrocyte death caused by inflammation, while enhancing the ISR by exogenous activation of PERK or deletion of GADD34 to diminish eIF2α dephosphorylation, protects oligodendrocytes from inflammation. Given its protective role in oligodendrocytes and known activation by hypoxia, the ISR, and specifically the PERK pathway, is a potential therapeutic target for DWMI.

Chapter 2 of This thesis reports on original work towards addressing the hypothesis that: *The PERK arm of the ISR plays an active role in hypoxia induced DWMI and that inhibition of this pathway will exacerbate DWMI while enhancement of the PERK pathway will protect oligodendrocytes and myelin from hypoxia induced DWMI.*

Hypoxia as an inhibitor of oligodendrocyte maturation can be modeled *in vitro* utilizing isolated primary OPCs (Yuen et al. 2014). OPCs exposed to 0.1% O_2 *in vitro* for 3 and 6 hours significantly increased phosphorylation of eIF2α in a time dependent manner characteristic of ISR activation (Fig. 2.3). The increase in phosphorylation of eIF2α driven by hypoxia was significantly diminished in OPCs generated from OL-PERK-null mice and expressing 95% less PERK protein compared to control OPCs (Fig 2.1 and 2.3). This data agrees with published work establishing PERK as the primary eIF2α kinase responsible for eIF2α phosphorylation in response to hypoxia. However, overlap between eIF2α kinases is known and GCN2 is also reported to respond to hypoxia. This overlap in eIF2α stress sensing is likely responsible for the substantially diminished increase in peIF2α in PERK ablated OPCs at 6 hours of 0.1% O_2 (Fig. 2.3). Still, OPCs with decreased PERK expression were significantly more susceptible to hypoxia during *in vitro* maturation to oligodendrocytes. Hypoxia decreased the percentage of MBP positive cells after 48hrs of differentiation in wild-type cells and to a significantly greater extent in cells lacking protective PERK signaling (Fig 2.4). These data demonstrate that PERK is activated and protects oligodendrocyte lineage cells from *in vitro* hypoxia.

The established MCH mouse model was used to study the ISR in *in vivo* hypoxia induced DWMI. The MCH model was shown to decrease myelin enriched mRNA and protein levels (Fig. 2.5 and 2.6), decrease MBP staining (Fig. 2.6), and decrease mature oligodendrocyte numbers in subcortical white matter (Fig. 2.6). MCH also increased peIF2α in total brain similar, although to a lesser extent than *in vitro* hypoxia (Fig. 2.7). However, OL-PERK-null mice challenged with MCH were not more vulnerable compared to OL-PERK-FL controls. In fact, there was no significant difference in MCH-induced DWMI in OL-PERK-null and OL-PERK-FL mice (Fig. 2.10). This differed from the predicted outcome since inhibition of the ISR via loss of PERK in

oligodendrocyte lineage cells was expected to exacerbate MCH-induced DWMI, similar to the results using *in vitro* hypoxia. The incongruent effects of PERK deletion *in vitro* and *in vivo* may be a result of the effective oxygen tension experienced by oligodendrocytes in each model. Culture cells are more accessible to hypoxic treatment and lack the confounding factor of systemic effects present in the whole animal, including intolerance of chronic hypoxic stress approaching anoxia. Therefore, it is likely oligodendrocyte lineage cells in culture are experiencing a higher severity of hypoxia compared to cells *in vivo*, and it is known that the ISR response to hypoxia depends on oxygen concentration with stronger ISR activation occurring in response to severe hypoxia (Koumenis et al. 2002). We also cannot rule out the possibility that while the effect on oligodendrocyte lineage cells and myelin are the same between control and OL-PERK-null mice, this does not mean that the underlying mechanism is the same. It is possible that effects the underlying mechanism that ultimately results in the same measurable phenotype. It is also possible that MCH does not activate the PERK arm of the ISR in oligodendrocyte lineage cells. A weakness of this work is that the cellular localization of MCH-induced peIF2α increase was not established. If the ISR in oligodendrocytes is refractor to MCH then oligodendrocyte specific ablation of *Perk* would be ineffective.

Although inhibition of the ISR had no effect on DWMI caused by MCH it was still possible that enhancing the ISR through *Gadd34* deletion could have a protective effect. Surprisingly though, global *Gadd34* deletion exacerbated MCH triggered DWMI (Fig. 2.11). Again this defied the predicted outcome, in addition, GADD34-null mice exposed to MCH weighed significantly less and had significantly higher mortality compared to GADD34-WT mice challenged with MCH. This pointed to a potential systemic and detrimental effect of combined MCH and loss of GADD34. A possibility is that GADD34 deficiency was leading to

accumulation of CHOP that in the face of unresolved stress is pro-apoptotic. To test this hypothesis, GADD34/CHOP double null mutant mice were exposed to MCH to determine whether CHOP removal rescued the increased mortality phenotype present in the MCH exposed GADD34-null mice. However, survival was not increased in GADD34/CHOP double null mutants challenged with MCH suggesting that accumulation of pro-apoptotic CHOP is not responsible. Although, it should be mentioned that a recent report shows overexpression of CHOP in myelinating glia does not cause apoptosis and therefore the function of CHOP within oligodendrocyte lineage cells is controversial (Southwood et al. 2016). Levels of peIF2α protein were measured in GADD34-WT and GADD34-null mice subjected to MCH to determine whether loss of GADD34 function enhances MCH driven eIF2α phosphorylation in the brain, which it did not (Fig. 2.12). Nevertheless, this was not due to a technical problem with the mouse line since these same mice exhibited increased peIF2α in GADD34-null heart compared to GADD34-WT heart (Fig. 2.13). Finally, because MCH is a global stress and the ISR is ubiquitous there are a myriad of systems in which the combination of MCH and loss of GADD34 could become lethal. In response to hypoxia erythropoiesis and increased hemoglobin production occur in order to adapt. Interestingly, a distinct GADD34 mutant mouse was characterized and shown to have a mild deficit in hemoglobin production (Patterson et al. 2006) that was tolerated under normal conditions but might increase susceptibility to hypoxia. Therefore, a pilot study was completed where a complete blood count was run on blood from GADD34-WT and GADD34-null pups after 4 days of MCH. GADD34-WT pups responded to MCH by increasing red blood cells and hemoglobin, while GADD34-null mice did not (Fig. 2.14). This deficit in hematopoietic adaptation to hypoxia is a possible mechanism for increased vulnerability of GADD34-null mice to MCH that requires further study.

Manipulation of the ISR in MCH is either ineffective or detrimental, despite the fact that OPCs lacking PERK are more susceptible to *in vitro* hypoxia. However, as discussed the severity of the *in vitro* hypoxia is likely greater than that of MCH, in addition, the *in vitro* hypoxic insult occurred over a much shorter time-frame. This combined with the presumptive switch from protective to pro-apoptotic that occurs under conditions of unresolved stress, makes it reasonable to suggest that within oligodendrocytes the ISR might be best suited for survival in the face of severe acute stress and not adaptation in the mild chronic stress. Therefore, the role of the ISR was examined in a newly developed SAH mouse model of DWMI.

SAH led to decreased levels of myelin enriched mRNA and protein levels (Fig. 2.15 and Fig. 2.16), decreased MBP staining (Fig 2.16), and decreased numbers of mature oligodendrocytes in subcortical white matter (Fig. 2.16). These results were very similar to the effect of MCH and as such SAH was validated as model of DWMI. Similar to MCH, SAH also increased peIF2α although more rapidly corresponding with the severe acute nature of the hypoxic insult (Fig. 2.17). OL-PERK-null and control OL-PERK-FL mice were challenged with SAH to determine whether loss of PERK signaling has an effect in in the severe acute stress compared to no effect in the mild chronic stress. Nonetheless, loss of PERK signaling in oligodendrocyte lineage cells did not have a significant effect on SAH-induced DWMI (Fig. 2.19). This supports the conclusion that PERK does not play a critical role in hypoxia induced DWMI regardless of severity or length of exposure. Next, GADD34-WT and GADD34-null mice were exposed to SAH. In contrast to the results from GADD34 null mutation and MCH, loss of GADD34 in mice exposed to SAH had no significant effect on DWMI (Fig. 2.20), nor did it have a significant effect on body weight or mortality. This supports the interpretation that

inhibition of eIF2α dephosphorylation via removal of GADD34 is not a valid therapeutic target in situations of chronic stress that requires adaptation rather than survival.

One intriguing finding from these studies is that none of the hypoxic insults examined lead to increased levels of ATF4 protein, despite causing increased levels of peIF2α (Fig. 2.3, 2.7, and 2.17). In fact, both MCH and SAH significantly decrease ATF4 protein levels during periods of increased peIF2α. Conventional understanding of the ISR conditions that increased peIF2α leads to higher translation of ATF4 and therefore higher levels of ATF4 protein. This does not hold true in these studies of hypoxia, which is surprising given reports of increased ATF4 protein after *in vitro* hypoxia (Blais et al. 2004; Halterman et al. 2010; Rzymski et al. 2010). However, none of these studies were performed on myelinating glia and as has been discussed, the PERK pathway within myelinating glia may respond differently. In addition, many studies were performed at anoxia. Interestingly, HIF1α, the major regulator of the hypoxic response, is reported to be a repressor of ATF4 and ATF4 targets (Guimarães-Camboa et al. 2015). This leads to the intriguing possibility that under anoxic conditions the transcriptional response driven by ATF4 is critical for survival, however, when oxygen is present, even at very low levels, the cell opts to repress ATF4 in favor of an adaptive transcriptional response driven by HIF1α.

In conclusion, the PERK pathway of the ISR plays a critical role in protecting oligodendrocyte lineage cells from *in vitro* hypoxia. However, genetic manipulation of the ISR under MCH or SAH stress is either ineffective or detrimental. Therefore, the ISR does not appear to be a valid therapeutic target for hypoxia induced DWMI.

The deleterious effects of neonatal hypoxia on oligodendrocyte lineage cells and CNS myelination are well known (Scafidi et al. 2014; Yuen et al. 2014; Fancy et al. 2011), however,

the effects of neonatal hypoxia on Schwann cells and PNS myelination have not been studied. Sensorimotor deficits are a common outcome of neonatal hypoxia and can effect a child's exploration of the environment and social interaction contributing to behavioral and cognitive deficits (Losch and Dammann 2004; Piek et al. 2008; Diamond 2000). Examining the effects of neonatal hypoxia on PNS myelination will further our understanding of the morbidities experienced by premature infants and has the potential to open up a previously underappreciated area for therapeutic intervention.

Chapter 3 of this thesis reports on original work towards addressing the hypothesis that: *Neonatal hypoxia disrupts developmental myelination within the PNS.*

A mouse model of *in vivo* neonatal hypoxia was used to examine the effects of hypoxia on Schwann cells and myelin in the developing PNS (Fig. 3.1). Electron microscopy was utilized to measure the thickness of myelin sheaths in control and hypoxia exposed mice. At every time point investigated, both during and after recovery from the hypoxic insult, hypoxia challenged mice exhibited thinner myelin sheaths compared to room air controls (Fig. 3.2). Thinner myelin sheaths were however, not associated with a decreased percentage of myelinated fibers (Fig. 3.2). In addition to myelination, Schwann cells surround axon bundles in the developing PNS and radial sort the growing axons as they increase in diameter with individual Schwann cells eventually removing the large caliber axons from the bundle and myelinating them in a 1:1 relationship (Feltri et al. 2016). Damage to Schwann cells during development can therefore cause myelination and/or sorting deficits. Using electron microscopy, the axon bundles in PNS of neonatal hypoxia exposed and control mice were examined. At P7 and P11, time points during the hypoxic challenge, mice exposed to neonatal hypoxia exhibited larger axon bundles with increased numbers of axons per bundle (Fig. 3.3). This is evidence of an early

radial sorting deficit that recovered when the mice were returned to room air. Together these data support the conclusion that neonatal hypoxia has an injurious effect on development of the PNS.

Neonatal hypoxia causes damage to the premature brain by first causing cell death of OPCs and then inhibiting maturation of the replenishing OPCs. This leads to a decrease in the number of mature oligodendrocytes and decreased expression of transcripts associated with mature oligodendrocytes (Fig. 2.5 and 2.6). To explore whether neonatal hypoxia leads to decreased numbers of Schwann cells in the PNS, P11 mice exposed to 8 days of either hypoxia or room air were fixed and stained for the mature Schwann cell marker KROX20. In agreement with the results of qPCR analysis, neonatal hypoxia had no effect on the total number of KROX20 positive Schwann cells in the PNS (Fig. 3.5). In fact, despite a significant decrease in total tissue area, the total numbers of Schwann cells did not change leading to higher Schwann cell density (Fig. 3.5). To validate this interpretation, RNA was collected from P7 mice exposed to 4 days of either hypoxia or room air, and quantitative real-time PCR analysis was performed using primers against immature Schwann cell markers Sox2 and GalC, and against mature Schwann cell markers KROX20, MAG, P0, and MBP. Neonatal hypoxia did not lead to a significant change in either immature or mature Schwann cell transcripts (Fig. 3.4) suggesting that neonatal hypoxia does not cause either death or arrested maturation of Schwann cells. These results support the conclusion that hypomyelination and axon bundle defects in the PNS of hypoxia exposed animals is not a result of decreased mature Schwann cell numbers.

Neonatal hypoxia in the CNS has been shown to increase Wnt signaling that damages OPCs contributing to the hypomyelination phenotype seen in neonatal hypoxia exposed mice Furthermore, increased Wnt signaling in PNS Schwann cells is known to cause disrupted myelination and radial sorting (Elbaz et al. 2016; Grigoryan et al. 2013). Hypoxic activation of

Wnt signaling in Schwann cells has not been reported. To determine whether neonatal hypoxia activates Wnt signaling in Schwann cells, expression levels of activated Wnt signaling markers Lef1, Axin2, and c-Myc were investigated. In contrast to the CNS, neonatal hypoxia did not have a significant effect on the expression of Lef1, Axin2, and c-Myc, suggesting that neonatal hypoxia does not activate Wnt signaling in PNS Schwann cells.

The mechanism of hypoxia induced damage to the developing CNS remains an open question. It is possible that the effects of neonatal hypoxia on Schwann cells are mild and driven by the decreased energy due to a switch from oxidative phosphorylation to glycolysis driven ATP production under hypoxic conditions. It was therefore important to determine whether the defects in the hypoxia challenged PNS are robust enough to produce an adverse behavioral and/or physiological phenotype. To that end, neonatal hypoxia and control mice were tested with a battery of motor tests from 4 weeks to 8 weeks of age. Neonatal hypoxia did not cause a significant deficit in performance on the rotarod, and a small but transient deficit in the grid test (Fig. 3.7). However, these tests are crude and are unable to detect subtle differences in motor performance. Upon a more sensitive examination of forelimb and hindlimb grip strength it was found that neonatal hypoxia caused a significant decrease in grip strength in both sets of limbs that did not recover over the time period tested (Fig. 3.7). This result showed that the decreased thickness of PNS myelin caused by neonatal hypoxia and still present in adulthood is robust enough to impair motor performance. Finally, electrophysiological measurements of compound action potentials from the sciatic nerve showed that at P60 mice previously exposed to neonatal hypoxia had significantly slower conduction velocity compared to controls (Fig. 3.7). This result is in agreement with the expected effect of thinner myelin sheaths seen at P60, and coincides with the motor deficits measured in adult mice previously challenged with neonatal hypoxia.

In conclusion, the results from this work suggest that deficits in PNS development represent an underappreciated injury associated with premature birth and neonatal hypoxia. It is crucial to further support these results with studies of PNS injury in human premature neonates. If present, PNS injury could represent a significant contributor to sensorimotor deficits experienced by over 50% of infants that survive premature birth, and holds the potential to open new therapeutic avenues for these children.

4.2 Potential interplay between the ISR and other hypoxia induced pathways

One interesting finding from my studies is that hypoxia, whether *in vitro* or *in vivo*, and whether mild and chronic or severe and acute, increases levels of peIF2α without the expected increase in ATF4 protein levels, and without the corresponding increase in expression of CHOP and GADD34 that would be expected. The mechanism of partial ISR activation in these hypoxic insults is not understood and requires further study. It is important to remember that stress pathways are often activated simultaneously within the same cell with the potential for interactions that increases the complexity of stress response. Activation of a partial ISR as a result of hypoxia may be an example of different hypoxia induced pathways interacting to provide the cell with appropriate molecular mechanisms to survive and adapt. As discussed in section 1.8, HIF1α has been reported to repress ATF4 expression and the expression of ATF4 target genes. In addition, it has been shown that the ISR is involved in translational control of HIF1α targets like carbonic anhydrase 9 and VEGF (van den Beucken et al. 2009; Barbosa, Peixeiro, and Romão 2013). It is unknown how many genes

are subject to translational control through uORFs and peIF2α, estimates have shown that approximately half of all human and mouse genes contain at least a single uORF (Pavitt and Ron 2012). This combination of transcriptional control through HIF1α and translational control through eIF2α phosphorylation provides cells with exquisite control over protein expression to survive and adapt to hypoxia.

Another control mechanism that effects gene and therefore protein expression is epigenetics, where DNA methylation and histone modification increases or decreases the availability of genes for transcription. Histone deacetylase proteins (HDACs) are known to influence oligodendrocyte differentiation (J. Liu and Casaccia 2010; S. Shen and Casaccia-Bonnefil 2008) and play a role in the regulation of hypoxic response gene expression (Tsai and Wu 2014). In addition, because epigenetic regulation of gene expression occurs prior to translation, epigenetic changes induced by hypoxia could affect the expression of ISR components. Therefore, it is an intriguing possibility that epigenetic changes are responsible for inhibiting the expression of ATF4 and other downstream ISR components under conditions of hypoxia induced eIF2α phosphorylation.

.

4.3 Future of neonatal hypoxia and PNS myelination.

Results have been presented here that show neonatal hypoxia damages the PNS leading to hypomyelination and persistent motor deficits. Being an initial investigation of this topic there are many questions that remain to be answered. Two that I believe need to be addressed in order for this work to progress. First, supportive evidence of PNS deficits in premature infants is needed. To my knowledge no such evidence exists. Is this because clinicians have not looked at the PNS instead focusing on CNS effects neonatal hypoxia, or because injury to the PNS does

not occur? This question needs to be addressed in order to judge the therapeutic potential of protecting the developing PNS from hypoxia. The second major remaining question is of the mechanism behind neonatal hypoxia induced PNS hypomyelination. Translation inhibition is a well-known adaptive response to hypoxia. Therefore, one interesting possibility is that, similar to what I've shown in the CNS, neonatal hypoxia activates the ISR in PNS Schwann cells. Chronic hypoxic activation of the ISR in Schwann cells could cause decreased protein and lipid synthesis, and due to the unique behavior of CHOP in myelinating glia, without causing apoptosis. Of course hypoxia is a promiscuous insult and activates multiple pathways including mTOR signaling that leads to reduced translation under prolonged exposure to hypoxia. While to this point I have focused on the potential direct effects of neonatal hypoxia on Schwann cells it is possible that neonatal hypoxia has a direct effect on axons in the PNS. In the PNS myelination is controlled by signals from the axon to Schwann cells, of which the NRG1/ErbB signaling pathway is crucial. NRG1 controls the amount of myelin produced by Schwann cells since overexpression of NRG1 type III significantly increases myelin thickness, while mice that are haploinsufficient for NRG1 type III have thinner PNS myelin. An investigation of the expression of molecules known to play a role in axon-glial should be one of the next steps taken to understand the mechanism behind neonatal hypoxia induced hypomyelination of the PNS.

4.4 Future of the SAH model of DWMI

Although the established model of DWMI involved mild chronic hypoxia over the course of a week, I present here evidence that severe acute hypoxia can lead to DWMI with only 24hrs of exposure. I believe that this new model of DWMI holds significant potential. Premature infants are challenged by both acute and chronic hypoxia and the effects of each insult on

oligodendrocyte lineage cells and myelin may be distinct. For example, in my work I found that mice exposed to chronic hypoxia were more vulnerable to disruption in GADD34 dependent dephosphorylation of eIF2α. However, mice exposed to acute hypoxia and lacking GADD34 were not significantly different than control mice exposed to acute hypoxia. Multiple pathways have been associated with MCH induced DWMI, including EGF receptor signaling and Wnt signaling. It would be of interest to know whether these pathways also play a role in SAH induced DWMI, and whether or not the experimental interventions targeted to those pathways are similarly beneficial in SAH. Further use of the SAH model has the potential to contribute to the fields understanding of the pathophysiology behind DWMI.

There are also many unanswered questions regarding the characterization of the SAH model itself. One weakness of the MCH model is that it does not generate gliosis that is a characteristic of the human disease. It would be interesting to know whether the outcomes of SAH include gliosis. Are there regional differences in SAH induced DWMI? White matter damage caused by MCH has been reported in the cortex, the cerebellum, and now the PNS. Is SAH similarly injurious to multiple regions within the nervous system? Finally, while not a focus of my thesis there is a growing appreciation for neuronal deficits caused by premature birth and neonatal hypoxia. These gray matter lesions seem to be caused in part by dysmaturation of GABAergic inhibitor interneurons (Back 2014; Zonouzi et al. 2015) and it would be of interest to determine whether SAH has similar effects on neurons or whether damage is restricted to oligodendrocyte lineage cells alone.

4.5 Future of the ISR and DWMI

The grand vision of this thesis was to establish the involvement of a novel pathway, the ISR, in hypoxia induced DWMI and show that manipulation of the ISR, specifically inhibition of GADD34, could be used to protect oligodendrocytes and white matter. However, the results of my studies show that the role of the ISR in hypoxia, whether MCH or SAH, induced DWMI is not critical and that manipulating the ISR is at best ineffective and at worst deleterious. These findings support the conclusion that the ISR is not a valid therapeutic target in hypoxia induced DWMI.

However, while hypoxia alone is a major contributor to DWMI it is not the only contributor to DWMI. Inflammation is also known to play a role in the pathogenesis of DWMI. In addition, the Popko lab has shown that the ISR is a significant player in inflammatory damage to oligodendrocytes in a model of multiple sclerosis and in a genetic approach where IFN-ɣ is expressed ectopically by astrocytes and causes oligodendrocyte death and hypomyelination. These findings are discussed in detail in section 1.5.1. Therefore, it is possible that the ISR plays a role in DWMI caused by inflammation instead of hypoxia. I performed preliminary studies using a systemic injection of gram-negative membrane component lipopolysaccharide (LPS) to model DWMI and did not see evidence of ISR activation nor an effect of genetic manipulation of the ISR. However, this model requires precise injection of LPS subcutaneously into P2 pups that is technically challenging. Therefore, it is possible that inconsistent injections were behind the lack of an association between inflammation and the ISR in the LPS model and a more focused investigation of the ISR in inflammation induced DWMI is warranted.

Although decreasing in prevalence severe white matter damage in premature infants caused by hypoxia and ischemia still occurs. As discussed in section 1.7.1 OGD is used as an *in*

vitro model of hypoxia and ischemia that causes OPC cell death. Moreover, OGD consists of two insults, hypoxia and glucose deprivation, which independently are activators of the ISR. This suggests that the ISR may play a larger role in OGD. I have data that show that OGD is a strong activator of the ISR, and preliminary data that suggests inhibition of the ISR may sensitize OPCs to OGD. As discussed in section 1.7.2 the Rice-Vannucci model of neonatal hypoxia and ischemia is a well-established model that generates more severe white matter injury, especially when paired with systemic inflammation caused by LPS injection, and would be applicable to studies using transgenic mice to investigate a potential role of the ISR. Importantly, one of the defining characteristics of the ISR, the integration of various stresses upon activation of a single peIF2α driven pathway, makes it uniquely position to respond to white matter injury caused by a combination of hypoxic, ischemic, and inflammatory insults.

4.6 Final thoughts

The power of targeting the ISR in diseases of myelin and myelinating disorders is clear. As discussed in section 1.5, many myelin disorders have known involvement of the ISR, specifically the PERK pathway. However, manipulation of a pathway central to protein synthesis without causing severe side effects will be difficult. In addition, within myelinating disorders manipulation of the ISR can have seemingly contradictory effects, for example deletion of CHOP is detrimental in mouse models of PMD (Southwood et al. 2002) but protective in mouse models of CMT1B (Pennuto et al. 2008) and has no effect on EAE (Deslauriers et al. 2011). Therefore, it will be important to have a full understanding of ISR signaling within each disease to better predict the effect that manipulating the ISR will have in patients. Presented in this thesis

is novel work that contributes to a better understanding of the ISR in hypoxia induced DWMI, a prevalent white matter disorder affecting premature infants.

Bibliography

Ameri, K, C E Lewis, M Raida, H Sowter, T Hai, and A L Harris. 2004. "Anoxic Induction of ATF-4 through HIF-1-independent Pathways of Protein Stabilization in Human Cancer Cells." *Blood* 103 (5): 1876–82. doi:10.1182/blood-2003-06-1859.

Auer, R N. 1994. "Automated Nerve Fibre Size and Myelin Sheath Measurement Using Microcomputer-based Digital Image Analysis: Theory, Method and Results." *Journal of Neuroscience Methods* 51 (2): 229–38. doi:10.1016/0165-0270(94)90015-9.

Baba, H, H Akita, T Ishibashi, Y Inoue, K Nakahira, and K Ikenaka. 1999. "Completion of Myelin Compaction, but Not the Attachment of Oligodendroglial Processes Triggers K+ Channel Clustering." *Journal of Neuroscience Research*, December. http://onlinelibrary.wiley.com/store/10.1002/(SICI)1097-4547(19991215)58:6%3C752::AID-JNR3%3E3.0.CO;2-D/asset/3_ftp.pdf?v=1&t=iirkk83p&s=2e7a4de49c473f6cb282bc9437f36b4f2fcbeb5d.

Back, S A. 2014. "Cerebral White and Gray Matter Injury in Newborns: New Insights into Pathophysiology and Management." *Clinics in Perinatology* 41 (1): 1–24. doi:10.1016/j.clp.2013.11.001.

Back, S A. 2015. "Brain Injury in the Preterm Infant: New Horizons for Pathogenesis and Prevention." *Pediatric Neurology* 53 (3): 185–92. doi:10.1016/j.pediatrneurol.2015.04.006.

Back, S A, A Craig, R J Kayton, N L Luo, C K Meshul, N Allcock, and R Fern. 2007. "Hypoxia-ischemia Preferentially Triggers Glutamate Depletion from Oligodendroglia and Axons in Perinatal Cerebral White Matter." *Journal of Cerebral Blood Flow and Metabolism* 27 (2): 334–47. doi:10.1038/sj.jcbfm.9600344.

Back, S A, A Craig, N L Luo, J Ren, R S Akundi, I Ribeiro, and S A Rivkees. 2006. "Protective Effects of Caffeine on Chronic Hypoxia-induced Perinatal White Matter Injury." *Annals of Neurology* 60 (6): 696–705. doi:10.1002/ana.21008.

Back, S A, X Gan, Y Li, P A Rosenberg, and J J Volpe. 1998. "Maturation-dependent Vulnerability of Oligodendrocytes to Oxidative Stress-induced Death Caused by Glutathione Depletion." *The Journal of Neuroscience* 18 (16): 6241–53.

Back, S A, N L Luo, R A Mallinson, J P O'Malley, L D Wallen, B Frei, J D Morrow, et al. 2005. "Selective Vulnerability of Preterm White Matter to Oxidative Damage Defined by F2-isoprostanes." *Annals of Neurology* 58 (1): 108–20. doi:10.1002/ana.20530.

Back, S A, and S P Miller. 2014. "Brain Injury in Premature Neonates: A Primary Cerebral Dysmaturation Disorder?" *Annals of Neurology* 75 (4): 469–86. doi:10.1002/ana.24132.

Back, S A, A Riddle, and M M McClure. 2007. “Maturation-dependent Vulnerability of Perinatal White Matter in Premature Birth.” *Stroke* 38 (2 Suppl): 724–30. doi:10.1161/01.STR.0000254729.27386.05.

Barbosa, C, I Peixeiro, and L Romão. 2013. “Gene Expression Regulation by Upstream Open Reading Frames and Human Disease.” *PLoS Genetics* 9 (8): e1003529. doi:10.1371/journal.pgen.1003529.

Barnett, M H, and J W Prineas. 2004. “Relapsing and Remitting Multiple Sclerosis: Pathology of the Newly Forming Lesion.” *Annals of Neurology* 55 (4): 458–68. doi:10.1002/ana.20016.

Barres, B A, M A Lazar, and M C Raff. 1994. “A Novel Role for Thyroid Hormone, Glucocorticoids and Retinoic Acid in Timing Oligodendrocyte Development.” *Development* 120 (5): 1097–1108.

Barres, B A, R Schmid, M Sendnter, and M C Raff. 1993. “Multiple Extracellular Signals Are Required for Long-term Oligodendrocyte Survival.” *Development* 118 (1): 283–95.

Bartlett, P F, M D Noble, R M Pruss, M C Raff, S Rattray, and C A Williams. 1981. “Rat Neural Antigen-2 (RAN-2): a Cell Surface Antigen on Astrocytes, Ependymal Cells, Müller Cells and Lepto-meninges Defined by a Monoclonal Antibody.”, January.

Beitner-Johnson, D, R T Rust, T C Hsieh, and D E Millhorn. 2001. “Hypoxia Activates Akt and Induces Phosphorylation of GSK-3 in PC12 Cells.” *Cellular Signalling* 13 (1): 23–27. doi:10.1016/S0898-6568(00)00128-5.

Bercury, K K, and W B Macklin. 2015. “Dynamics and Mechanisms of CNS Myelination.” *Developmental Cell* 32 (4): 447–58. doi:10.1016/j.devcel.2015.01.016.

Blais, J D, C L Addison, R Edge, T Falls, H Zhao, K Wary, C Koumenis, et al. 2006. “Perk-dependent Translational Regulation Promotes Tumor Cell Adaptation and Angiogenesis in Response to Hypoxic Stress.” *Molecular and Cellular Biology* 26 (24): 9517–32. doi:10.1128/MCB.01145-06.

Blais, J D, V Filipenko, M Bi, H P Harding, D Ron, C Koumenis, B G Wouters, and J C Bell. 2004. “Activating Transcription Factor 4 Is Translationally Regulated by Hypoxic Stress.” *Molecular and Cellular Biology* 24 (17): 7469–82. doi:10.1128/MCB.24.17.7469-7482.2004.

Bondarenko, A, and M Chesler. 2001a. “Rapid Astrocyte Death Induced by Transient Hypoxia, Acidosis, and Extracellular Ion Shifts.” *Glia* 34 (2): 134–42.

Bondarenko, A, and M Chesler. 2001b. “Calcium Dependence of Rapid Astrocyte Death Induced by Transient Hypoxia, Acidosis, and Extracellular Ion Shifts.” *Glia* 34 (2): 143–49.

Boyce, M, K F Bryant, C Jousse, K Long, H P Harding, D Scheuner, R J Kaufman, et al. 2005. "A Selective Inhibitor of eIF2alpha Dephosphorylation Protects Cells from ER Stress." *Science (New York)* 307 (5711): 935–39. doi:10.1126/science.1101902.

Buser, J R, J Maire, A Riddle, X Gong, T Nguyen, K Nelson, N L Luo, et al. 2012. "Arrested Preoligodendrocyte Maturation Contributes to Myelination Failure in Premature Infants." *Annals of Neurology* 71 (1): 93–109. doi:10.1002/ana.22627.

Buttermore, E D, C L Thaxton, and M A Bhat. 2013. "Organization and Maintenance of Molecular Domains in Myelinated Axons." *Journal of Neuroscience Research* 91 (5): 603–22. doi:10.1002/jnr.23197.

Cai, J, C M Tuong, Y Zhang, C B Shields, G Guo, H Fu, and D Gozal. 2012. "Mouse Intermittent Hypoxia Mimicking Apnoea of Prematurity: Effects on Myelinogenesis and Axonal Maturation." *The Journal of Pathology* 226 (3): 495–508. doi:10.1002/path.2980.

Calfon, M, H Zeng, F Urano, J H Till, S R Hubbard, H P Harding, S G Clark, and D Ron. 2002. "IRE1 Couples Endoplasmic Reticulum Load to Secretory Capacity by Processing the XBP-1 mRNA." *Nature* 415 (6867): 92–96. doi:10.1038/415092a.

Cao, S S, and R J Kaufman. 2012. "Unfolded Protein Response." *Current Biology* 22 (16): R622–R626. doi:10.1016/j.cub.2012.07.004.

Chakrabarty, A, M M Danley, and S M LeVine. 2004. "Immunohistochemical Localization of Phosphorylated Protein Kinase R and Phosphorylated Eukaryotic Initiation Factor-2 Alpha in the Central Nervous System of SJL Mice with Experimental Allergic Encephalomyelitis." *J Neurosci Res* 76 (6): 822–33. doi:10.1002/jnr.20125.

Chakrabarty, A, K K Fleming, J G Marquis, and S M LeVine. 2005. "Quantifying Immunohistochemical Staining of phospho-eIF2alpha, Heme Oxygenase-2 and NADPH Cytochrome P450 Reductase in Oligodendrocytes During Experimental Autoimmune Encephalomyelitis." *J Neurosci Methods* 144 (2): 227–34. doi:10.1016/j.jneumeth.2004.11.010.

Chen, J J. 2007. "Regulation of Protein Synthesis by the Heme-regulated eIF2alpha Kinase: Relevance to Anemias." *Blood* 109 (7): 2693–99. doi:10.1182/blood-2006-08-041830.

Chen, N, Y W Jiang, H J Hao, T T Ban, K Gao, Z B Zhang, J M Wang, and Y Wu. 2015. "Different Eukaryotic Initiation Factor 2Bε Mutations Lead to Various Degrees of Intolerance to the Stress of Endoplasmic Reticulum in Oligodendrocytes." *Chin Med J* 128 (13): 1772–77. doi:10.4103/0366-6999.159353.

Ching, W, G Zanazzi, S R Levinson, and J L Salzer. 1999. "Clustering of Neuronal Sodium Channels Requires Contact with Myelinating Schwann Cells." *Journal of Neurocytology* 28 (4-5): 295–301.

Clayton, B L, and B Popko. 2016. “Endoplasmic Reticulum Stress and the Unfolded Protein Response in Disorders of Myelinating Glia.” *Brain Research*, April. doi:10.1016/j.brainres.2016.03.046.

Cooke, R W, and L Foulder-Hughes. 2003. “Growth Impairment in the Very Preterm and Cognitive and Motor Performance at 7 Years.”, June.

Counsell, S J, A D Edwards, A T Chew, M Anjari, L E Dyet, L Srinivasan, J P Boardman, et al. 2008. “Specific Relations Between Neurodevelopmental Abilities and White Matter Microstructure in Children Born Preterm.” *Brain: A Journal of Neurology* 131 (Pt 12): 3201–8. doi:10.1093/brain/awn268.

Cunnea, P, A N Mháille, S McQuaid, M Farrell, J McMahon, and U FitzGerald. 2011. “Expression Profiles of Endoplasmic Reticulum Stress-related Molecules in Demyelinating Lesions and Multiple Sclerosis.” *Mult Scler* 17 (7): 808–18. doi:10.1177/1352458511399114.

D’Antonio, M, M L Feltri, and L Wrabetz. 2009. “Myelin Under Stress.” *J Neurosci Res* 87 (15): 3241–49. doi:10.1002/jnr.22066.

D’Antonio, M, N Musner, C Scapin, D Ungaro, U Del Carro, D Ron, M L Feltri, and L Wrabetz. 2013. “Resetting Translational Homeostasis Restores Myelination in Charcot-Marie-Tooth Disease Type 1B Mice.” *J Exp Med* 210 (4): 821–38. doi:10.1084/jem.20122005.

Dar, A C, T E Dever, and F Sicheri. 2005. “Higher-order Substrate Recognition of eIF2alpha by the RNA-dependent Protein Kinase PKR.” *Cell* 122 (6): 887–900. doi:10.1016/j.cell.2005.06.044.

Das, I, A Krzyzosiak, K Schneider, L Wrabetz, M D’Antonio, N Barry, A Sigurdardottir, and A Bertolotti. 2015. “Preventing Proteostasis Diseases by Selective Inhibition of a Phosphatase Regulatory Subunit.” *Science* 348 (6231): 239–42. doi:10.1126/science.aaa4484.

Davidson, J O, G Wassink, L G van den Heuij, L Bennet, and A J Gunn. 2015. “Therapeutic Hypothermia for Neonatal Hypoxic-Ischemic Encephalopathy - Where to from Here?” *Frontiers in Neurology* 6 (September): 198. doi:10.3389/fneur.2015.00198.

De Kieviet, J F, J P Piek, C S Aarnoudse-Moens, and J Oosterlaan. 2009. “Motor Development in Very Preterm and Very Low-birth-weight Children from Birth to Adolescence: a Meta-analysis.”, November.

Deguchi, J O, H Yamazaki, E Aikawa, and M Aikawa. 2009. “Chronic Hypoxia Activates the Akt and Beta-catenin Pathways in Human Macrophages.” *Arteriosclerosis, Thrombosis, and Vascular Biology* 29 (10): 1664–70. doi:10.1161/ATVBAHA.109.194043.

Deng, W. 2010. “Neurobiology of Injury to the Developing Brain.” *Nature Reviews. Neurology* 6 (6): 328–36. doi:10.1038/nrneurol.2010.53.

Deng, W, P A Rosenberg, J J Volpe, and F E Jensen. 2003. “Calcium-permeable AMPA/kainate Receptors Mediate Toxicity and Preconditioning by Oxygen-glucose Deprivation in Oligodendrocyte Precursors.” *Proceedings of the National Academy of Sciences of the United States of America* 100 (11): 6801–6. doi:10.1073/pnas.1136624100.

Deslauriers, A M, A Afkhami-Goli, A M Paul, R K Bhat, S Acharjee, K K Ellestad, F Noorbakhsh, M Michalak, and C Power. 2011. “Neuroinflammation and Endoplasmic Reticulum Stress Are Coregulated by Crocin to Prevent Demyelination and Neurodegeneration.” *Journal of Immunology* 187 (9): 4788–99. doi:10.4049/jimmunol.1004111.

Deval, C, C Chaveroux, A C Maurin, Y Cherasse, L Parry, V Carraro, D Milenkovic, et al. 2009. “Amino Acid Limitation Regulates the Expression of Genes Involved in Several Specific Biological Processes through GCN2-dependent and GCN2-independent Pathways.” *The FEBS Journal* 276 (3): 707–18. doi:10.1111/j.1742-4658.2008.06818.x.

Diamond, A. 2000. “Close Interrelation of Motor Development and Cognitive Development and of the Cerebellum and Prefrontal Cortex.” *Child Development* 71 (1): 44–56. doi:10.1111/1467-8624.00117.

Dickson, K M, J J Bergeron, I Shames, J Colby, D T Nguyen, E Chevet, D Y Thomas, and G J Snipes. 2002. “Association of Calnexin with Mutant Peripheral Myelin Protein-22 Ex Vivo: a Basis for ‘Gain-of-function’ ER Diseases.” *Proc Natl Acad Sci U S A* 99 (15): 9852–57. doi:10.1073/pnas.152621799.

Domercq, M, E Etxebarria, A Pérez-Samartín, and C Matute. 2005. “Excitotoxic Oligodendrocyte Death and Axonal Damage Induced by Glutamate Transporter Inhibition.” *Glia* 52 (1): 36–46. doi:10.1002/glia.20221.

Donnelly, N, A M Gorman, S Gupta, and A Samali. 2013. “The eIF2α Kinases: Their Structures and Functions.” *Cellular and Molecular Life Sciences* 70 (19): 3493–3511. doi:10.1007/s00018-012-1252-6.

Dugas, J C, and B Emery. 2013. “Purification and Culture of Oligodendrocyte Lineage Cells.” *Cold Spring Harbor Protocols* 2013 (9): 810–14. doi:10.1101/pdb.top074898.

Elbaz, B, M Traka, R B Kunjamma, D Dukala, A B Lutz, E S Anton, B A Barres, B Soliven, and B Popko. 2016. “Adenomatous Polyposis Coli Regulates Radial Axonal Sorting and Myelination in the PNS.”, May.

Emery, B. 2010. “Transcriptional and Post-transcriptional Control of CNS Myelination.” *Current Opinion in Neurobiology* 20 (5): 601–7. doi:10.1016/j.conb.2010.05.005.

Emery, B, and J C Dugas. 2013. “Purification of Oligodendrocyte Lineage Cells from Mouse Cortices by Immunopanning.” *Cold Spring Harbor Protocols* 2013 (9): 854–68. doi:10.1101/pdb.prot073973.

Fagel, D M, Y Ganat, J Silbereis, T Ebbitt, W Stewart, H Zhang, L R Ment, and F M Vaccarino. 2006. “Cortical Neurogenesis Enhanced by Chronic Perinatal Hypoxia.” *Experimental Neurology* 199 (1): 77–91. doi:10.1016/j.expneurol.2005.04.006.

Fancy, S P, E P Harrington, S E Baranzini, J C Silbereis, L R Shiow, T J Yuen, E J Huang, S Lomvardas, and D H Rowitch. 2014. “Parallel States of Pathological Wnt Signaling in Neonatal Brain Injury and Colon Cancer.” *Nature Neuroscience* 17 (4): 506–12. doi:10.1038/nn.3676.

Fancy, S P, E P Harrington, T J Yuen, J C Silbereis, C Zhao, S E Baranzini, C C Bruce, et al. 2011. “Axin2 as Regulatory and Therapeutic Target in Newborn Brain Injury and Remyelination.” *Nature Neuroscience* 14 (8): 1009–16. doi:10.1038/nn.2855.

Fels, D R, and C Koumenis. 2006. “The PERK/eIF2alpha/ATF4 Module of the UPR in Hypoxia Resistance and Tumor Growth.” *Cancer Biology & Therapy* 5 (7): 723–28.

Feltri, M L, Y Poitelon, and S C Previtali. 2016. “How Schwann Cells Sort Axons: New Concepts.” *The Neuroscientist* 22 (3): 252–65. doi:10.1177/1073858415572361.

Finer, N N, R Higgins, J Kattwinkel, and R J Martin. 2006. “Summary Proceedings from the Apnea-of-prematurity Group.” *Pediatrics* 117 (3 Pt 2): S47–S51. doi:10.1542/peds.2005-0620H.

Folkerth, R D, R L Haynes, N S Borenstein, R A Belliveau, F Trachtenberg, P A Rosenberg, J J Volpe, and H C Kinney. 2004. “Developmental Lag in Superoxide Dismutases Relative to Other Antioxidant Enzymes in Premyelinated Human Telencephalic White Matter.” *Journal of Neuropathology and Experimental Neurology* 63 (9): 990–99.

Franklin, R J, C ffrench-Constant, J M Edgar, and K J Smith. 2012. “Neuroprotection and Repair in Multiple Sclerosis.” *Nature Reviews. Neurology* 8 (11): 624–34. doi:10.1038/nrneurol.2012.200.

Fünfschilling, U, L M Supplie, D Mahad, S Boretius, A S Saab, J Edgar, B G Brinkmann, et al. 2012. “Glycolytic Oligodendrocytes Maintain Myelin and Long-term Axonal Integrity.” *Nature* 485 (7399): 517–21. doi:10.1038/nature11007.

Garbern, J Y. 2007. “Pelizaeus-Merzbacher Disease: Genetic and Cellular Pathogenesis.” *Cell Mol Life Sci* 64 (1): 50–65. doi:10.1007/s00018-006-6182-8.

Geva, M, Y Cabilly, Y Assaf, N Mindroul, L Marom, G Raini, D Pinchasi, and O Elroy-Stein. 2010. “A Mouse Model for Eukaryotic Translation Initiation Factor 2B-leucodystrophy

Reveals Abnormal Development of Brain White Matter." *Brain* 133 (Pt 8): 2448–61. doi:10.1093/brain/awq180.

Gow, A, and R A Lazzarini. 1996. "A Cellular Mechanism Governing the Severity of Pelizaeus-Merzbacher Disease." *Nat Genet* 13 (4): 422–28. doi:10.1038/ng0896-422.

Grallert, B, and E Boye. 2007. "The Gcn2 Kinase as a Cell Cycle Regulator." *Cell Cycle* 6 (22): 2768–72. doi:10.4161/cc.6.22.4933.

Greer, J M, and M B Lees. 2002. "Myelin Proteolipid Protein--the First 50 Years." *The International Journal of Biochemistry & Cell Biology* 34 (3): 211–15. doi:10.1016/S1357-2725(01)00136-4.

Griffiths, I, M Klugmann, T Anderson, D Yool, C Thomson, M H Schwab, A Schneider, et al. 1998. "Axonal Swellings and Degeneration in Mice Lacking the Major Proteolipid of Myelin." *Science (New York)* 280 (5369): 1610–13.

Grigoryan, T, S Stein, J Qi, H Wende, A N Garratt, K A Nave, C Birchmeier, and W Birchmeier. 2013. "Wnt/Rspondin/β-catenin Signals Control Axonal Sorting and Lineage Progression in Schwann Cell Development." *Proceedings of the National Academy of Sciences of the United States of America* 110 (45): 18174–79. doi:10.1073/pnas.1310490110.

Grunau, R E, M F Whitfield, and T B Fay. 2004. "Psychosocial and Academic Characteristics of Extremely Low Birth Weight (< or =800 G) Adolescents Who Are Free of Major Impairment Compared with Term-born Control Subjects." *Pediatrics* 114 (6): e725–e732. doi:10.1542/peds.2004-0932.

Guimarães-Camboa, N, J Stowe, I Aneas, N Sakabe, P Cattaneo, L Henderson, M S Kilberg, et al. 2015. "HIF1α Represses Cell Stress Pathways to Allow Proliferation of Hypoxic Fetal Cardiomyocytes." *Developmental Cell* 33 (5): 507–21. doi:10.1016/j.devcel.2015.04.021.

Hack, M, D J Flannery, M Schluchter, L Cartar, E Borawski, and N Klein. 2002. "Outcomes in Young Adulthood for Very-low-birth-weight Infants." *The New England Journal of Medicine* 346 (3): 149–57. doi:10.1056/NEJMoa010856.

Halterman, M W, M Gill, C DeJesus, M Ogihara, N F Schor, and H J Federoff. 2010. "The Endoplasmic Reticulum Stress Response Factor CHOP-10 Protects Against Hypoxia-induced Neuronal Death." *The Journal of Biological Chemistry* 285 (28): 21329–40. doi:10.1074/jbc.M109.095299.

Hansen, A J. 1985. "Effect of Anoxia on Ion Distribution in the Brain." *Physiological Reviews* 65 (1): 101–48.

Harding, H P, Y Zhang, D Scheuner, J J Chen, R J Kaufman, and D Ron. 2009. "Ppp1r15 Gene Knockout Reveals an Essential Role for Translation Initiation Factor 2 Alpha (eIF2alpha)

Dephosphorylation in Mammalian Development." *Proceedings of the National Academy of Sciences of the United States of America* 106 (6): 1832–37. doi:10.1073/pnas.0809632106.

Harding, H P, Y Zhang, H Zeng, I Novoa, P D Lu, M Calfon, N Sadri, et al. 2003. "An Integrated Stress Response Regulates Amino Acid Metabolism and Resistance to Oxidative Stress." *Molecular Cell* 11 (3): 619–33. doi:10.1016/S1097-2765(03)00105-9.

Hemgren, E, and K Persson. 2009. "Deficits in Motor Co-ordination and Attention at 3 Years of Age Predict Motor Deviations in 6.5-year-old Children Who Needed Neonatal Intensive Care.", January.

Hoyle, J C, M C Isfort, J Roggenbuck, and W D Arnold. 2015. "The Genetics of Charcot-Marie-Tooth Disease: Current Trends and Future Implications for Diagnosis and Management." *Appl Clin Genet* 8 (October): 235–43. doi:10.2147/TACG.S69969.

Hussien, Y, D R Cavener, and B Popko. 2014. "Genetic Inactivation of PERK Signaling in Mouse Oligodendrocytes: Normal Developmental Myelination with Increased Susceptibility to Inflammatory Demyelination." *Glia* 62 (5): 680–91. doi:10.1002/glia.22634.

Jablonska, B, J Scafidi, A Aguirre, F Vaccarino, V Nguyen, E Borok, T L Horvath, D H Rowitch, and V Gallo. 2012. "Oligodendrocyte Regeneration after Neonatal Hypoxia Requires FoxO1-mediated p27Kip1 Expression." *The Journal of Neuroscience* 32 (42): 14775–93. doi:10.1523/JNEUROSCI.2060-12.2012.

Jousse, C, S Oyadomari, I Novoa, P Lu, Y Zhang, H P Harding, and D Ron. 2003. "Inhibition of a Constitutive Translation Initiation Factor 2alpha Phosphatase, CReP, Promotes Survival of Stressed Cells." *The Journal of Cell Biology* 163 (4): 767–75. doi:10.1083/jcb.200308075.

Juliano, C, S Sosunov, Z Niatsetskaya, J A Isler, I Utkina-Sosunova, I Jang, V Ratner, and V Ten. 2015. "Mild Intermittent Hypoxemia in Neonatal Mice Causes Permanent Neurofunctional Deficit and White Matter Hypomyelination." *Experimental Neurology* 264 (February): 33–42. doi:10.1016/j.expneurol.2014.11.010.

Kantor, L, D Pinchasi, M Mintz, Y Hathout, A Vanderver, and O Elroy-Stein. 2008. "A Point Mutation in Translation Initiation Factor 2B Leads to a Continuous Hyper Stress State in Oligodendroglial-derived Cells." *PLoS ONE* 3 (11): e3783. doi:10.1371/journal.pone.0003783.

Karussis, D. 2014. "The Diagnosis of Multiple Sclerosis and the Various Related Demyelinating Syndromes: A Critical Review." *Journal of Autoimmunity* 48-49 (February): 134–42. doi:10.1016/j.jaut.2014.01.022.

Klugmann, M, M H Schwab, A Pühlhofer, A Schneider, F Zimmermann, I R Griffiths, and K A Nave. 1997. “Assembly of CNS Myelin in the Absence of Proteolipid Protein.” *Neuron* 18 (1): 59–70. doi:10.1016/S0896-6273(01)80046-5.

Koumenis, C, M Bi, J Ye, D Feldman, and A C Koong. 2007. “Hypoxia and the Unfolded Protein Response.” *Methods in Enzymology* 435: 275–93. doi:10.1016/S0076-6879(07)35014-3.

Koumenis, C, C Naczki, M Koritzinsky, S Rastani, A Diehl, N Sonenberg, A Koromilas, and B G Wouters. 2002. “Regulation of Protein Synthesis by Hypoxia via Activation of the Endoplasmic Reticulum Kinase PERK and Phosphorylation of the Translation Initiation Factor eIF2alpha.” *Molecular and Cellular Biology* 22 (21): 7405–16. doi:10.1128/MCB.22.21.7405-7416.2002.

Kraskiewicz, H, and U FitzGerald. 2011. “Partial XBP1 Knockdown Does Not Affect Viability of Oligodendrocyte Precursor Cells Exposed to New Models of Hypoxia and Ischemia in Vitro.” *Journal of Neuroscience Research* 89 (5): 661–73. doi:10.1002/jnr.22583.

Kucharova, K, and W B Stallcup. 2015. “NG2-proteoglycan-dependent Contributions of Oligodendrocyte Progenitors and Myeloid Cells to Myelin Damage and Repair.” *Journal of Neuroinflammation* 12 (September): 161. doi:10.1186/s12974-015-0385-6.

Kumar, R, S Azam, J M Sullivan, C Owen, D R Cavener, P Zhang, D Ron, et al. 2001. “Brain Ischemia and Reperfusion Activates the Eukaryotic Initiation Factor 2alpha Kinase, PERK.” *Journal of Neurochemistry* 77 (5): 1418–21.

Lappe-Siefke, C, S Goebbels, M Gravel, E Nicksch, J Lee, P E Braun, I R Griffiths, and K A Nave. 2003. “Disruption of Cnp1 Uncouples Oligodendroglial Functions in Axonal Support and Myelination.” *Nature Genetics* 33 (3): 366–74. doi:10.1038/ng1095.

Lee, Y, B M Morrison, Y Li, S Lengacher, M H Farah, P N Hoffman, Y Liu, et al. 2012. “Oligodendroglia Metabolically Support Axons and Contribute to Neurodegeneration.” *Nature* 487 (7408): 443–48. doi:10.1038/nature11314.

Lees, J R, and A H Cross. 2007. “A Little Stress Is Good: IFN-gamma, Demyelination, and Multiple Sclerosis.” *J Clin Invest* 117 (2): 297–99. doi:10.1172/JCI31254.

Li, Y, Y Guo, J Tang, J Jiang, and Z Chen. 2014. “New Insights into the Roles of CHOP-induced Apoptosis in ER Stress.” *Acta Biochimica et Biophysica Sinica* 46 (8): 629–40. doi:10.1093/abbs/gmu048.

Lin, W, S L Bailey, H Ho, H P Harding, D Ron, S D Miller, and B Popko. 2007. “The Integrated Stress Response Prevents Demyelination by Protecting Oligodendrocytes Against Immune-mediated Damage.” *J Clin Invest* 117 (2): 448–56. doi:10.1172/JCI29571.

Lin, W, H P Harding, D Ron, and B Popko. 2005. “Endoplasmic Reticulum Stress Modulates the Response of Myelinating Oligodendrocytes to the Immune Cytokine Interferon-gamma.” *The Journal of Cell Biology* 169 (4): 603–12. doi:10.1083/jcb.200502086.

Lin, W, A Kemper, J L Dupree, H P Harding, D Ron, and B Popko. 2006. “Interferon-gamma Inhibits Central Nervous System Remyelination through a Process Modulated by Endoplasmic Reticulum Stress.” *Brain* 129 (Pt 5): 1306–18. doi:10.1093/brain/awl044.

Lin, W, P E Kunkler, H P Harding, D Ron, R P Kraig, and B Popko. 2008. “Enhanced Integrated Stress Response Promotes Myelinating Oligodendrocyte Survival in Response to Interferon-gamma.” *The American Journal of Pathology* 173 (5): 1508–17. doi:10.2353/ajpath.2008.080449.

Lin, W, Y Lin, J Li, A G Fenstermaker, S W Way, B Clayton, S Jamison, H P Harding, D Ron, and B Popko. 2013. “Oligodendrocyte-specific Activation of PERK Signaling Protects Mice Against Experimental Autoimmune Encephalomyelitis.” *The Journal of Neuroscience* 33 (14): 5980–91. doi:10.1523/JNEUROSCI.1636-12.2013.

Lin, Y, G Huang, S Jamison, J Li, H P Harding, D Ron, and W Lin. 2014. “PERK Activation Preserves the Viability and Function of Remyelinating Oligodendrocytes in Immune-mediated Demyelinating Diseases.” *The American Journal of Pathology* 184 (2): 507–19. doi:10.1016/j.ajpath.2013.10.009.

Lin, Y, X Pang, G Huang, S Jamison, J Fang, H P Harding, D Ron, and W Lin. 2014. “Impaired Eukaryotic Translation Initiation Factor 2B Activity Specifically in Oligodendrocytes Reproduces the Pathology of Vanishing White Matter Disease in Mice.” *J Neurosci* 34 (36): 12182–91. doi:10.1523/JNEUROSCI.1373-14.2014.

Lindström, K, B Winbladh, B Haglund, and A Hjern. 2007. “Preterm Infants as Young Adults: a Swedish National Cohort Study.” *Pediatrics* 120 (1): 70–77. doi:10.1542/peds.2006-3260.

Liu, J, and P Casaccia. 2010. “Epigenetic Regulation of Oligodendrocyte Identity.” *Trends in Neurosciences* 33 (4): 193–201. doi:10.1016/j.tins.2010.01.007.

Liu, Y, C László, Y Liu, W Liu, X Chen, S C Evans, and S Wu. 2010. “Regulation of G(1) Arrest and Apoptosis in Hypoxia by PERK and GCN2-mediated eIF2alpha Phosphorylation.” *Neoplasia* 12 (1): 61–68.

Losch, H, and O Dammann. 2004. “Impact of Motor Skills on Cognitive Test Results in Very-low-birthweight Children.” *Journal of Child Neurology* 19 (5): 318–22.

Lossos, A, N Elazar, I Lerer, O Schueler-Furman, Y Fellig, B Glick, B E Zimmerman, et al. 2015. “Myelin-associated Glycoprotein Gene Mutation Causes Pelizaeus-Merzbacher Disease-like Disorder.” *Brain* 138 (Pt 9): 2521–36. doi:10.1093/brain/awv204.

Marciniak, S J, C Y Yun, S Oyadomari, I Novoa, Y Zhang, R Jungreis, K Nagata, H P Harding, and D Ron. 2004. "CHOP Induces Death by Promoting Protein Synthesis and Oxidation in the Stressed Endoplasmic Reticulum." *Genes & Development* 18 (24): 3066–77. doi:10.1101/gad.1250704.

Marlow, N, D Wolke, M A Bracewell, M Samara, and EPICure Study Group. 2005. "Neurologic and Developmental Disability at Six Years of Age after Extremely Preterm Birth." *The New England Journal of Medicine* 352 (1): 9–19. doi:10.1056/NEJMoa041367.

Martin, R J, K Wang, O Köroğlu, J Di Fiore, and P Kc. 2011. "Intermittent Hypoxic Episodes in Preterm Infants: Do They Matter?" *Neonatology* 100 (3): 303–10. doi:10.1159/000329922.

McMahon, J M, S McQuaid, R Reynolds, and U F FitzGerald. 2012. "Increased Expression of ER Stress- and Hypoxia-associated Molecules in Grey Matter Lesions in Multiple Sclerosis." *Multiple Sclerosis* 18 (10): 1437–47. doi:10.1177/1352458512438455.

Ment, L R, M Schwartz, R W Makuch, and W B Stewart. 1998. "Association of Chronic Sublethal Hypoxia with Ventriculomegaly in the Developing Rat Brain." *Developmental Brain Research* 111 (2): 197–203. doi:10.1016/S0165-3806(98)00139-4.

Mháille, A N, S McQuaid, A Windebank, P Cunnea, J McMahon, A Samali, and U FitzGerald. 2008. "Increased Expression of Endoplasmic Reticulum Stress-related Signaling Pathway Molecules in Multiple Sclerosis Lesions." *J Neuropathol Exp Neurol* 67 (3): 200–211. doi:10.1097/NEN.0b013e318165b239.

Miller, S P, D M Ferriero, C Leonard, R Piecuch, D V Glidden, J C Partridge, M Perez, P Mukherjee, D B Vigneron, and A J Barkovich. 2005. "Early Brain Injury in Premature Newborns Detected with Magnetic Resonance Imaging Is Associated with Adverse Early Neurodevelopmental Outcome." *The Journal of Pediatrics* 147 (5): 609–16. doi:10.1016/j.jpeds.2005.06.033.

Mounir, Z, J L Krishnamoorthy, S Wang, B Papadopoulou, S Campbell, W J Muller, M Hatzoglou, and A E Koromilas. 2011. "Akt Determines Cell Fate through Inhibition of the PERK-eIF2α Phosphorylation Pathway." *Science Signaling* 4 (192): ra62. doi:10.1126/scisignal.2001630.

Mullen, K M, B R Vohr, K H Katz, K C Schneider, C Lacadie, M Hampson, R W Makuch, A L Reiss, R T Constable, and L R Ment. 2011. "Preterm Birth Results in Alterations in Neural Connectivity at Age 16 Years." *Neuroimage* 54 (4): 2563–70. doi:10.1016/j.neuroimage.2010.11.019.

Nave, K A. 2010. "Myelination and Support of Axonal Integrity by Glia." *Nature* 468 (7321): 244–52. doi:10.1038/nature09614.

Nave, K A, and H Ehrenreich. 2014. “Myelination and Oligodendrocyte Functions in Psychiatric Diseases.” *JAMA Psychiatry* 71 (5): 582–84. doi:10.1001/jamapsychiatry.2014.189.

Nave, K A, and H B Werner. 2014. “Myelination of the Nervous System: Mechanisms and Functions.” *Annual Review of Cell and Developmental Biology* 30: 503–33. doi:10.1146/annurev-cellbio-100913-013101.

Ní Fhlathartaigh, M, J McMahon, R Reynolds, D Connolly, E Higgins, T Counihan, and U Fitzgerald. 2013. “Calreticulin and Other Components of Endoplasmic Reticulum Stress in Rat and Human Inflammatory Demyelination.” *Acta Neuropathol Commun* 1 (July): 37. doi:10.1186/2051-5960-1-37.

Novoa, I, H Zeng, H P Harding, and D Ron. 2001. “Feedback Inhibition of the Unfolded Protein Response by GADD34-mediated Dephosphorylation of eIF2alpha.” *The Journal of Cell Biology* 153 (5): 1011–22.

Numasawa-Kuroiwa, Y, Y Okada, S Shibata, N Kishi, W Akamatsu, M Shoji, A Nakanishi, et al. 2014. “Involvement of ER Stress in Dysmyelination of Pelizaeus-Merzbacher Disease with PLP1 Missense Mutations Shown by iPSC-derived Oligodendrocytes.” *Stem Cell Reports* 2 (5): 648–61. doi:10.1016/j.stemcr.2014.03.007.

Onuki, R, Y Bando, E Suyama, T Katayama, H Kawasaki, T Baba, M Tohyama, and K Taira. 2004. “An RNA-dependent Protein Kinase Is Involved in Tunicamycin-induced Apoptosis and Alzheimer’s Disease.” *The EMBO Journal* 23 (4): 959–68. doi:10.1038/sj.emboj.7600049.

Pandit, A S, E Robinson, P Aljabar, G Ball, I S Gousias, Z Wang, J V Hajnal, et al. 2014. “Whole-brain Mapping of Structural Connectivity in Infants Reveals Altered Connection Strength Associated with Growth and Preterm Birth.” *Cerebral Cortex* 24 (9): 2324–33. doi:10.1093/cercor/bht086.

Patterson, A D, M C Hollander, G F Miller, and A J Fornace. 2006. “Gadd34 Requirement for Normal Hemoglobin Synthesis.” *Molecular and Cellular Biology* 26 (5): 1644–53. doi:10.1128/MCB.26.5.1644-1653.2006.

Patzkó, A, Y Bai, M A Saporta, I Katona, X Wu, D Vizzuso, M L Feltri, et al. 2012. “Curcumin Derivatives Promote Schwann Cell Differentiation and Improve Neuropathy in R98C CMT1B Mice.” *Brain: A Journal of Neurology* 135 (Pt 12): 3551–66. doi:10.1093/brain/aws299.

Pavitt, G D, and D Ron. 2012. “New Insights into Translational Regulation in the Endoplasmic Reticulum Unfolded Protein Response.” *Cold Spring Harbor Perspectives in Biology* 4 (6). doi:10.1101/cshperspect.a012278.

Pennuto, M, E Tinelli, M Malaguti, U Del Carro, M D’Antonio, D Ron, A Quattrini, M L Feltri,

and L Wrabetz. 2008. “Ablation of the UPR-mediator CHOP Restores Motor Function and Reduces Demyelination in Charcot-Marie-Tooth 1B Mice.” *Neuron* 57 (3): 393–405. doi:10.1016/j.neuron.2007.12.021.

Peschek, J, D Acosta-Alvear, A S Mendez, and P Walter. 2015. “A Conformational RNA Zipper Promotes Intron Ejection During Non-conventional XBP1 mRNA Splicing.” *EMBO Reports* 16 (12): 1688–98. doi:10.15252/embr.201540955.

Pfaffl, M W. 2001. “A New Mathematical Model for Relative Quantification in Real-time RT-PCR.” *Nucleic Acids Research* 29 (9): e45.

Pfeiffer, S E, A E Warrington, and R Bansal. 1993. “The Oligodendrocyte and Its Many Cellular Processes.” *Trends in Cell Biology* 3 (6): 191–97.

Piek, J P, L Dawson, L M Smith, and N Gasson. 2008. “The Role of Early Fine and Gross Motor Development on Later Motor and Cognitive Ability.” *Human Movement Science* 27 (5): 668–81. doi:10.1016/j.humov.2007.11.002.

Poole, K L, L A Schmidt, C Missiuna, S Saigal, M H Boyle, and R J Van Lieshout. 2015. “Motor Coordination and Mental Health in Extremely Low Birth Weight Survivors During the First Four Decades of Life.”, September.

Popko, B, J G Corbin, K D Baerwald, J Dupree, and A M Garcia. 1997. “The Effects of Interferon-gamma on the Central Nervous System.” *Mol Neurobiol* 14 (1-2): 19–35. doi:10.1007/BF02740619.

Rasband, M N, E Peles, J S Trimmer, S R Levinson, S E Lux, and P Shrager. 1999. “Dependence of Nodal Sodium Channel Clustering on Paranodal Axoglial Contact in the Developing CNS.” *The Journal of Neuroscience* 19 (17): 7516–28.

Reid, D W, A S Tay, J R Sundaram, I C Lee, Q Chen, S E George, C V Nicchitta, and S Shenolikar. 2016. “Complementary Roles of GADD34- and CReP-Containing Eukaryotic Initiation Factor 2α Phosphatases During the Unfolded Protein Response.” *Molecular and Cellular Biology* 36 (13): 1868–80. doi:10.1128/MCB.00190-16.

Rice, J E, R C Vannucci, and J B Brierley. 1981. “The Influence of Immaturity on Hypoxic-ischemic Brain Damage in the Rat.” *Annals of Neurology* 9 (2): 131–41. doi:10.1002/ana.410090206.

Riddle, A, N L Luo, M Manese, D J Beardsley, L Green, D A Rorvik, K A Kelly, et al. 2006. “Spatial Heterogeneity in Oligodendrocyte Lineage Maturation and Not Cerebral Blood Flow Predicts Fetal Ovine Periventricular White Matter Injury.” *The Journal of Neuroscience* 26 (11): 3045–55. doi:10.1523/JNEUROSCI.5200-05.2006.

Rinholm, J E, N B Hamilton, N Kessaris, W D Richardson, L H Bergersen, and D Attwell. 2011.

"Regulation of Oligodendrocyte Development and Myelination by Glucose and Lactate." *The Journal of Neuroscience* 31 (2): 538–48. doi:10.1523/JNEUROSCI.3516-10.2011.

Roberts, G, P J Anderson, L W Doyle, and Victorian Infant Collaborative Study Group. 2009. "Neurosensory Disabilities at School Age in Geographic Cohorts of Extremely Low Birth Weight Children Born Between the 1970s and the 1990s." *The Journal of Pediatrics* 154 (6): 829–34.e1. doi:10.1016/j.jpeds.2008.12.036.

Rosenbluth, J, K A Nave, A Mierzwa, and R Schiff. 2006. "Subtle Myelin Defects in PLP-null Mice." *Glia* 54 (3): 172–82. doi:10.1002/glia.20370.

Rzymski, T, M Milani, L Pike, F Buffa, H R Mellor, L Winchester, I Pires, E Hammond, I Ragoussis, and A L Harris. 2010. "Regulation of Autophagy by ATF4 in Response to Severe Hypoxia." *Oncogene* 29 (31): 4424–35. doi:10.1038/onc.2010.191.

Salmaso, N, B Jablonska, J Scafidi, F M Vaccarino, and V Gallo. 2014. "Neurobiology of Premature Brain Injury." *Nature Neuroscience* 17 (3): 341–46. doi:10.1038/nn.3604.

Salt, A, and M Redshaw. 2006. "Neurodevelopmental Follow-up after Preterm Birth: Follow up after Two Years.", March.

Salzer, J L. 2015. "Schwann Cell Myelination." *Cold Spring Harbor Perspectives in Biology* 7 (8): a020529. doi:10.1101/cshperspect.a020529.

Saporta, M A, B R Shy, A Patzko, Y Bai, M Pennuto, C Ferri, E Tinelli, et al. 2012. "MpzR98C Arrests Schwann Cell Development in a Mouse Model of Early-onset Charcot-Marie-Tooth Disease Type 1B." *Brain: A Journal of Neurology* 135 (Pt 7): 2032–47. doi:10.1093/brain/aws140.

Scafidi, J, D M Fagel, L R Ment, and F M Vaccarino. 2009. "Modeling Premature Brain Injury and Recovery." *International Journal of Developmental Neuroscience* 27 (8): 863–71. doi:10.1016/j.ijdevneu.2009.05.009.

Scafidi, J, T R Hammond, S Scafidi, J Ritter, B Jablonska, M Roncal, K Szigeti-Buck, et al. 2014. "Intranasal Epidermal Growth Factor Treatment Rescues Neonatal Brain Injury." *Nature* 506 (7487): 230–34. doi:10.1038/nature12880.

Schmitz, T, S Endesfelder, L J Chew, I Zaak, and C Bührer. 2012. "Minocycline Protects Oligodendroglial Precursor Cells Against Injury Caused by Oxygen-glucose Deprivation." *Journal of Neuroscience Research* 90 (5): 933–44. doi:10.1002/jnr.22824.

Schüller, U, V M Heine, J Mao, A T Kho, A K Dillon, Y G Han, E Huillard, et al. 2008. "Acquisition of Granule Neuron Precursor Identity Is a Critical Determinant of Progenitor Cell Competence to Form Shh-induced Medulloblastoma." *Cancer Cell* 14 (2): 123–34. doi:10.1016/j.ccr.2008.07.005.

Sharp, F R, and M Bernaudin. 2004. “HIF1 and Oxygen Sensing in the Brain.” *Nature Reviews. Neuroscience* 5 (6): 437–48. doi:10.1038/nrn1408.

Shen, S, and P Casaccia-Bonnefil. 2008. “Post-translational Modifications of Nucleosomal Histones in Oligodendrocyte Lineage Cells in Development and Disease.” *Journal of Molecular Neuroscience* 35 (1): 13–22. doi:10.1007/s12031-007-9014-x.

Shen, Y, J M Plane, and W Deng. 2010. “Mouse Models of Periventricular Leukomalacia.” *Journal of Visualized Experiments*, no. 39 (May). doi:10.3791/1951.

Silver, I, and M Erecińska. 1998. “Oxygen and Ion Concentrations in Normoxic and Hypoxic Brain Cells.” *Advances in Experimental Medicine and Biology* 454: 7–16.

Simons, M, and K A Nave. 2016. “Oligodendrocytes: Myelination and Axonal Support.” *Cold Spring Harbor Perspectives in Biology* 8 (1): a020479. doi:10.1101/cshperspect.a020479.

Smit, E, X Liu, S Jary, F Cowan, and M Thoresen. 2015. “Cooling Neonates Who Do Not Fulfil the Standard Cooling Criteria - Short- and Long-term Outcomes.” *Acta Paediatrica* 104 (2): 138–45. doi:10.1111/apa.12784.

Sommer, I, and M Schachner. 1981. “Monoclonal Antibodies (O1 to O4) to Oligodendrocyte Cell Surfaces: An Immunocytological Study in the Central Nervous System.” *Developmental Biology* 83 (2): 311–27. doi:10.1016/0012-1606(81)90477-2.

Southwood, C M, B Fykkolodziej, F Dachet, and A Gow. 2013. “Potential For Cell-mediated Immune Responses In Mouse Models Of Pelizaeus-Merzbacher Disease.” *Brain Sci* 3 (4): 1417–44. doi:10.3390/brainsci3041417.

Southwood, C M, B Fykkolodziej, K J Maheras, D M Garshott, M Estill, A M Fribley, and A Gow. 2016. “Overexpression of CHOP in Myelinating Cells Does Not Confer a Significant Phenotype Under Normal or Metabolic Stress Conditions.” *The Journal of Neuroscience* 36 (25): 6803–19. doi:10.1523/JNEUROSCI.1118-15.2016.

Southwood, C M, J Garbern, W Jiang, and A Gow. 2002. “The Unfolded Protein Response Modulates Disease Severity in Pelizaeus-Merzbacher Disease.” *Neuron* 36 (4): 585–96. doi:10.1016/S0896-6273(02)01045-0.

Stone, S, and W Lin. 2015. “The Unfolded Protein Response in Multiple Sclerosis.” *Front Neurosci* 9 (July): 264. doi:10.3389/fnins.2015.00264.

Tagliavacca, L, A Caretti, P Bianciardi, and M Samaja. 2012. “In Vivo Up-regulation of the Unfolded Protein Response after Hypoxia.” *Biochimica et Biophysica Acta* 1820 (7): 900–906. doi:10.1016/j.bbagen.2012.02.016.

Theocharopoulou, G, and P Vlamos. 2015. “Modeling Protein Misfolding in Charcot-marie-tooth

Disease." *Adv Exp Med Biol* 820: 91–102. doi:10.1007/978-3-319-09012-2_7.

Topilko, P, S Schneider-Maunoury, G Levi, A Baron-Van Evercooren, A B Chennoufi, T Seitanidou, C Babinet, and P Charnay. 1994. "Krox-20 Controls Myelination in the Peripheral Nervous System." *Nature* 371 (6500): 796–99. doi:10.1038/371796a0.

Traka, M, J R Podojil, D P McCarthy, S D Miller, and B Popko. 2015. "Oligodendrocyte Death Results in Immune-mediated CNS Demyelination." *Nature Neuroscience*, December. doi:10.1038/nn.4193.

Tsai, Y P, and K J Wu. 2014. "Epigenetic Regulation of Hypoxia-responsive Gene Expression: Focusing on Chromatin and DNA Modifications." *International Journal of Cancer* 134 (2): 249–56. doi:10.1002/ijc.28190.

Tsaytler, P, H P Harding, D Ron, and A Bertolotti. 2011. "Selective Inhibition of a Regulatory Subunit of Protein Phosphatase 1 Restores Proteostasis." *Science* 332 (6025): 91–94. doi:10.1126/science.1201396.

Van den Beucken, T, M Koritzinsky, H Niessen, L Dubois, K Savelkouls, H Mujcic, B Jutten, et al. 2009. "Hypoxia-induced Expression of Carbonic Anhydrase 9 Is Dependent on the Unfolded Protein Response." *The Journal of Biological Chemistry* 284 (36): 24204–12. doi:10.1074/jbc.M109.006510.

Van der Knaap, M S, J C Pronk, and G C Scheper. 2006. "Vanishing White Matter Disease." *Lancet Neurol* 5 (5): 413–23. doi:10.1016/S1474-4422(06)70440-9.

Van der Voorn, J P, B van Kollenburg, G Bertrand, K Van Haren, G C Scheper, J M Powers, and M S van der Knaap. 2005. "The Unfolded Protein Response in Vanishing White Matter Disease." *J Neuropathol Exp Neurol* 64 (9): 770–75. doi:10.1097/01.jnen.0000178446.41595.3a.

Van Kollenburg, B, J van Dijk, J Garbern, A A Thomas, G C Scheper, J M Powers, and M S van der Knaap. 2006. "Glia-specific Activation of All Pathways of the Unfolded Protein Response in Vanishing White Matter Disease." *J Neuropathol Exp Neurol* 65 (7): 707–15. doi:10.1097/01.jnen.0000228201.27539.50.

Volpe, J J. 2001. "Neurobiology of Periventricular Leukomalacia in the Premature Infant." *Pediatric Research* 50 (5): 553–62. doi:10.1203/00006450-200111000-00003.

Volpe, J J. 2009. "Brain Injury in Premature Infants: a Complex Amalgam of Destructive and Developmental Disturbances." *Lancet Neurology* 8 (1): 110–24. doi:10.1016/S1474-4422(08)70294-1.

Walter, P, and D Ron. 2011. "The Unfolded Protein Response: From Stress Pathway to Homeostatic Regulation." *Science (New York)* 334 (6059): 1081–86.

doi:10.1126/science.1209038.

Watzlawik, J O, R J Kahoud, R J O'Toole, K A White, A R Ogden, M M Painter, B Wootla, et al. 2015. "Abbreviated Exposure to Hypoxia Is Sufficient to Induce CNS Dysmyelination, Modulate Spinal Motor Neuron Composition, and Impair Motor Development in Neonatal Mice." *Plos One* 10 (5): e0128007. doi:10.1371/journal.pone.0128007.

Way, S W, J R Podojil, B L Clayton, A Zaremba, T L Collins, R B Kunjamma, A P Robinson, et al. 2015. "Pharmaceutical Integrated Stress Response Enhancement Protects Oligodendrocytes and Provides a Potential Multiple Sclerosis Therapeutic." *Nat Commun* 6 (March): 6532. doi:10.1038/ncomms7532.

Way, S W, and B Popko. 2016. "Harnessing the Integrated Stress Response for the Treatment of Multiple Sclerosis." *Lancet Neurology* 15 (4): 434–43. doi:10.1016/S1474-4422(15)00381-6.

Wilson-Costello, D, H Friedman, N Minich, A A Fanaroff, and M Hack. 2005. "Improved Survival Rates with Increased Neurodevelopmental Disability for Extremely Low Birth Weight Infants in the 1990s." *Pediatrics* 115 (4): 997–1003. doi:10.1542/peds.2004-0221.

Woodward, L J, P J Anderson, N C Austin, K Howard, and T E Inder. 2006. "Neonatal MRI to Predict Neurodevelopmental Outcomes in Preterm Infants." *The New England Journal of Medicine* 355 (7): 685–94. doi:10.1056/NEJMoa053792.

Wouters, B G, T van den Beucken, M G Magagnin, M Koritzinsky, D Fels, and C Koumenis. 2005. "Control of the Hypoxic Response through Regulation of mRNA Translation." *Seminars in Cell & Developmental Biology* 16 (4-5): 487–501. doi:10.1016/j.semcdb.2005.03.009.

Wrabetz, L, M D'Antonio, M Pennuto, G Dati, E Tinelli, P Fratta, S Previtali, et al. 2006. "Different Intracellular Pathomechanisms Produce Diverse Myelin Protein Zero Neuropathies in Transgenic Mice." *J Neurosci* 26 (8): 2358–68. doi:10.1523/JNEUROSCI.3819-05.2006.

Wu, X, X Qu, Q Zhang, F Dong, H Yu, C Yan, D Qi, M Wang, X Liu, and R Yao. 2014. "Quercetin Promotes Proliferation and Differentiation of Oligodendrocyte Precursor Cells after Oxygen/glucose Deprivation-induced Injury." *Cellular and Molecular Neurobiology* 34 (3): 463–71. doi:10.1007/s10571-014-0030-4.

Ye, J, M Kumanova, L S Hart, K Sloane, H Zhang, D N De Panis, E Bobrovnikova-Marjon, J A Diehl, D Ron, and C Koumenis. 2010. "The GCN2-ATF4 Pathway Is Critical for Tumour Cell Survival and Proliferation in Response to Nutrient Deprivation." *The EMBO Journal* 29 (12): 2082–96. doi:10.1038/emboj.2010.81.

Ye, J, R B Rawson, R Komuro, X Chen, U P Davé, R Prywes, M S Brown, and J L Goldstein. 2000. “ER Stress Induces Cleavage of Membrane-bound ATF6 by the Same Proteases That Process SREBPs.” *Molecular Cell* 6 (6): 1355–64.

Yerlikaya, A, S R Kimball, and B A Stanley. 2008. “Phosphorylation of eIF2alpha in Response to 26S Proteasome Inhibition Is Mediated by the Haem-regulated Inhibitor (HRI) Kinase.” *The Biochemical Journal* 412 (3): 579–88. doi:10.1042/BJ20080324.

Yuen, T J, J C Silbereis, A Griveau, S M Chang, R Daneman, S P Fancy, H Zahed, E Maltepe, and D H Rowitch. 2014. “Oligodendrocyte-encoded HIF Function Couples Postnatal Myelination and White Matter Angiogenesis.” *Cell* 158 (2): 383–96. doi:10.1016/j.cell.2014.04.052.

Zhang, P, B McGrath, S Li, A Frank, F Zambito, J Reinert, M Gannon, K Ma, K McNaughton, and D R Cavener. 2002. “The PERK Eukaryotic Initiation Factor 2 Alpha Kinase Is Required for the Development of the Skeletal System, Postnatal Growth, and the Function and Viability of the Pancreas.” *Molecular and Cellular Biology* 22 (11): 3864–74.

Zhang, Y, K Chen, S A Sloan, M L Bennett, A R Scholze, S O’Keeffe, H P Phatnani, et al. 2014. “An RNA-sequencing Transcriptome and Splicing Database of Glia, Neurons, and Vascular Cells of the Cerebral Cortex.” *The Journal of Neuroscience* 34 (36): 11929–47. doi:10.1523/JNEUROSCI.1860-14.2014.

Zhu, K, H Jiao, S Li, H Cao, D L Galson, Z Zhao, X Zhao, et al. 2013. “ATF4 Promotes Bone Angiogenesis by Increasing VEGF Expression and Release in the Bone Environment.” *Journal of Bone and Mineral Research* 28 (9): 1870–84. doi:10.1002/jbmr.1958.

Zinszner, H, M Kuroda, X Wang, N Batchvarova, R T Lightfoot, H Remotti, J L Stevens, and D Ron. 1998. “CHOP Is Implicated in Programmed Cell Death in Response to Impaired Function of the Endoplasmic Reticulum.” *Genes & Development* 12 (7): 982–95.

Zonouzi, M, J Scafidi, P Li, B McEllin, J Edwards, J L Dupree, L Harvey, et al. 2015. “GABAergic Regulation of Cerebellar NG2 Cell Development Is Altered in Perinatal White Matter Injury.” *Nature Neuroscience* 18 (5): 674–82. doi:10.1038/nn.3990.